Investigation of the structure of exopolysaccharides produced by lactic acid bacteria

Elisabeth J. Faber

Investigation of the structure of exopolysaccharides produced by lactic acid bacteria

Investigation of the structure of exopolysaccharides produced by lactic acid bacteria

Struktuuronderzoek van exopolysachariden geproduceerd door melkzuurbacteriën

(met een samenvatting in het Nederlands)

Proefschrift

ter verkrijging van de graad van doctor
aan de Universiteit Utrecht
op gezag van de Rector Magnificus, Prof. Dr. H.O. Voorma,
ingevolge het besluit van het College voor Promoties
in het openbaar te verdedigen
op woensdag 6 december 2000 des middags te 14.30 uur

door

Elisabeth Johanna Faber
geboren op 13 juni 1970 te Minnertsga

Promotores: **Prof. Dr. J.P. Kamerling**
en
Prof. Dr. J.F.G. Vliegenthart

Verbonden aan de sectie Bio-Organische Chemie van het Bijvoet Centrum voor Biomoleculair Onderzoek van de Faculteit Scheikunde van de Universiteit Utrecht

Het in dit proefschrift beschreven onderzoek is uitgevoerd bij de sectie Bio-Organische Chemie van het Bijvoet Centrum voor Biomoleculair Onderzoek van de Faculteit Scheikunde van de Universiteit Utrecht. Het onderzoek werd mogelijk gemaakt door het onderzoekproject exopolysachariden van de Programmatische Bedrijfsgerichte Technologische Stimulering (PBTS) met financiële ondersteuning van het Ministerie van Economische Zaken en het Integrale Structuurplan voor Noord-Nederland van de Nederlandse Ontwikkelingsmaatschappij (NOM).

Structural knowledge of naturally occurring, biologically important molecules is at the very foundation of modern biochemistry and biology. When an unprecedented and unanticipated type of molecular structure is suddenly discovered, one therefore imagines that either 'the microscope has got bigger', or that someone was lucky and stumbled onto something.

O. Hindsgaul, Nature, 399 (1999) 644-645.

Oan Heit en Mem
Voor Hans

Cover *Streptococcus thermophilus*
Lactobacillus delbrueckii subsp. *bulgaricus*

CIP-GEGEVENS KONINKLIJKE BIBLIOTHEEK, DEN HAAG

Faber, Elisabeth Johanna

Investigation of the structural of exopolysaccharides produced by lactic acid bacteria / Elisabeth Johanna Faber. – Utrecht: Universiteit Utrecht, Faculteit Scheikunde.

Thesis Universiteit Utrecht. – With Ref. – With summary in Dutch.

ISBN 90-393-2557-X

Subject headings: exopolysaccharides / lactic acid bacteria / structural analysis

Contents

General Introduction

Exopolysaccharides

Contents

Introduction

For centuries lactic acid bacteria have been involved in the preparation of a wide variety of fermented food products such as sourdough, fermented meat (*e.g.* sausages), fermented vegetables (*e.g.* olives, cabbage), and dairy products. One of the most important properties of lactic acid bacteria during these fermentation processes is the production of lactate causing acidification of the food product and thereby preservation against microbial spoilage. Besides the inhibition of spoilage, it is often the presence of fermenting lactic acid bacteria that gives the food product its characteristic properties. The proteolytic activity exerted by most lactic acid bacteria has a large impact on the development of flavor and texture of food products. In addition to lactate production and proteolytic activity, a large variety of other substances are produced that contribute to the flavor, texture and consistency of fermented products. In this respect the extracellular polysaccharides produced by lactic acid bacteria play a crucial role in the rheological properties of fermented food products. In some cases this results in undesired ropiness [1,2], however, often these polymers are used to improve body and texture of the fermented products [3]. Besides these interesting physical properties, some of these polysaccharides have been reported to exhibit health-beneficial properties, such as antitumor [4,5], anti-ulcer [6], immune stimulating [7], and cholesterol-lowering [8] activities. However, despite the numerous health claims, care should be taken when interpreting the results of these studies, since not all of these health claims are supported by solid scientific evidence [9].

Microbial production of extracellular polysaccharides is a phenomenon that is not confined to lactic acid bacteria alone. In fact, these polysaccharides are of widespread occurrence, being produced by a variety of bacterial and fungal cultures. Extracellular polysaccharides produced by bacteria are either located outside the cell wall as a capsule intimately associated with the cell surface or secreted into the environment in the form of slime. Exopolysaccharides should not be confused with capsular polysaccharides (CPSs). The latter play an important role in determining the immunological properties of the bacterial cell [10]. Slime polysaccharides, or exopolysaccharides (EPSs) in their natural environment, are thought to have a function in the protection of the cell against desiccation, phagocytosis and predation by protozoas, adhesion to surfaces and in cellular recognition. EPSs do not appear to function as energy sources, since EPS-producing bacteria are usually not capable of catabolizing the polysaccharides they synthesize [11,12].

In this thesis the structural and conformational characterization of EPSs produced by several lactic acid bacteria is described. The research is stimulated by the industrial interest in

microbial polysaccharides originating from bacteria, which carry the 'generally recognized as safe' (GRAS) status [13]. In this chapter, a survey is given of the current application of exopolysaccharides in industry, followed by an overview of the structures of EPSs produced by lactic acid bacteria known in literature. The strategies and techniques commonly used for the elucidation of EPS structures, including an introduction into the concepts of conformational analysis of carbohydrates, are given. Moreover, the relationship between the structure of EPSs and their physical properties, as well as recent studies on the biochemistry and genetics of EPS biosynthesis in lactic acid bacteria will be outlined. With the growing knowledge of EPS structures and biosynthesis, doors open to EPS engineering. Finally, the use of this knowledge for current and future aspects of polysaccharide engineering will be discussed.

1. Polysaccharides in food industry

Most high-molecular-weight polysaccharides used in food industry are derived from plants (cellulose, pectin, and starch), seaweeds (alginate and carrageenan), and bacteria (alginate, gellan, and xanthan). A number of these polysaccharides are employed to alter the

Table 1. *Established applications of microbial exopolysaccharides in foods [14].*

Polymer	Bacterial source	Application
Xanthan	*Xanthomonas campestris*	Inhibitor of crystal formation Stabilizing agent Suspending agent Viscosity control
Acetan	*Acetobacter xylinum*	Gelling agent Viscosity control
Dextran	*Leuconostoc mesenteroides* [a] *Leuconostoc dextranicus*	Stabilizing agent Viscosity control
Gellan	*Sphingomonas* species	Gelling agent Stabilizing agent Suspending agent
EPS of LAB	*Lactobacillus* ssp. *Lactococcus lactis*	Hydrating agent Viscosity control

[a] main dextran-producing bacterium

rheological behavior and the texture of food products. In 1878 the first reported microbial polysaccharide, produced by *Leuconostoc mesenteroides*, was intentionally used as a thickener of sugar beat and sugar cane syrups [15]. Microbial polysaccharides represent only a small fraction of the current biopolymers, since they have to compete with other natural or synthetic polymers which are much cheaper to produce and market. On the other hand, microbial polysaccharides possess unique physical properties that make their applications in food widespread (Table 1).

Xanthan. — The anionic polysaccharide xanthan produced by the plant pathogenic bacterium *Xanthomonas campestris* received approval for industrial applications as food additive by the U.S. Food and Drug Administration in 1969, and is nowadays commercially the most important microbial EPS. Xanthan (**1**) consists of a cellulose backbone carrying a side-chain composed of D-mannose and D-glucuronic acid. Mutants, different parental strains and different nutrition conditions yield a range of polysaccharides that correspond to the same general structure but have variable ratios of acetylation and pyruvation. Because of its physical properties, the low cost isolation procedures, and the relatively high yields, xanthan is widely used as a thickener or viscosifier in both food and non-food applications. Recently, the genetics and biochemistry of xanthan biosynthesis as well as of the industrial production and application of xanthan have been reviewed [16].

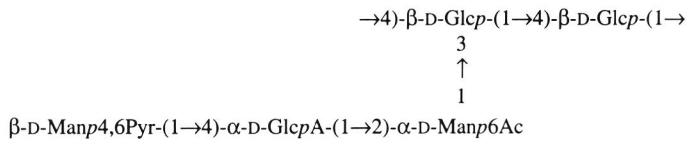

1

Acetan. — The *Acetobacter xylinum* bacterium secretes a xanthan-like polysaccharide named acetan (**2**). This polysaccharide resembles xanthan in having a cellulose backbone substituted on alternate glucose residues with a pentasaccharide side-chain. Although the lengths of the side-chains are different, the residues and linkage types adjacent to the backbone are identical. The polysaccharide can be partially acetylated at O-6 of the branching glucose and the mannose residues. Chemical mutagenesis of *A. xylinum* has allowed selection of mutants that produce acetan-like polysaccharides containing side-chains of reduced length. Deacetylated acetan shows massive increases in viscosity and the

development of gel-like properties when mixed with locust bean gum or konjan mannan [17]. Due to its resemblance in properties to the commercially important xanthan, acetan is a potential thickening and gelling agent.

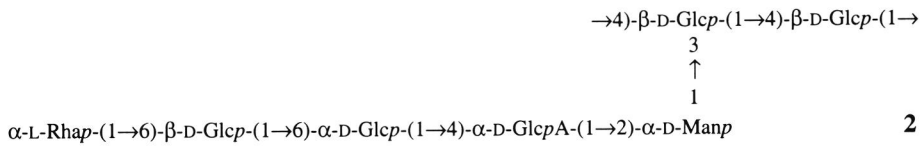

2

Dextran. — Dextran is a name given to a class of neutral branched polysaccharides composed of a linear backbone of (1→6)-linked α-D-glucopyranosyl residues. In most dextrans branching occurs mainly at O-3, and to a lesser extent at O-2 or O-4 [18]. As for xanthan, the type of dextran formed is dependent on the bacterial strain and the nutrition conditions. The bacteria that produce dextran belong to the genera *Lactobacillus*, *Leuconostoc*, and *Streptococcus*, from which the main dextran-producing bacterium used in industry is *Leuconostoc mesenteroides*. Dextran is chemically inert, compatible with most food ingredients, shows high resistance to hydrolytic depolymerization and has effective emulsifying and stabilizing properties in oil-in-water emulsions. In food industry dextran is used as stabilizing agent and for viscosity control, although the largest market for dextran and its derivatives is the pharmaceutical and fine-chemical industry.

Gellan. — Other examples of microbial EPSs of potential industrial importance are collected under the name Gellan. These structurally related polysaccharides are synthesized by *Sphingomonas* species such as *Sphingomonas paucimobilis.* The native polymers are composed of linear tetrasaccharide repeating units (**3**) with different ratios of *O*-acetyl and *O*-glyceryl substituents. With the trade names Kelcogel or Gelrite, gellan is approved in the United States and Europe for use in food applications.

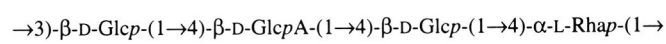

3

Exopolysaccharides produced by lactic acid bacteria. — In contrast to microbial polysaccharides such as xanthan, acetan, dextran, and gellan, which are applied as additives

in food products in order to obtain texturizing properties, there are a number of bacterial fermentations in which polysaccharides are produced *in situ*. For example, the application of EPS-producing lactic acid bacteria in a large number of fermented milk products such as yogurt and villi (traditional Finnish fermentation product). This *in situ* production of EPS results in the enhancement of body, texture, smoothness and mouth feel of these products. Furthermore, research demonstrated that EPS-producing lactic acid bacteria can increase moisture retention in low fat Mozzarella cheese, thereby improving its melting properties [19].

The use of microbial EPSs in food is not strictly related to their physical properties. There is a growing awareness of the widespread use of additives in consumer products and an increase in the popularity of 'natural' food products. Therefore, it is relevant for the food industry to consider natural alternatives for these food additives. The use of EPS-producing lactic acid bacteria, a class of microorganisms possessing the GRAS status, as a natural source of food thickeners receives a great deal of attention. In the prospect of the industrial applications of these EPSs, the understanding of their physical properties in relationship to their structure, the so-called structure-function relationship, plays a crucial role.

2. Exopolysaccharides produced by lactic acid bacteria

Since the primary structures of EPSs are at the base of their physical properties, a detailed knowledge of these structures is required to establish the structure-function relationship of EPSs. In general, EPSs produced by lactic acid bacteria can be divided into homopolysaccharides, containing a single type of monosaccharides, and heteropolysaccharides, possessing repeating units in which different monosaccharides are present.

Homopolysaccharides produced by lactic acid bacteria can be divided into three groups of structurally related polymers, α-D-glucans, β-D-glucans, and fructans (Table 2). The various homopolysaccharides belonging to these three groups have main backbone structures and strain specific differences by a variable degree of branching and different linking sides; for dextrans various degrees of (1→2)-linked, (1→3)-linked and (1→4)-linked α-D-Glc*p* branchings have been reported (*vide infra*). The polygalactan produced by *L. lactis* subsp. *cremoris* H414 [20] is generally assigned as a fourth group of homopolysaccharides. This homopolymer consists of a pentameric repeating unit and therefore resembles more the structures of the heteropolysaccharides produced by lactic acid bacteria (*vide infra*). For this reason, the EPS produced by *L. lactis* subsp. *cremoris* H414 is included in the overview of

heteropolysaccharide structures (Table 3). The production, chemical composition, structure and biosynthesis of homopolysaccharides produced by lactic acid bacteria have been reviewed [11].

Table 2. *Structures of homopolysaccharides produced by lactic acid bacteria.*

EPS	Lactic acid bacteria	Main backbone structure
α-D-glucans		
dextran	*Leuconostoc mesenteroides* subsp. *mesenteroides* *Leuconostoc mesenteroides* subsp. *dextranicum* *Pediococcus pentosaceus* *Lactobacillus reuteri*	(1→6)-linked α-D-Glc*p*
mutant	*Streptococcus mutans* *Streptococcus sobrinus*	(1→3)-linked α-D-Glc*p*
alternan	*Leuconostoc mesenteroides* subsp. *mesenteroides*	alternating (1→3)- and (1→6)-linked α-D-Glc*p*
β-D-glucans	*Pediococcus* spp. *Streptococcus* spp.	(1→6)-linked β-D-Glc*p*
fructans		
levan	*Lactobacillus reuteri* *Streptococcus salivarius*	(2→6)-linked β-D-Fru*f*

Heteropolysaccharides produced by lactic acid bacteria contain repeating units varying in size from trisaccharides to heptasaccharides. The molecular weight of the EPSs ranges from 4 to $6 \cdot 10^3$ kDa, and the number of repeating units per molecule may surpass one thousand. The production of the heteropolysaccharides varies from 0.05 – 0.60 g/L, depending on the EPS-producing strain. Optimization of culturing conditions can increase the EPS production; for example, EPS production of *Lb. sake* 0-1 is as high as approximately 1.4 g/L when grown anaerobically at 20 °C and pH 5.8 [21]. In the last decade compositional studies have been performed on heteropolysaccharides produced by various species of the *Lactobacillus*, *Lactococcus*, and *Streptococcus* genera [9]. The primary structures of heteropolysaccharides produced by lactic acid bacteria obtained from more detailed structural studies are illustrated in Table 3.

Table 3. *Primary structures of heteropolysaccharides produced by lactic acid bacteria.*

***Lactobacillus acidophilus* LMG 9433** β-D-Glc*p*NAc 1 ↓ 3 →4)-β-D-Glc*p*A-(1→6)-α-D-Glc*p*-(1→4)-β-D-Gal*p*-(1→4)-β-D-Glc*p*-(1→	[22]
Lactobacillus brevis [a] →6)-β-D-Glc*p*-[1→2(6)]-β-D-Gal*p*-(1→4)-α-D-Gal*p*-(1→3)-β-D-Gal*p*-(1→4)-β-D-Glc*p*-(1→ 6(2) ↑ 1 β-D-Glc*p*	[23,24]
***Lactobacillus delbrueckii* subsp. *bulgaricus* rr** β-D-Gal*p* β-D-Gal*p* α-L-Rha*p* 1 1 1 ↓ ↓ ↓ 3 4 3 →2)-α-D-Gal*p*-(1→3)-β-D-Glc*p*-(1→3)-β-D-Gal*p*-(1→4)-α-D-Gal*p*-(1→	[25]
***Lactobacillus helveticus* 766** β-D-Gal*f* 1 ↓ 3 →3)-β-D-Glc*p*-(1→4)-β-D-Glc*p*-(1→6)-α-D-Glc*p*-(1→6)-α-D-Gal*p*-(1→6)-α-D-Glc*p*-(1→	[26]
***Lactobacillus helveticus* 2091** β-D-Gal*p* 1 ↓ 6 →6)-β-D-Gal*p*-(1→4)-α-D-Gal*p*-(1→3)-β-D-Gal*p*-(1→4)-β-D-Glc*p*-(1→6)-β-D-Glc*p*-(1→	[27]
***Lactobacillus helveticus* Lb161** →4)-α-D-Glc*p*-(1→4)-β-D-Gal*p*-(1→3)-α-D-Gal*p*-(1→2)-α-D-Glc*p*-(1→3)-β-D-Glc*p*-(1→ 3 3 ↑ ↑ 1 1 β-D-Glc*p* β-D-Glc*p*	[28]

(continued on the next page)

Table 3. *Continued.*

***Lactobacillus helveticus* TN-4**, and **Lh59** β-D-Gal*p*-(1→4)-β-D-Glc*p* 1 ↓ 3 →3)-α-D-Gal*p*-(1→3)-α-D-Glc*p*-(1→3)-β-D-Glc*p*-(1→5)-β-D-Gal*f*-(1→	[29,30]
***Lactobacillus helveticus* TY1-2** β-D-Gal*p*-(1→4)-β-D-Glc*p* 1 ↓ 6 →6)-β-D-Glc*p*-(1→3)-β-D-Glc*p*-(1→6)-α-D-Glc*p*NAc-(1→3)-β-D-Gal*p*-(1→ 4 ↑ 1 (α-D-Gal*p*)$_{0.8}$	[31]
***Lactobacillus kefiranofaciens* K1**[b] β-D-Glc-{1→2(6)}-β-D-Gal-(1→4)-α-D-Gal-(1→3)-β-D-Gal-(1→4)-D-Glc 6(2) ↑ 1 β-D-Gal or β-D-Glc-(1→6)-β-D-Gal	[32]
***Lactobacillus paracasei* 34-1** →3)-β-D-Gal*p*NAc-(1→4)-β-D-Gal*p*-(1→6)-β-D-Gal*p*-(1→6)-β-D-Gal*p*-(1→ 3 ↑ *sn*-glycerol 3-phosphate	[33]
***Lactobacillus rhamnosus* C83** →3)-α-D-Glc*p*-(1→2)-β-D-Gal*f*-(1→6)-α-D-Gal*p*-(1→6)-α-D-Glc*p*-(1→3)-β-D-Gal*f*-(1→	[34]
***Lactobacillus sake* 0-1** β-D-Glc*p* 1 ↓ 6 →4)-β-D-Glc*p*-(1→4)-α-D-Glc*p*-(1→3)-β-L-Rha*p*2Ac$_{0.85}$-(1→ 3 ↑ 1 *sn*-glycerol 3-phosphate→4)-α-L-Rha*p*	[35]

Table 3. *Continued.*

***Lactococcus lactis* subsp. *cremoris* H414** →4)-β-D-Gal*p*-(1→3)-β-D-Gal*p*-(1→4)-α-D-Gal*p*-(1→ 3 ↑ 1 β-D-Gal*p*-(1→3)-β-D-Gal*p*	[20]
***Lactococcus lactis* subsp. *cremoris* SBT 0495, and NIZO B40** α-L-Rha*p* 1 ↓ 2 →4)-β-D-Glc*p*-(1→4)-β-D-Gal*p*-(1→4)-β-D-Glc*p*-(1→ 3 ↑ α-D-Gal*p*-(1→phosphate	[36,37]
***Lactococcus lactis* subsp. *cremoris* NIZO B39** β-D-Gal*p*-(1→4)-β-D-Glc*p* 1 ↓ 4 →3)-α-D-Gal*p*-(1→3)-α-L-Rha*p*-(1→2)-α-L-Rha*p*-(1→2)-α-D-Gal*p*-(1→3)-α-D-Glc*p*-(1→	[38]
***Lactococcus lactis* subsp. *cremoris* NIZO B891** β-D-Gal*p*-(1→4)-β-D-Glc*p*6Ac $_{0.5}$ 1 ↓ 6 →4)-α-D-Glc*p*-(1→4)-β-D-Gal*p*-(1→4)-β-D-Glc*p*-(1→	[39]
***Streptococcus macedonicus* Sc136** β-D-Gal*f*-(1→6)-β-D-Glc*p*-(1→6)-β-D-Glc*p*NAc 1 ↓ 3 →4)-α-D-Gal*p*-(1→4)-β-D-Gal*p*-(1→4)-β-D-Glc*p*-(1→	[40]
***Streptococcus thermophilus* Sfi6** α-D-Gal*p* 1 ↓ 6 →3)-β-D-Gal*p*-(1→3)-β-D-Glc*p*-(1→3)-α-D-Gal*p*NAc-(1→	[41-43]

(continued on the next page)

Table 3. *Continued.*

***Streptococcus thermophilus* Sfi39** β-D-Gal*p* 1 ↓ 6 →3)-α-D-Glc*p*-(1→3)-β-D-Glc*p*-(1→3)-β-D-Gal*f*-(1→	[44]
***Streptococcus thermophilus* Sfi12** β-D-Gal*p* 1 ↓ 4 →3)-α-D-Gal*p*-(1→3)-α-L-Rha*p*-(1→2)-α-L-Rha*p*-(1→2)-α-D-Gal*p*-(1→3)-α-D-Glc*p*-(1→	[44]
***Streptococcus thermophilus* OR 901** β-D-Gal*p*-(1→6)-β-D-Gal*p* 1 ↓ 4 →3)-α-D-Gal*p*-(1→3)-α-L-Rha*p*-(1→2)-α-L-Rha*p*-(1→2)-α-D-Gal*p*-(1→3)-α-D-Gal*p*-(1→	[45]

[a] no strain specified.
[b] ring configuration not determined.

As is clear from the EPSs described in Table 3, EPSs produced by lactic acid bacteria have only a limited amount of structural features. The EPSs consist mainly of combinations of D-Glc, D-Gal and/or L-Rha, and to a minor extent of D-GlcNAc, D-GalNAc or D-GlcA. In some cases non-carbohydrate substituents such as phosphate and acetyl functions, and glycerol groups are present. A structural similarity of the majority of the EPSs produced by lactic acid bacteria is the presence of a side chain. Moreover, the side-chains themselves show structural analogies. For example, the repeating units of the EPSs produced by several strains of *Lb. helveticus* [29-31] and *L. lactis* subsp. *cremoris* [38,39] carry a lactosyl side-chain attached to the polysaccharide backbone. Further structural analogies are observed for the EPSs produced by *L. lactis* subsp. *cremoris* B39 [38], *S. thermophilus* Sfi12 [44] and *S. thermophilus* OR 901 [45]. These EPSs are characterized by the presence of a pentameric backbone containing the →3)-α-D-Gal*p*-(1→3)-α-L-Rha*p*-(1→2)-α-L-Rha*p*-(1→2)-α-D-Gal*p*-(1→3)-Hex*p*-(1→ sequence, wherein the fifth residue is α-D-Glc*p* in B39 and Sfi12, and α-D-

Gal*p* in the EPSs produced by OR 901. A further remarkable structural feature of the EPSs produced by several lactic acid bacteria is the coexistence of galactopyranosyl and galactofuranosyl residues [29,30,34, 40,44]. From the existence of the furanose form it can be concluded that these lactic acid bacteria have a mechanism for converting the pyranose into the furanose form [46].

The hexasaccharide repeating unit produced by *S. macedonicus* [40] contains the trisaccharide sequence β-D-Glc*p*NAc-(1→3)-β-D-Gal*p*-(1→4)-β-D-Glc*p*. This sequence corresponds to the internal backbone of lacto-*N*-tetraose and lacto-*N*-neotetraose, which serve as a structural basis for the large majority of human milk oligosaccharides [47]. The presence of this sequence in the *S. macedonicus* EPS may offer an important potential for the development of improved infant nutrition products.

3. Structure elucidation of polysaccharides

Primary structure

The primary structure of a polysaccharide is defined by the monosaccharide composition including the absolute and anomeric configurations, the sequence and ring size of the constituting monosaccharides, the location of the glycosidic linkages, and the type and location of non-carbohydrate substituents. Finally, the mass distribution of the polysaccharides needs to be determined. No single technique is available, which is capable of assigning all these parameters in terms of a unique carbohydrate structure. Therefore, structure elucidation involves the application of several techniques such as nuclear magnetic resonance (NMR) spectroscopy, gas chromatography (GC), and mass spectrometry (MS). Over the years strategies for the structural determination of bacterial polysaccharides have been developed including chemical or enzymatic depolymerization of polysaccharides, yielding mono- or oligosaccharides, and derivatization of monosaccharides into alditol acetates, trimethylsilylated methyl glycosides, and trimethylsilylated (-)-2-butyl glycosides [48-51]. But, although the techniques and strategies mentioned are generally used, the elucidation of the primary structure of a polysaccharide is, due to the diversity in structural features, no routine job. A full description of strategies and techniques used for the elucidation of the primary structure of bacterial polysaccharides is beyond the scope of this introduction; for more details see [49-53].

Three-dimensional structure

Although the elucidation of the primary structure of polysaccharides can be performed using the previously mentioned techniques, detailed knowledge of the three-dimensional structure or conformation is needed to gain insight into the relationship between the structure and physical properties of polysaccharides. For a comprehensive overview of the conformational analysis of carbohydrates, see [54]. In addition to conformational analysis, the dynamics of the polymer and its interaction with other molecules provide insight into the structure-function relationship. To obtain the three-dimensional structure of a polysaccharide both the time averaged ring conformation of the monosaccharide residues and the relative orientations of adjacent monosaccharides have to be determined. The conformation of the glycosidic linkage plays a key role in the overall conformation of carbohydrate chains. This linkage can be defined by two dihedral angles (ϕ,ψ; Figure 1A). In case of a (1→6)-linkage, an additional dihedral angle (ω) is defined (Figure 1B).

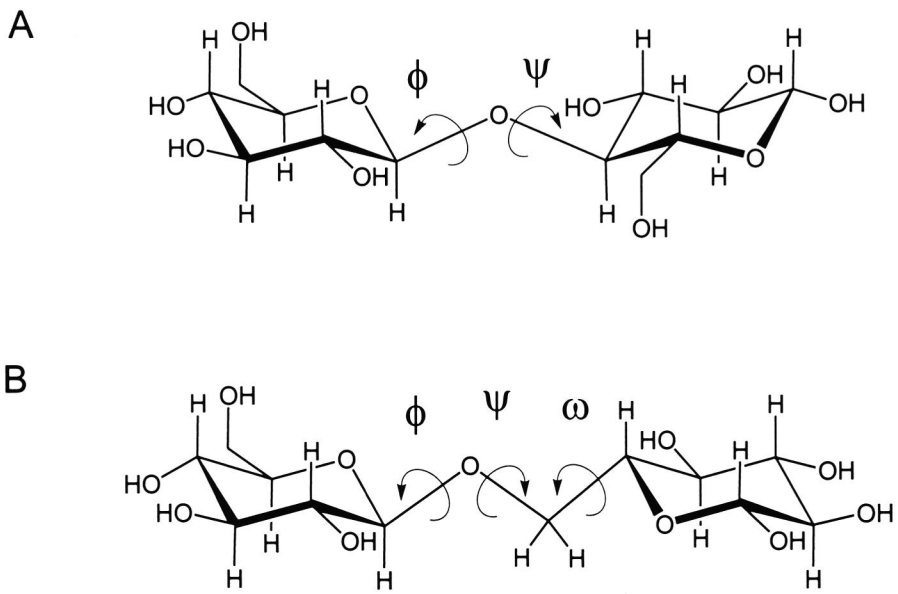

Figure 1. *Molecular model of (A) methyl β-cellobioside and (B) methyl β-gentiobioside. The indicated dihedral angles are* $\phi = \theta(O'_5\text{-}C'_1\text{-}O_X\text{-}C_X)$, $\psi = \theta(C'_1\text{-}O_X\text{-}C_X\text{-}C_{(X-1)})$ *and* $\omega = \theta(O_6\text{-}C_6\text{-}C_5\text{-}O_5)$.

The major techniques used to obtain conformational data on polysaccharides are X-ray diffraction, NMR spectroscopy, molecular mechanics calculations, and molecular dynamics simulations. Less frequently used methods such as light scattering and neutron diffraction can also provide conformational information. Light scattering leads to estimates of the molecular mass and macroscopic dimensions such as the end-to-end distance, radius of gyration, and persistent length [55]. In neutron fiber diffraction studies deuteration, replacing ^{1}H by ^{2}H, is used to change the relative scattering power of chosen groups making them easier to locate. For carbohydrates deuteration of hydroxyl groups and substitution of ^{1}H covalently bound to ^{13}C can be used. In the next paragraphs the techniques employed in the present study for the characterization of the three-dimensional structure of EPSs will be discussed briefly.

Nuclear Magnetic Resonance. — NMR spectroscopy is often used to study the conformation of biomolecules in solution. The most valuable NMR parameter for conformational analysis is the proton-proton Nuclear Overhauser effect (NOE). However, due to the geometry of the glycosidic linkages, the number of NOEs in polysaccharides in solution is often not sufficient for a straightforward interpretation of the data in terms of conformation. Scalar coupling data (*J*-couplings) are valuable complements to the NOEs. Both homo- and heteronuclear *J*-couplings are used to determine the orientation of substituents of ring atoms and to assign the ring conformation. Furthermore, heteronuclear vicinal *J*-couplings ($^{3}J_{C,H}$) between atoms on opposite sides of the glycosidic linkage can be related to their dihedral angles by an improved version of the Karplus equation [56,57]:

$$^{3}J_{C,H} = A\cos^{2}(\theta) + B\cos(\theta) + C \qquad (eq.\ 1)$$

Wherein θ is the dihedral angle ϕ or ψ and A, B, and C are experimentally determined constants, which depend on the nature and orientation of the substituents along the coupling pathway [57]. *J*-couplings have an advantage over NOEs since the averaging of scalar coupling values over multiple conformations is a simple linear average over individual conformers.

Additional conformational aspects of EPSs form the intramolecular hydrogen bonds. ^{1}H NMR spectroscopy provides several parameters for exchangeable protons that can be used to study intramolecular hydrogen bonding [58,59]. The chemical shift of hydroxyl protons tends to increase upon hydrogen bonding, due to the accompanying deshielding effect. The

chemical shift temperature coefficient $d\delta/dT$ provides useful information for the existence of intramolecular hydrogen bonds. The chemical shifts of hydroxyl protons that are hydrogen bonded to solvent molecules have a marked temperature dependence, due to changes in mobility of the solvent molecules. However, changes in temperature have less influence on the chemical shifts of protons involved in intramolecular hydrogen bonds, because they have weaker interactions with the solvent molecules. A third parameter is the vicinal *J*-coupling $^3J_{H\text{-}O\text{-}C\text{-}H}$. The dihedral angles related to these couplings show whether hydroxyl groups are directed towards other oxygen atoms within the molecule. Unfortunately, it is generally not possible to derive dihedral angles from the observed coupling constants, because they are often time averages of several conformations. Finally, the exchange rates of exchangeable protons involved in intramolecular hydrogen bonds are lower than for those interacting with solvent molecules. These exchange rates are calculated from cross-peak intensities in ROESY experiments [58].

Computational analysis. — It is not always possible to get enough information from experimental methods to come to a sufficient definition of the conformational equilibrium. In these cases computational methods can be used to obtain more conformational details. Many different molecular modeling techniques are available. For a review of the techniques used for the analysis of oligosaccharides in solution, see [60]. In principle, *ab initio* calculations can be used for the computational analysis of solute-solvent systems. However, the computational time required for these quantum mechanical calculations increases rapidly with the number of atoms in the system. For this reason, the fully empirical Molecular Mechanics (MM) and Molecular Dynamics (MD) calculations have been developed.

MM is a technique to calculate the energy or geometry of a molecule using a force field. This force field is an expression that represents the energy of a molecule as a function of the coordinates of the individual atoms. The force field can be divided into energy functions for bonds, angles, torsions, van der Waals interactions, and electrostatic interactions [61]. It is used to analyze the minimal energies of all possible combinations of the torsion angle (a grid search) in order to find minimal-energy conformations of small carbohydrates. For larger systems like oligo- or polysaccharides such an approach is not possible, because the number of conformers to consider increases exponentially with the size of the molecule. A further restriction on MM calculations is that it can not be applied to molecules in solution, due to the endless number of possible solvent configurations that should be considered. MD is a force field method that can overcome both problems.

In MD simulations molecules can move according to classical motional equations, and conformation transitions of the molecule can be determined in time. A drawback of MD is

that the simulation time is sometimes too short to monitor all transitions, and important energy minima might be overlooked. In order to obtain statistical information on dihedral angle distributions, a molecular dynamics technique has been developed using the umbrella potential sampling procedure [61]. During an MD simulation the umbrella potential of one dihedral angle in a molecule is improved in order to obtain the potential of mean force (PMF) of this dihedral angle. From this simulation probability distribution profiles can be extracted in order to obtain statistical information on the dihedral angle distributions.

4. Structure-function relationship of exopolysaccharides

Studies of physical properties of EPSs involve the application of a wide range of techniques including electron microscopy, rheometry, viscometry, and light scattering techniques. The interpretation of the results requires a thorough knowledge of the chemical structure of the polymer since the main factors influencing the physical properties of EPSs are of structural origin: molecular mass, stiffness of the polymer, presence of side chains, substituents and charged groups.

Most food products in which EPSs are applied contain fat, oil particles and/or proteins that may interact with the EPSs. The interaction of EPSs with other biopolymers and dispersed particles needs to be considered to get an overall picture of structure-function relationships of EPSs in food products. For example, xanthan can form stable gels when mixed together with a number of galactomannans [62].

Exopolysaccharides and yogurt. — In an attempt to obtain a better understanding of the influence of EPSs on the physical properties of yogurts, the concentration of EPS in various yogurts and the apparent viscosity as a function of the shear rate of these yogurts were determined [63]. Since no direct relationship between apparent viscosity and EPS concentration was observed, it was concluded that the EPS concentration alone could not explain the differences in the physical properties of these yogurts. Further research was focused on the molecular properties of the EPS produced by *L. lactis* subsp. *cremoris* NIZO B40 [64]. The molecular mass, the radius of gyration and the hydrodynamic radius of the EPS in solution were determined using light scattering techniques. Furthermore, investigations were directed towards the physical properties of the EPS, and the interaction between the EPS and relevant colloidal particles present in milk (*e.g.* whey protein, casein micelles). The theoretical models, which describe the results obtained, can serve as tools to gain insight into the textural contribution of EPS to yogurt.

5. Biosynthesis and genetics of exopolysaccharides

The biosynthesis of polysaccharides can be divided into different pathways, mainly depending on composition (homo- and heteropolysaccharides) of the EPS. For a number of homopolysaccharides, including dextrans, mutans, alternans and levans, the biosynthesis process is extracellular and requires the exogeneous substrate sucrose. The highly specific glycosyltransferase sucrase is involved in the polymerization reaction, whereas the energy needed for polymerization is obtained from the hydrolysis of sucrose [46].

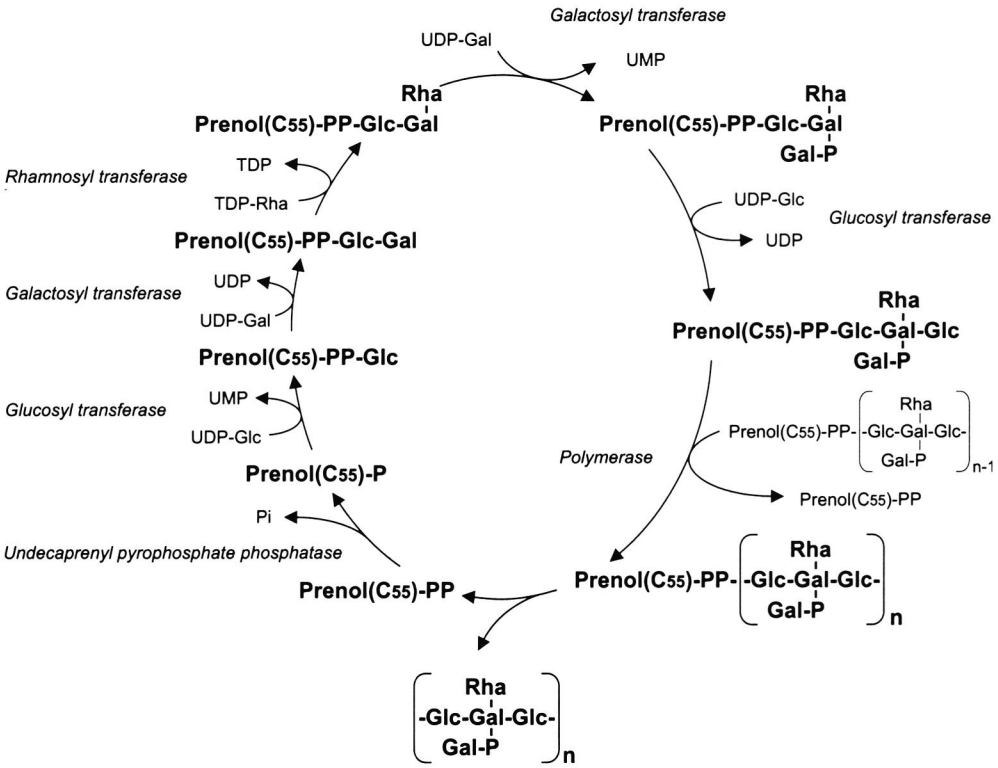

Figure 2. *Proposed biosynthesis of the exopolysaccharide produced by* Lactococcus lactis *subsp.* cremoris *SBT 0495 [9].*

The pathway for the biosynthesis of heteropolysaccharides produced by lactic acid bacteria is far more complex in polymerizing repeating unit precursors formed on a lipid carrier located in the cytoplasmic membrane of the cell. The biosynthesis of EPSs of lactic acid bacteria is thought to proceed in a similar way as that of O-antigens and several types of capsular EPSs [14]. The biosynthetic pathway proposed for the production of the EPS by *L. lactis* subsp. *cremoris* SBT 0495 is depicted in Figure 2. The different steps represent the preparation of the membrane-embedded lipid carrier, the stepwise assembly of the repeating unit, the polymerization of the lipid-linked repeating units, followed by the transport and release of the EPS [9]. Recently, a similar model was proposed for the EPS-biosynthesis route for *L. lactis* subsp. *cremoris* NIZO B40 [65]; a strain producing an EPS, which is identical to the EPS produced by *L. lactis* subsp. *cremoris* SBT 0495. This model differs from that for the *L. lactis* subsp. *cremoris* SBT 0495 in the residue attached to the lipid carrier, consequently resulting in a differently initiated repeating unit.

Biosynthesis of heteropolysaccharides is genetically controlled by *eps* gene clusters. For several *L. lactis* subsp. *cremoris* and two *Lb. casei* strains, these gene clusters have been shown to be located on plasmids, and their loss resulted in the inability to produce EPS [66-69]. On the other hand, the EPS-production of thermophilic lactic acid bacteria has not been found to be linked to plasmids [11,68], and genes required for the EPS synthesis seem to be chromosomally located.

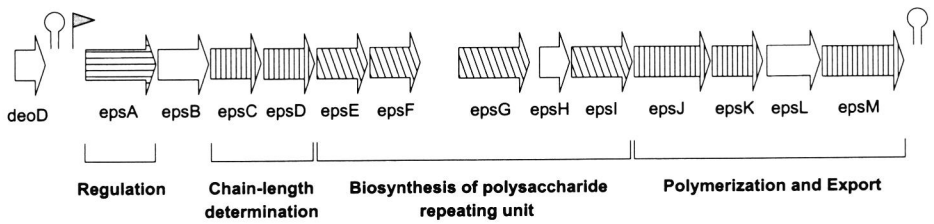

Figure 3. *Organization of the eps gene cluster of* S. thermophilus *Sfi6. Flag and hairpin indicate the eps gene cluster promoter and terminator respectively. Genes are grouped according to the homologies of their predicted proteins, with proteins of known functions that are a regulatory protein (horizontal hatching), polysaccharide polymerase and chain length determinator (vertical hatching) and glycosyl-transferases (diagonal hatching) [42].*

The first genetic work concerning the EPS production of lactic acid bacteria was performed on the *eps* gene cluster from *S. thermophilus* Sfi6 [42]. In succession, complete or parts of the gene clusters of other lactic acid bacteria strains, including *S. thermophilus* NCBF 2393 [70] and *L. lactis* subsp. *cremoris* NIZO B40 [37], were identified and characterized. The clusters are organized into functional regions encoding for enzymes involved in the polymerization and export of the EPS, genes encoding for the glycosyltransferases required for the biosynthesis of the EPS-repeating unit, and genes encoding for regulatory enzymes, polymerization, chain-length determination, and export of the polysaccharides (Figure 3).

During the biosynthesis of EPSs there is a requirement for activated precursors of the constituting monosaccharides: the sugar nucleotides. These sugar nucleotides are general precursors for biosynthetic processes such as the production of cell wall polymers and glycans. As well as the activated forms of the constituting monosaccharides, the synthesis of an EPS demands a precursor of any other group present in the polymer. For example, studies focused on xanthan biosynthesis indicated that acetyl groups are added from acetyl-CoA [16].

6. Engineering of exopolysaccharides

One of the aims for polysaccharide engineering is altering physical properties by changing the primary structure of these polymers. In addition, engineering polysaccharide structures creates the possibility to obtain polymers with closer related structures, which may provide insight into the relationship between structure and physical properties of EPSs. Furthermore, engineering of polysaccharides on the level of biosynthesis may open the door to generate oligosaccharides beneficial for human health (*vide infra*). The engineering of polysaccharides can be performed in several ways.

Chemical modifications. — Structural modifications of polysaccharides can be achieved by controlled treatment with acids, bases, or oxidizing agents. Often these types of modifications are used to obtain structural information [53], but in cases where the target sugar is located in the side-chain of the polysaccharide, these treatments can be applied to alter polymers. For example, uronic acid-containing polymers can be subjected to a specific β-elimination protocol, which results in the elimination of the uronic acid residue and part of the residue attached to its non-reducing side. Likewise, EPSs containing 2-acetamido-2-deoxy sugars can be depolymerized by selective cleavage of the linkage between the 2-acetamido-2-deoxy sugar and the succeeding monosaccharide by means of de-*N*-acetylation followed by deamination. Furthermore, the addition or removal of functional groups like

O-acetyl groups has a great impact on the physical properties of the polymers [71].

Enzymatic modifications. — A different method to tailor the structure of polysaccharides is the modification by means of hydrolytic enzymes. In the field of oligosaccharide sequencing glycosidases have proven to be extremely useful in providing information about glycan structures [72]. These enzymes can also be utilized to alter polysaccharides in order to create wanted physical properties. In principle, enzymes that can be used in EPS modifications are endo- and exo-glycosidases. The former giving rise to depolymerization or to cleavage of glycosidic linkages between internal monosaccharides in extended side-chains, the latter to cleavage of monosaccharides at terminal non-reducing positions. Since heteropolysaccharides have unique repeating units, their hydrolysis is most commonly achieved by highly specific enzymes [12]. Unfortunately, the only enzymatic modification of heteropolysaccharides produced by lactic acid bacteria known thus far, is the cleavage of the terminal Gal*p* residue from a lactosyl side-chain attached to the polysaccharide backbone, using a β-galactosidase [28,31,38,39].

Genetic engineering. — Over the past ten years, important progress has been made in the characterization of the *eps* gene cluster of several EPS-producing lactic acid bacteria (*vide supra*). The availability of knowledge on the functioning of these genes opened the way to genetic EPS-engineering.

→3)-β-D-Glc*p*-(1→3)-α-D-Gal*p*-(1→3)-β-D-Gal*p*-(1→ **4**

α-D-Gal*p*
1
↓
6
→3)-β-D-Glc*p*-(1→3)-α-D-Gal*p*NAc-(1→3)-β-D-Gal*p*-(1→ **5**

In the field of lactic acid bacteria, random mutagenesis of *Lb. sake* 0-1 has yielded a strain that produces an EPS with a different monosaccharide composition [73]. Stingele *et al.* [43] showed that the production of an EPS with an altered repeating unit but of a similar molecular weight was possible. The gene cluster, encoding for the biosynthesis of the EPS

produced by *S. thermophilus* Sfi6, was transferred into the non-EPS producing lactic acid bacterium *L. lactis* MG1363, yielding a high-molecular-weight EPS with a structure different from the EPS produced by the native host. The structure of the recombinant EPS was determined to be as **4**, whereas the structure of the native EPS was shown to be as **5**. The study indicated that *L. lactis* MG1393 was lacking UDP-*N*-acetylglucosamine C4-epimerase activity, which would provide the sugar nucleotide UDP-GalNAc for the incorporation of GalNAc into the EPS. The absence of this enzyme probably caused the substitution of GalNAc by Gal, whereby the α-1,3-*N*-acetylgalactosaminytransferase used UDP-Gal instead of UDP-GalNAc as donor molecule. A further modification consists of a conversion of the tetrameric branched repeating unit with an (1→6)-linked α-D-Gal*p* side-chain (**5**) into a trimeric linear repeating unit (**4**). An explanation for the absence of the branching in the altered EPS could be that the *S. thermophilus* α-1,6-galactosyltransferase, required for the attachment of the side-chain to β-D-Glc, relies on the presence of the *N*-acetyl group of the neighboring α-D-GalNAc unit in order to be functional. Interestingly, the β-1,3-glucosyltransferase, needed for the incorporation of Glc, does not seem to recognize the *N*-acetyl group of the GalNAc residue, since Glc is transferred to Gal in the *L. lactis* EPS. The modification of the EPS further implies that the repeating unit polymerase can recognize and polymerize repeating units that differ in the backbone as well as in the side-chain from their native substrates.

At this moment, a wide variety of polysaccharide gene clusters and polysaccharides are being studied, and will result in a collection of glycosyltransferase genes and a better understanding of polymerization and export processes. The understanding of the biosynthetic pathway of EPSs may not only result in successful polysaccharide engineering, but may as well open the way to the synthesis of oligosaccharide fragments. Because the biosynthesis of heteropolysaccharides starts with the synthesis of the repeating unit precursor on a lipid carrier, interference at the polymerization level of the biosynthesis may provide a tool for biochemical oligosaccharide synthesis. This, in combination with a collection of glycosyl-transferase genes could provide us with a unique opportunity to synthesize biologically important oligosaccharides. For example, the use of modified lactic acid bacteria for the production of fermented products would give the additional advantage to generate oligosaccharides, which resemble beneficial milk oligosaccharides in food products in order to improve their nutritional value.

7. Outline of this thesis

Microbial exopolysaccharides (EPS) are employed in the food industry as viscosifying, stabilizing, emulsifying and gelling agents. The texturizing properties of EPSs in fermented dairy products in combination with the GRAS (Generally Recognized as Safe) status of EPS-producing lactic acid bacteria make these EPSs of interest for the food industry. To understand the relationship between the structure of EPSs and their physical properties, knowledge of their compositions, structures, and producers are required. Moreover, insight into the biochemistry and genetics of the EPS biosynthesis in lactic acid bacteria is needed in order to influence production levels as well as composition, structure and size of the EPS. The aim of this thesis is to characterize the primary and three-dimensional structure of EPSs produced by different lactic acid bacteria in order to gain knowledge on the relationship between the structure and the physical properties of these EPSs.

The study described in this thesis was part of the PBTS (Programmatische Bedrijfsgerichte Technologische Stimulering) project exopolysaccharides. The aim of this project was to create a better understanding of the relationship between the structure and the physical properties of exopolysaccharides produced by lactic acid bacteria in order to increase the number of applications in the food industry. In order to reach this goal, a number of research topics were formulated including the development of new sources of exopolysaccharides and structurizing agents from which the source should have the GRAS status. In addition, techniques to interfere in the biosynthesis of EPSs in order to influence the structure of the EPS were to be developed. Furthermore, it was recognized that more fundamental knowledge on the relationship between the structure and the physical properties of the EPS was needed in order to select EPS-producing lactic acid bacteria for the application in foods, either by *in situ* production of EPS in food or by the addition of food grade EPSs. From monosaccharide analysis performed on the large number of EPSs produced by lactic acid bacteria belonging to the culture collection of NIZO food research (Ede, The Netherlands), *S. thermophilus* Rs, Sts and S3 were selected for further study, based on comparable monosaccharide compositions of the EPSs produced. Furthermore, the EPS produced by *S. thermophilus* 8S was selected, since the monosaccharide analysis revealed an unusual monosaccharide composition making the EPS of this lactic acid bacteria an intriguing research topic. The EPS-producing lactic acid bacterium *Lb. delbrueckii* subsp. *bulgaricus* 291 (WISBY, Niebüll, Germany) was included in the studies, because this bacterium produces a CPS rather then an EPS in its early stage of growth. Furthermore, the EPS produced by *Lb. helveticus* 766 (Unilever Research; NCDO 766) was selected for a

detailed structural study since this EPS is of interest to the food industry for its good growth characteristics and excellent acidifying properties.

In order to obtain fundamental knowledge on the relationship between the structure and physical properties of these EPSs, the primary structure of the EPSs produced by *S. thermophilus* Rs and Sts (Chapter 1), *S. thermophilus* S3 (Chapter 2), and *Lb. delbrueckii* subsp. *bulgaricus* 291 (Chapter 3) were determined. The EPS produced by *S. thermophilus* 8S has been shown to contain a novel substituent, which was isolated and characterized (Chapter 4); furthermore, the primary structure of the complete *S. thermophilus* 8S EPS was elucidated (Chapter 5). Finally, a more detailed conformational analysis of the EPS produced by *Lb. helveticus* 766 is described (Chapter 6). The primary structure of this EPS, elucidated by Robijn *et al.* [26], was applied to a new Molecular Modeling method for obtaining the conformation of an EPS in solution.

References

[1] M.C. Mance de Nadra, A.M. Strasser de Saad, *J. Food Microbiol.*, 27 (1995) 101-106.

[2] M.T. Dueñas-Chasco, M.A. Rodríguez-Carvajal, P. Tejero-Mateo, J.L. Espartero, A. Irastorza-Iribas, A.M. Gil-Serrano, *Carbohydr. Res.*, 307 (1998) 125-133.

[3] J. Cerning, C. Bouillanne, M.J. Desmazeaud, M. Landon, *Biotechnol. Lett.*, 10 (1988) 255-260.

[4] H. Kitazawa, T. Toba, T. Itoh, S. Adachi, N. Kumano, *Agric. Biol. Chem.*, 9 (1988) 2331-2332.

[5] H. Kitazawa, M. Nomura, T. Itoh, T. Yamaguchi, *J. Dairy Sci.*, 74 (1991) 2082-2088.

[6] M. Nagaoka, S. Hashimoto, T. Watanabe, T. Yokokura, Y. Mori, *Biol. Pharm. Bull.*, 17 (1994) 1012-1017.

[7] H. Nakajima, T. Toba, S. Toyoda, *Int. J. Food Microbiol.*, 25 (1995) 153-158.

[8] H. Nakajima, Y. Suzuki, H. Kaizu, T. Hirota, *J. Food Sci.*, 57 (1992) 1327-1329.

[9] J. Sikkema, T. Oba, *Snow Brand R&D Reports*, 107 (1998) 1-31.

[10] L. Kenne, B. Lindberg, in G.O. Aspinall (Ed.), *The Polysaccharides*, Vol. 2, Academic Press, New York, 1983, pp. 287-363.

[11] J. Cerning, *FEMS Microbiol. Rev.*, 87 (1990) 113-130.

[12] I.W. Sutherland, *Carbohydr. Polym.*, 38 (1999) 319-328.

[13] D.J. Stancioff, D.W. Renn, *ACS Symp. Ser.*, 15 (1975) 282-295.

[14] R. van Kranenburg, I.C. Boels, M. Kleerebezem, W.M. de Vos, *Curr. Opin. Biotechnol.*, 10 (1999) 498-504.

[15] V. Crescenzi, *Biotechnol. Prog.*, 11 (1995) 251-259.

[16] A. Becker, F. Katzer, A. Pühler, L. Ielpi, *Appl. Microbiol. Biotechnol.*, 50 (1998) 145-152.

[17] C. Ojinnaka, G.J. Brownsey, E.R. Morris, V.J. Morris, *Carbohydr. Res.*, 305 (1998) 101-108.

[18] J.F. Robyt, in S.B. Petersen, B. Svensson, S. Peterson (Ed.), *Carbohydrate Bioengineering*, Elsevier, Amsterdam, 1995, pp. 295-312.

[19] D.B. Perry, D.J. McMahon, C.J. Oberg, *J. Dairy Sci.*, 80 (1997) 799-805.

[20] M. Gruter, B.R. Leeflang, J. Kuiper, J.P. Kamerling, J.F.G. Vliegenthart, *Carbohydr. Res.*, 231 (1992) 273-291.

[21] D.J.C. van den Berg, G.W. Robijn, A.C. Janssen, M.L.F. Giuseppin, R. Vreeker, J.P. Kamerling, J.F.G. Vliegenthart, A.M. Ledeboer, C.T. Verrips, *Appl. Environ. Microbiol.*, 61 (1995) 2840-2844.

[22] G.W. Robijn, R. Gutiérrez Gallego, D.J.C. van den Berg, H. Haas, J.P. Kamerling, J.F.G. Vliegenthart, *Carbohydr. Res.*, 288 (1996) 203-218.

[23] P. Kooiman, *Carbohydr. Res.*, 7 (1968) 200-211.

[24] L. Micheli, D. Uccelletti, C. Palleschi, V. Crescenzi, *Appl. Microbiol. Biotechnol.*, 53 (1999) 69-74.

[25] M. Gruter, B.R. Leeflang, J. Kuiper, J.P. Kamerling, J.F.G. Vliegenthart, *Carbohydr. Res.*, 239 (1993) 209-226.

[26] G.W. Robijn, J.R. Thomas, H. Haas, D.J.C. van den Berg, J.P. Kamerling, J.F.G. Vliegenthart,

Carbohydr. Res., 276 (1995) 137-154.
[27] M. Staaf, G. Widmalm, Z. Yang, E. Huttunen, *Carbohydr. Res.*, 291 (1996) 155-164.
[28] M. Staaf, Z. Yang, E. Huttunen, G. Widmalm, *Carbohydr. Res.*, 326 (2000) 113-119.
[29] Y. Yamamoto, T. Nunome, R. Yamauchi, K. Kato, Y. Sone, *Carbohydr. Res.*, 275 (1995) 319-332.
[30] F. Stingele, J. Lemoine, J.-R. Neeser, *Carbohydr. Res.*, 302 (1997) 197-202.
[31] Y. Yamamoto, S. Murosaki, R. Yamauchi, K. Kato, Y. Sone, *Carbohydr. Res.*, 261 (1994) 67-78.
[32] T. Mukai, T. Toba, T. Itoh, S. Adachi, *Carbohydr. Res.*, 204 (1990) 227-232.
[33] G.W. Robijn, H.L.J. Wienk, D.J.C. van den Berg, H. Haas, J.P. Kamerling, J.F.G. Vliegenthart, *Carbohydr. Res.*, 285 (1996) 129-139.
[34] C. Vanhaverbeke, C. Bosso, P. Colin-Morel, C. Gey, L. Gamar-Nourani, K. Blondeau, J.-M. Simonet, A. Heyraud, *Carbohydr. Res.*, 314 (1998) 211-220.
[35] G.W. Robijn, D.J.C. van den Berg, H. Haas, J.P. Kamerling, J.F.G. Vliegenthart, *Carbohydr. Res.*, 276 (1995) 117-136.
[36] H. Nakajima, T. Hirota, T. Toba, T. Itoh, S. Adachi, *Carbohydr. Res.*, 224 (1992) 245-253.
[37] R. van Kranenburg, J.D. Marugg, I.I. van Swam, N.J. Willem, W.M. de Vos, *Mol. Microbiol.*, 24 (1997) 387-397.
[38] W.H.M. van Casteren, C. Dijkema, H.A. Schols, G. Beldman, A.G.J. Voragen, *Carbohydr. Res.*, 324 (2000) 170-181.
[39] W.H.M. van Casteren, P. de Waard, C. Dijkema, H.A. Schols, A.G.J. Voragen, *Carbohydr. Res.*, 327 (2000) 411-422.
[40] S.J.F. Vincent, E.J. Faber, J.-R. Neeser, F. Stingele, J.P. Kamerling, *Glycobiology*, in press.
[41] T. Doco, J.-M. Wieruszeski, B. Fournet, D. Carcano, P. Ramos, A. Loones, *Carbohydr. Res.*, 198 (1990) 313-321.
[42] F. Stingele, J.-R. Neeser, B. Mollet, *J. Bacteriol.*, 178 (1996) 1680-1690.
[43] F. Stingele, S.J.F. Vincent, E.J. Faber, J.W. Newell, J.P. Kamerling, J.-R. Neeser, *Mol. Microbiol.*, 32 (1999) 1287-1295.
[44] J. Lemoine, F. Chirat, J.-M. Wieruszeski, G. Strecker, N. Favre, J.-R. Neeser, *Appl. Environ. Microbiol.*, 63 (1997) 3512-3518.
[45] W.A. Bubb, T. Urashima, R. Fujiwara, T. Shinnai, H. Ariga, *Carbohydr. Res.*, 301 (1997) 41-50.
[46] I.W. Sutherland, *Biotechnology of microbial exopolysaccharides*, Cambridge University Press, Cambridge, 1990.
[47] D.S. Newburg, S.H. Neubauer, in R.G. Jensen (Ed.), *Handbook of Milk Composition*, Academic Press, New York, 1995, pp. 273-350.
[48] M.F. Chaplin, *Anal. Biochem.*, 123 (1982) 336-341.
[49] J.P. Kamerling, J.F.G. Vliegenthart, in A.M. Lawson (Ed.), *Clinical Biochemistry - Principles, Methods, Applications. Vol. 1, Mass Spectrometry*, Walter de Gruyter, Berlin, 1989, pp. 176-263.
[50] G.J. Gerwig, J.P. Kamerling, J.F.G. Vliegenthart, *Carbohydr. Res.*, 62 (1978) 349-357.
[51] G.J. Gerwig, J.P. Kamerling, J.F.G. Vliegenthart, *Carbohydr. Res.*, 77 (1979) 1-7.

[52] M.F. Chaplin (Ed.), J.F. Kennedy, *Carbohydrate analysis; a practical approach*, IRL Press, Oxford, 1986.

[53] G.O. Aspinall, in G.O. Aspinall (Ed.), *The Polysaccharides*, Vol. 1, Academic Press, New York, 1982, pp. 35-131.

[54] V.S.R. Rao, P.K. Qasba, P.V. Balaji, R. Chandrasekaran, *Conformation of Carbohydrates*, Harwood Academic Publishers, Amsterdam, 1998.

[55] R. Tuinier, P. Zoon, C. Olieman, M.A. Cohen Stuart, G.J. Fleer, C.G. de Kruif, *Biopolymers*, 49 (1999) 1-9.

[56] M. Karplus, *J. Chem. Phys.*, 30 (1959) 11-15.

[57] C.A.G. Haasnoot, F.A.A.M. de Leeuw, C. Altona, *Tetrahedron*, 36 (1980) 2783-2792.

[58] B.R. Leeflang, J.F.G. Vliegenthart, L.M.J. Kroon-Batenburg, B.P. van Eijck, J. Kroon, *Carbohydr. Res.*, 230 (1992) 41-61.

[59] J. Kroon, L.M.J. Kroon-Batenburg, B.R. Leeflang, J.F.G. Vliegenthart, *J. Mol. Struct.*, 322 (1994) 27-31.

[60] R.J. Woods, in K.B. Lipkowitz, D.B. Boys (Ed.), *Computational Chemistry*, Vol. 9., VCH Publishers Inc., New York, 1996, pp. 129-165.

[61] R.W.W. Hooft, PhD Thesis Utrecht University, The Netherlands, 1993.

[62] G.W. Robijn, PhD Thesis Utrecht University, The Netherlands, 1996.

[63] M.E. van Marle, P. Zoon, *Neth. Milk Dairy J.*, 49 (1995) 47-65.

[64] R. Tuinier, PhD Thesis Wageningen University, The Netherlands, 1999.

[65] R. van Kranenburg, PhD Thesis Wageningen University, The Netherlands, 1999.

[66] H. Neve, A. Geis, M. Teuber, *Biochimie*, 70 (1988) 437-442.

[67] E.R. Vedamuthu, J.M. Neville, *Appl. Environ. Microbiol.*, 51 (1986) 677-682.

[68] M. Vescovo, G.L. Scolari, V. Bottazzi, *Biotechnol. Lett.*, 11 (1989) 709-712.

[69] A. von Wright, S. Tynkkynen, *Appl. Environ. Microbiol.*, 53 (1987) 1385-1386.

[70] A.M. Griffin, V.J. Morris, M.J. Gasson, *Gene*, 183 (1996) 23-27.

[71] I.W. Sutherland, *Pure & Appl. Chem.*, 69 (1997) 1911-1917.

[72] P.M. Rudd, G.R. Guile, B. Küster, D.J. Harvey, G. Opdenakker, R.A. Dwek, *Nature*, 388 (1997) 205-207.

[73] M. Breedveld, K. Bonting, L. Dijkhuizen, *FEMS Microbiol. Lett.*, 169 (1998) 241-249.

Chapter 1

The exopolysaccharides produced by *Streptococcus thermophilus* Rs and Sts have the same repeating unit but differ in viscosity of their milk cultures

Elisabeth J. Faber [a], Pieternella Zoon [b], Johannis P. Kamerling [a], and Johannes F.G. Vliegenthart [a]

[a] *Bijvoet Center, Department of Bio-Organic Chemistry, Utrecht University, PO Box 80.075, NL-3508 TB Utrecht, The Netherlands.*

[b] *NIZO food research, PO Box 20, NL-6710 BA Ede, The Netherlands.*

Abstract

The polysaccharides produced by *Streptococcus thermophilus* Rs and Sts in skimmed milk consist of D-galactose and L-rhamnose in a molar ratio of 5:2. Linkage analysis and 1D/2D NMR (^{1}H and ^{13}C) studies revealed that both polysaccharides have the same branched heptasaccharide repeating unit:

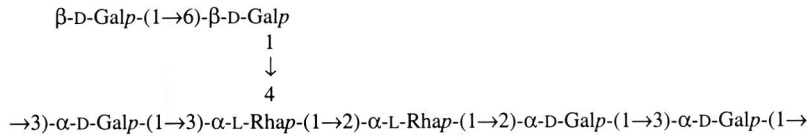

Remarkably, the two strains differ in their effects on the viscosity of stirred milk cultures. The milk culture of *S. thermophilus* Rs is non-ropy and affords 135 mg/L polysaccharide with an average molecular mass of 2.6×10^3 kDa. In contrast, the milk culture of *S. thermophilus* Sts is ropy and produces 127 mg/L polysaccharide with an average molecular mass of 3.7×10^3 kDa. Permeability measurements of non-stirred milk cultures of both strains suggest that both strains have a similar effect on the protein-polysaccharide network. Therefore, the only clear difference between both strains, which may cause the difference in ropiness of the milk cultures, is the difference in molecular mass of the polysaccharide.

Elisabeth J. Faber, Pieternella Zoon, Johannis P. Kamerling, and Johannes F.G. Vliegenthart, *Carbohydr. Res.*, 310 (1998) 269-276.

1.1. Introduction

Microbial exopolysaccharides (EPSs) are widely applied as gelling and stabilizing agents in the food industry [1]. The EPSs produced by lactic acid bacteria which carry the GRAS (Generally Recognized as Save) status, are promising as a new generation of food thickeners. For that reason, detailed structural studies have been performed on exopolysaccharides produced by several lactic acid bacteria strains including *Lactococcus lactis* subsp. *cremoris* [2,3], *Lactobacillus delbrueckii* subsp. *bulgaricus* rr [4], *Lb. helveticus* [5-9], *Lb. acidophilus* [10], *Lb. paracasei* [11], *Lb. sake* [12], and *Streptococcus thermophilus* [13-15].

S. thermophilus strains are used in combination with *Lb. delbrueckii* subsp. *bulgaricus* strains as commercial yogurt starters. Since it is assumed that the ropiness of yogurt is caused by the EPSs produced by these bacteria many investigations have been directed towards those EPSs. Polysaccharides produced by various *S. thermophilus* strains contain mainly rhamnose, glucose, galactose, and 2-acetamido-2-deoxygalactose [13-16]. Although the similarities in these structures are striking, little is known about the relationship between the structures and the consistency of the EPS-containing milk cultures. An exploratory study to establish the main factors determining the consistency of EPS-containing yogurt showed that its apparent viscosity, which increases with increasing ropiness, was not simply related to the EPS concentration [17]. Furthermore, it is stated that the permeability of milk gels before stirring, which reveals information about the structure of the protein-EPS network, was affected by the type of yogurt starter.

In this study, *S. thermophilus* Rs and Sts strains were selected on the basis of huge differences in viscosifying properties of their milk cultures. Both strains produce approximately 100 mg/L EPS which contain galactose and rhamnose in a molar ratio of 5:2. Due to these similarities the strains may give a better insight into the relationship between structures of exopolysaccharides and viscosity of milk cultures. Therefore, we have characterized the EPSs produced by both strains. Furthermore, we have studied the permeability and viscosity of milk cultures produced by both strains.

1.2. Results and discussion

Isolation, purification, and composition of the exopolysaccharides

The exopolysaccharides produced by *S. thermophilus* Rs and Sts in skimmed milk were isolated via ethanol precipitation of the supernatant of the TCA-treated medium, followed by

acetone precipitation and lyophilization of the precipitated polysaccharides. The purity of the polysaccharides was confirmed by 1D ^{1}H NMR spectroscopy (*vide infra*). From the *S. thermophilus* Rs culture 135 mg/L polysaccharide with an average molecular mass of 2.6×10^3 kDa was isolated, whereas the *S. thermophilus* Sts culture yielded 127 mg/L polysaccharide with an average molecular mass of 3.7×10^3 kDa (Table 1). The results show a difference of 1.1×10^3 kDa in molecular mass between both EPSs.

Table 1. *Physical properties of milk cultures and concentration and molecular mass of EPS, produced by* S. thermophilus *Rs and Sts.*

Strain	B [a] (10^{-14} m^2)	Posthumus [b] viscosity (s)	EPS yield (mg/L)	Molecular mass (10^3 kDa)
Rs	11.2 (± 0.2)	39 (± 3)	135 (± 8)	2.6 (± 0.4)
Sts	13.0 (± 0.6)	126 (± 15)	127 (± 13)	3.7 (± 0.7)

[a] Permeability coefficient B measured at 20 °C
[b] Posthumus viscosity measured at 5 °C

Quantitative monosaccharide analysis using procedures I and II, together with the determination of absolute configurations, revealed the presence of D-Gal and L-Rha in a molar ratio of 5:2 for both EPSs. Methylation analyses (Table 2) indicated that the EPSs are composed of branched heptasaccharide repeating units, whereby, according to NMR experiments (*vide infra*), all monosaccharides are in the pyranose ring form.

The 1D ^{1}H NMR spectra (Figure 1) of *S. thermophilus* Rs and Sts EPS are indistinguishable and contain six signals in the anomeric region (δ 5.4 – 4.4). Because the proton signal at δ 5.18 stems from two anomeric protons, the repeating units are heptasaccharides. The sugar residues are designated **A-G** according to increasing chemical shift of the anomeric protons. The chemical shifts and coupling constants of the anomeric signals at δ 4.480 (residue **A**, $^{3}J_{1,2}$ 7.8 Hz) and δ 4.671 (residue **B**, $^{3}J_{1,2}$ 7.8 Hz) indicate two β-Gal*p* residues, and the anomeric signal at δ 5.278 (residue **G**, $^{3}J_{1,2}$ 3.9 Hz) indicates an α-Gal*p* residue. Coupling constants of the remaining anomeric signals could not be measured. The spectra show two high-field doublets at δ 1.312 (residue **F**, $^{3}J_{5,6}$ 5.9 Hz) and δ 1.347 (residue **C**, $^{3}J_{5,6}$ 5.9 Hz), arising from the methyl groups of two Rha residues. The specific residue assignments follow from 2D NMR experiments (*vide infra*).

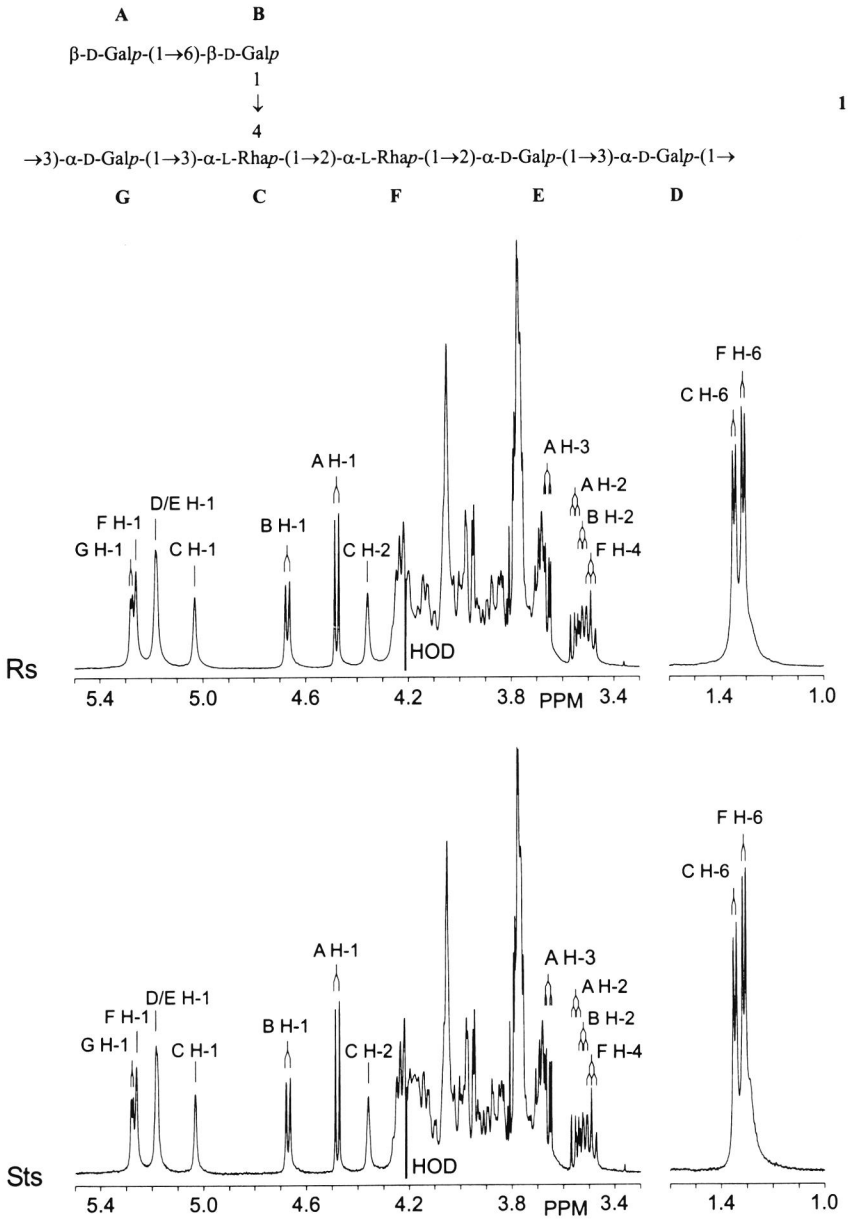

Figure 1. *500-MHz ^1H NMR spectra of EPS from* S. thermophilus *Rs and Sts, recorded in D_2O at 80 °C.*

Table 2. *Methylation analysis data of* S. thermophilus *Rs and Sts EPS.*

Derivative	Molar amounts [a]	
	Rs	Sts
3,4-Rha[b]	0.9	0.9
2-Rha	1.0	1.1
2,3,4,6-Gal	1.0	0.9
2,3,4-Gal	0.9	0.9
3,4,6-Gal	1.0	1.0
2,4,6-Gal	2.0	2.2

[a] 3,4,6-Gal is taken as 1.0.
[b] 3,4-Rha = 1,2,5-tri-*O*-acetyl-3,4-di-*O*-methyl-rhamnitol-*1-d*, *etc.*

2D NMR spectroscopy

Since 2D COSY, 2D TOCSY, 2D NOESY and ^{13}C-^{1}H HSQC spectra of both EPSs are essentially identical, assignments of ^{1}H and ^{13}C chemical shifts and coupling constants of the EPSs were performed using 2D NMR spectra of Sts EPS.

Assignments of the ^{1}H chemical shifts and coupling constants of Sts EPS (Table 3) were performed by means of 2D COSY, 2D TOCSY, 2D NOESY and ^{13}C-^{1}H HSQC-TOCSY experiments. The TOCSY spectrum with a mixing time of 250 ms and the ^{13}C-^{1}H HSQC-TOCSY spectrum are depicted in Figures 2 and 3, respectively. Starting points for the interpretation of the spectra were the H-1 signals of residues **A–G** and the methyl signals of rhamnose residues **C** and **F**.

The TOCSY **A** H-1 track (δ 4.480) shows cross-peaks with **A** H-2,3,4,5. The chemical shifts of the **A** H-6 resonances were assigned through cross-peaks on the TOCSY **A** H-5 track. On the TOCSY **B** H-1 track (δ 4.671), cross-peaks were observed with **B** H-2,3,4. An intraresidual H-1,H-5 contact in the NOESY spectrum (Figure 5) allowed the assignment of **B** H-5. The resonances for **B** H-6a,6b were found via connectivities with **B** H-5 in both the COSY and the TOCSY spectra. The chemical shifts of the H-6 protons of the Gal residue **B** could also be interpreted from cross-peaks on the **B** C-5 track in the HSQC-TOCSY spectrum. From the anomeric carbon signal of residue **D** (δ 98.4) a single cross-peak could be observed in the HSQC-TOCSY spectrum. The spectrum provides evidence that this signal derives from both the **D** H-2 and **D** H-3 atoms, since **D** C-2 and **D** C-3 have different chemical shifts. A connectivity with **D** H-4 was observed on the TOCSY **D** H-1 track, whereas the **D** H-5 signal could be deduced from the intraresidual H-1,H-5 contact in the

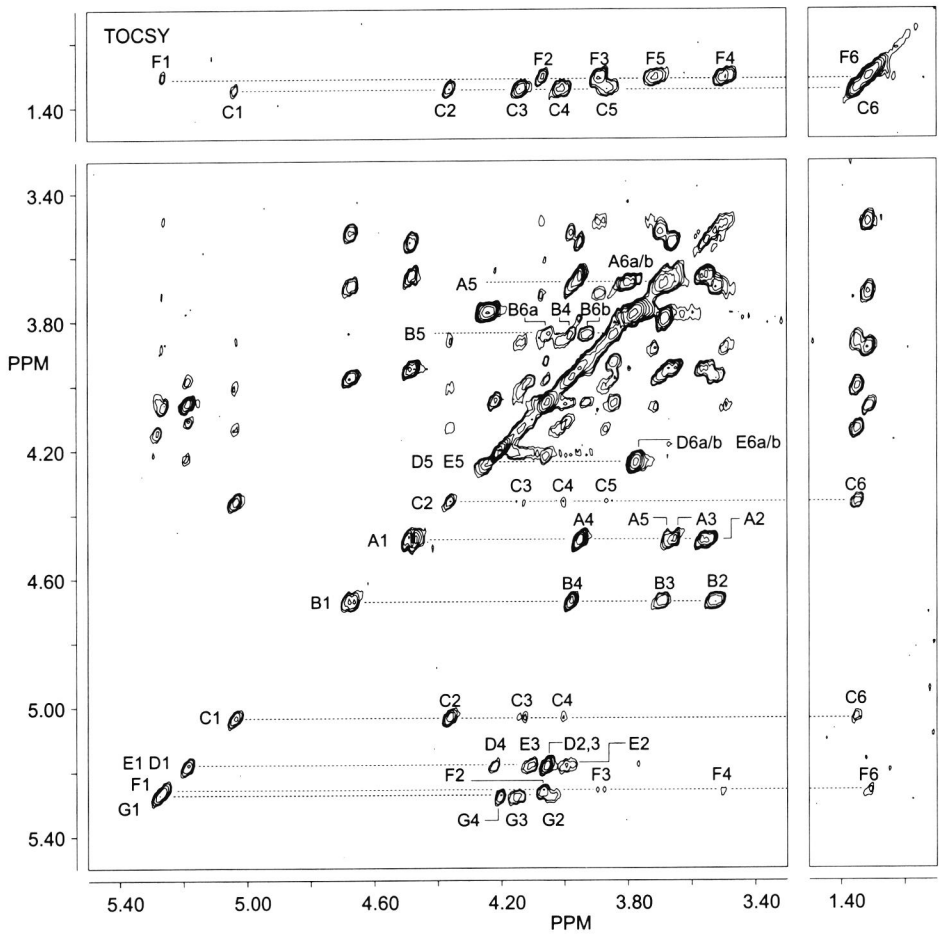

Figure 2. *500-MHz 2D TOCSY spectrum (mixing time 250 ms) of Sts EPS, recorded in D_2O at 80 °C. Diagonal peaks of the anomeric protons, of H-2 of residue* ***C****, of H-5 of residue* ***A****,* ***B****,* ***D*** *and* ***E****, and of H-6 of residues* ***C*** *and* ***F*** *are indicated. Cross-peaks belonging to the same scalar-coupling network are indicated near a dotted line starting from the corresponding diagonal peak.*

NOESY spectrum. Finally the **D** H-6 signals were determined on the **D** C-5 track in the HSQC-TOCSY spectrum. For residue **E**, well resolved H-2 and H-3 connectivities were found on the HSQC-TOCSY **E** C-1 track (δ 97.8), whereas H-4 and H-5,6 were detected on the HSQC-TOCSY **E** C-3 and **E** C-4 track, respectively. On the TOCSY H-6 tracks of the

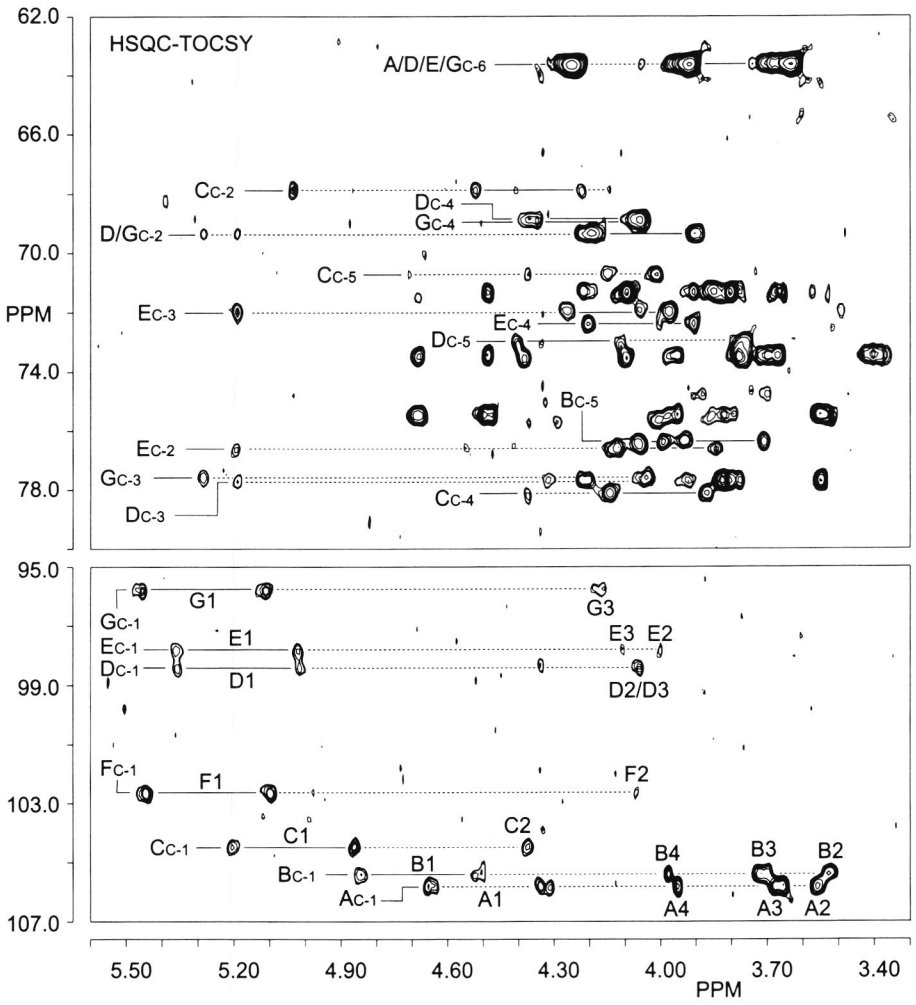

Figure 3. *500-MHz 2D ^{13}C-^{1}H undecoupled HSQC-TOCSY spectrum (mixing time 80 ms) of Sts EPS, recorded in D_2O at 67 °C. The code AC-1 denotes the chemical shift of C-1 of residue* **A**, *etc. Cross-peaks between carbons and protons belonging to the same scalar-coupling network are indicated near a dotted line.*

Rha residues **C** (δ 1.347) and **F** (δ 1.312), the complete series of cross-peaks with H-1,2,3,4,5 are observed. The H-2,3,4 atoms of residue **G** were identified on the basis of cross-peaks on the TOCSY **G** H-1 track (δ 5.278). Assignment of the H-6 proton resonances of

Table 3. *^1H NMR chemical shifts[a] of Sts EPS, recorded in D_2O at 80 °C. Coupling constants (Hz) are included in parentheses.*

Residue	H-1	H-2	H-3	H-4	H-5	H-6a	H-6b	CH_3
A	4.480 (7.8)	3.551 (9.8)	3.660 (3.4)	3.95	3.68	3.81	3.78	-
B	4.671 (7.8)	3.523 (9.3)	3.70	3.98	3.82	4.05	3.93	-
C	5.032	4.36	4.14	4.00	3.86	-	-	1.347 (5.9)
D	5.180	4.05	4.05	4.22	4.25	3.80 - 3.74		-
E	5.185	3.99	4.11	4.05	4.23	3.80 - 3.74		-
F	5.261	4.07	3.89	3.491 (9.3)	3.71	-	-	1.312 (5.9)
G	5.278 (3.9)	4.04	4.15	4.20	n.d.[b]	3.80 - 3.74		-

[a] In ppm relative to the signal of internal acetone at δ 2.225.
[b] n.d., not determined.

residue **G** was deduced from the HSQC-TOCSY spectrum, whereas the **G** H-5 signal could not be detected.

The 2D ^{13}C-^1H HSQC spectrum of Sts EPS (Figure 4) allowed the assignment of the ^{13}C resonances (Table 4). The one bond coupling constants of the anomeric carbon atoms of residues **A** and **B** ($^1J_{C\text{-}1,H\text{-}1}$162 Hz) prove that their anomeric configurations are β, and those of residues **C**, **D**, **E** and **G** ($^1J_{C\text{-}1,H\text{-}1}$ 170–171 Hz) are α [18]. The one bond coupling constant for residue **F** ($^1J_{C\text{-}1,H\text{-}1}$ 174 Hz) is indicative of an α configuration. The relatively high coupling constant of this residue is most likely caused by the 2-substitution.

Table 4. *^{13}C NMR chemical shifts[a] of Sts EPS, as determined from 2D ^{13}C-^1H HSQC experiments, recorded in D_2O at 67 °C. $^1J_{C\text{-}1,H\text{-}1}$ Values (Hz) are included in parentheses.*

Residue	C-1	C-2	C-3	C-4	C-5	C-6
A	105.8 (162)	73.5	75.5	71.4	77.7	63.7
B	105.4 (162)	73.5	75.5	71.5	76.1	71.3
C	104.5 (171)	68.0	75.8	78.2	70.8	19.8
D	98.4 (171)	69.6	77.7	68.9	73.0	63.7
E	97.8 (170)	76.7	72.0	72.4	73.5	63.7
F	102.6 (174)	81.4	72.7	74.9	71.9	19.3
G	95.8 (171)	69.6	77.6	68.9	n.d.[b]	63.7

[a] In ppm relative to the α-anomeric signal of external [1-^{13}C]glucose at δ 92.9.
[b] n.d., not determined.

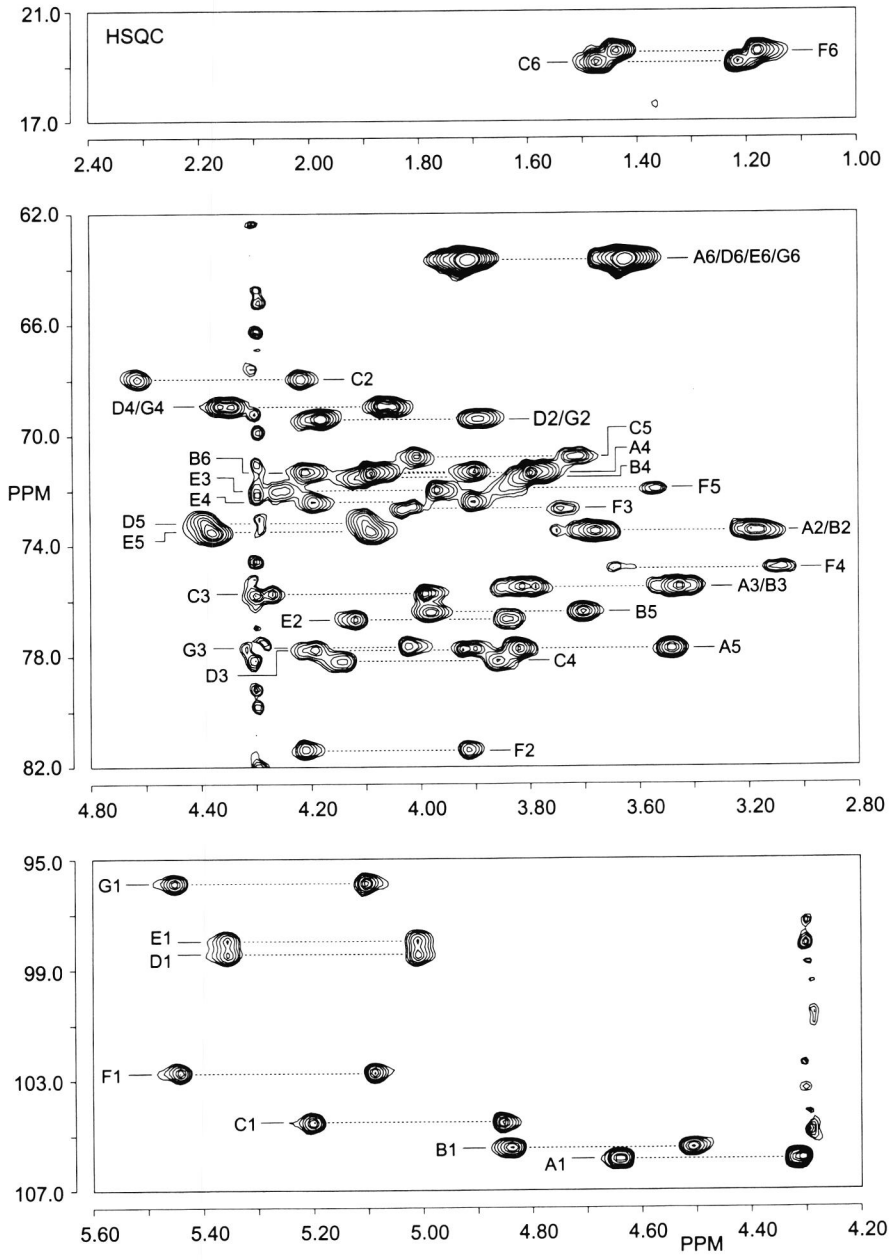

Figure 4. *500-MHz 2D ^{13}C-^{1}H undecoupled HSQC spectrum of Sts EPS, recorded in D_2O at 67 °C. A1 stands for the set of cross-peaks between H-1 and C-1 of residue* **A**, *etc.*

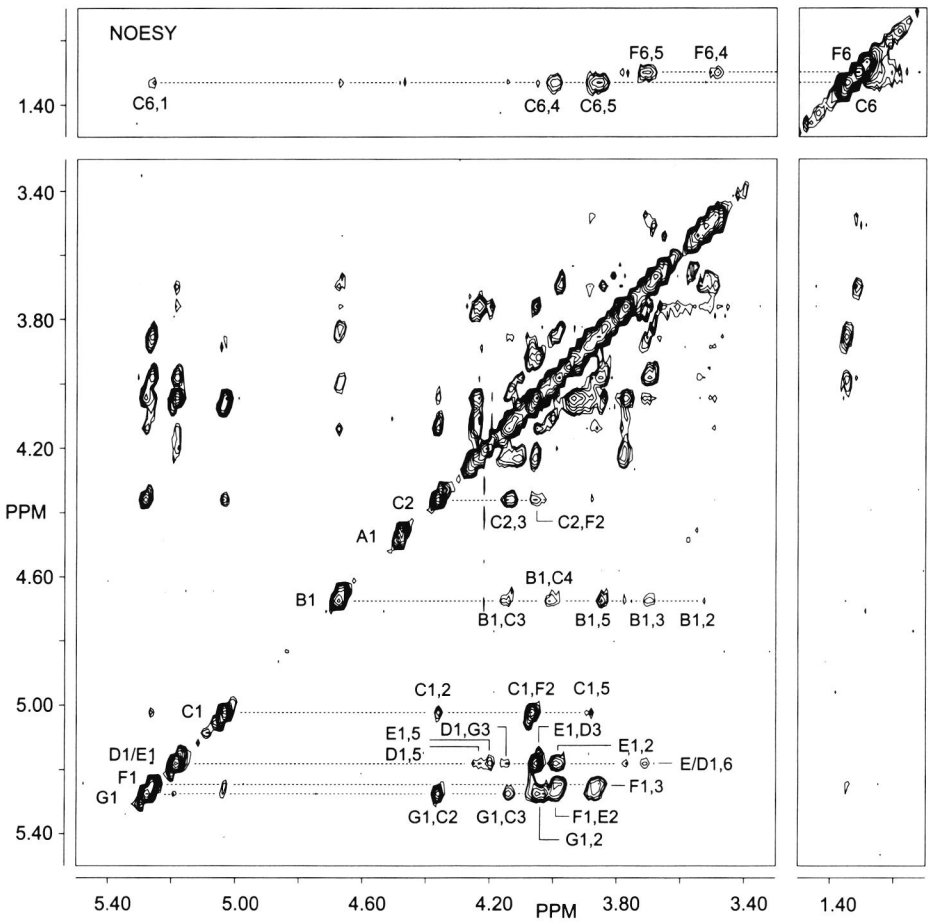

Figure 5. *500-MHz 2D NOESY spectrum (mixing time 150 ms) of Sts EPS, recorded in D_2O at 80 °C. G1 corresponds to the diagonal peak belonging to residue* **G** *H-1; G1,2 refers to an intraresidual cross-peak between* **G** *H-1 and* **G** *H-2, and G1,C2 means an interresidual connectivity between* **G** *H-1 and* **C** *H-2, etc.*

In agreement with published chemical shift data of methyl aldosides [19], and methylation analysis, residue **A** was identified as the terminal β-Gal*p* residue, whereas the downfield chemical shift of **B** C-6 (δ 71.3) demonstrated residue **B** to represent the 6-substituted β-Gal*p* residue. The downfield chemical shifts for C-3 of residues **D** and **G** indicate that these α-Gal*p* units are 3-substituted, whereas the downfield chemical shifts of **E** C-2 (δ 76.7) and **F** C-2 (δ

81.4) show that both residues are 2-substituted. The remaining **C** residue could be assigned as the 3,4-disubstituted α-Rha*p* unit, since **C** C-3 (δ 75.8) and **C** C-4 (δ 78.2) are downfield shifted.

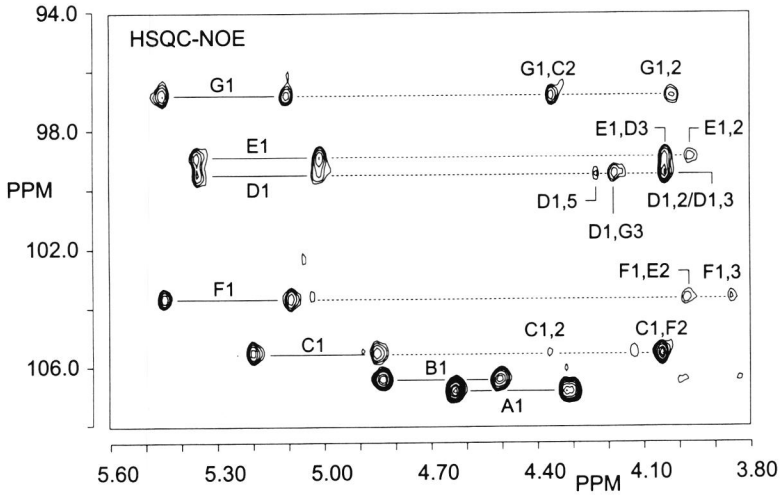

Figure 6. *500-MHz 2D ^{13}C-^{1}H undecoupled HSQC-NOE spectrum (mixing time 80 ms) of the anomeric region of Sts EPS, recorded in D_2O at 67 °C. G1 denotes for the set of cross-peaks between C-1 and H-1 of residue* **G**, *G1,2 refers to an intraresidual cross-peak between* **G** *C-1 and* **G** *H-2, and G1,C2 means an interresidual connectivity between* **G** *C-1 and* **C** *H-2, etc.*

By means of NOESY and HSQC-NOE experiments (Figures 5 and 6) the sequence of the monosaccharide residues in the EPS was established. On the NOESY **C** H-1 track a cross-peak with **F** H-2 was observed, suggesting a **C**(1→2)**F** sequence, whereas a well-resolved interresidual connectivity **F** H-1,**E** H-2 in the HSQC-NOE spectrum demonstrates a **F**(1→2)**E** linkage. Likewise, the NOE between **E** H-1 and **D** H-2,3, observed in the HSQC-NOE spectrum, indicates a **E**(1→3)**D** linkage, since residue **D** has proven to be a 3-substituted galactose. The NOE between **D** H-1 and **G** H-3 in the HSQC-NOE spectrum reveals a **D**(1→3)**G** linkage. Furthermore, a strong NOE between **G** H-1 and **C** H-2 and a weak NOE between **G** H-1 and **C** H-3 were observed. The NOE cross-peaks indicate a **G**(1→3)**C** linkage, since methylation analysis in combination with carbon chemical shifts demonstrate that residue **C** is 3,4-disubstituted. The NOE cross-peak between **G** H-1 and **C** H-2 does not

reflect the glycosidic linkage. The observation of such non-glycosidic NOE cross-peaks have been reported for several (1→3)-linked disaccharide methyl glycosides [20]. On the NOESY **B** H-1 track a NOE cross-peak with **C** H-3 was observed, suggesting a **B**(1→3)**C** sequence. The **A**(1→6)**B** linkage could not be confirmed by NOESY and HSQC-NOE analysis.

The intraresidual connectivities in the NOESY spectra of Sts EPS confirm the anomeric configurations of the various monosaccharide residues in the polysaccharide. Intraresidual connectivities between H-1 and H-5 of residue **C** and of H-1 and H-6 of residues **C**, **D** and **E** are brought about by spin diffusion.

The combined results, from chemical and NMR studies, have proven the EPSs of both *S. thermophilus* Rs and *S. thermophilus* Sts to be composed of a heptasaccharide repeating unit with the following structure:

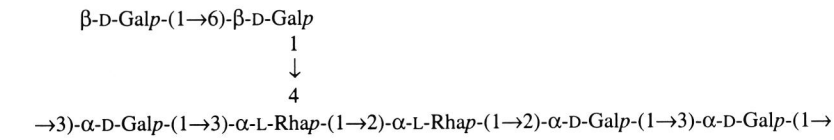

This structure is identical to the EPS produced by *S. thermophilus* OR 901 [14]. Since *S. thermophilus* Rs and Sts are distinct strains with different viscosifying properties but the same repeating unit it is presumed that OR 901 is a third strain with an identical repeating unit but other viscosifying properties.

Physical properties of the milk cultures

Permeability and viscosity data from milk cultures of *S. thermophilus* Rs and Sts are shown in Table 1. The stirred milk culture of *S. thermophilus* Rs looked thin and lumpy, whereas that of *S. thermophilus* Sts looked very thick. The Posthumus viscosity (Table 1) of the stirred yogurt increased with increasing ropiness of the milk cultures, which is in agreement with earlier findings [17]. The permeability coefficient B of the milk cultures is fairly equal, which suggests that the strains have a similar effect on the protein-EPS network in the milk cultures. Finally, the rate of protein digestion in the Rs and Sts milk cultures was evaluated by SDS-PAGE, showing a high similarity between both protein profiles.

Concluding remarks

Polysaccharides produced by *S. thermophilus* Rs and Sts have the same branched heptasaccharide repeating unit. Permeability measurements of non-stirred milk cultures suggest that the cultures have a similar effect on the protein-EPS network. Consequently, the only detected difference which might explain the differences in ropiness of the milk cultures lies in the molecular mass of the polysaccharides.

1.3. Experimental

Organisms. — *S. thermophilus* Rs and Sts were obtained from the Netherlands Institute of Dairy Research (NIZO food research, Ede, The Netherlands).

Physical properties of milk cultures. — Milk and milk cultures were made as described [17]. *S. thermophilus* Rs or Sts were inoculated in such a concentration that the pH of the milk reached a value of 4.3 after 16 h at 32 °C. Permeability measurements, calculations of the permeability coefficient B and viscosity measurements were performed as described [17].

Exopolysaccharide concentration. — Trichloroacetic acid was added to milk cultures (final concentration 12% w/w). After stirring for 1 h, cells and precipitated proteins were removed by centrifugation (20 min, 16,300 *g*, 4 °C). Supernatants were collected, extensively dialyzed against running tap water and subsequently lyophilized. Samples were re-dissolved in water and analyzed by HP-GPC with RI detection. Dextran was used as a standard to determine the EPS concentrations.

Culture conditions of microorganisms and isolation of exopolysaccharides. — Cultures were grown for 16 h at 32 °C in pasteurized reconstituted skim milk [17] containing 0.2% (w/w) casitone. After the addition of trichloroacetic acid to a final concentration of 4% (w/w), cultures were stirred for 1 h. Cells and precipitated proteins were removed by centrifugation (2 × 30 min, 16,300 *g*, 4 °C), and EPSs from the supernatants were precipitated with two vols of cold EtOH. Aqueous solutions of the precipitated materials were extensively dialyzed against running tap water and after removal of insoluble material by centrifugation again two vols of EtOH were added. The precipitates formed were re-dissolved in water, and purified further by precipitation at 40% (v/v) acetone.

Molecular mass determination. — The average molecular masses of the polysaccharides were determined, using a modified method combining gel permeation chromatography, static light scattering, and differential refraction analysis, as described [21].

High performance gel permeation chromatography, gas-liquid chromatography, and mass spectrometry. — HP-GPC analyses were achieved on a TSK G6000 PW column (300 × 7.5 mm, Progel) using a RI detector (Erna ERC-7510). Elution was performed with 0.1 M $NaNO_3$ at a flow rate of 0.6 mL/min. GLC measurements were performed on a Chrompack CP9002 gas chromatograph, equipped with a CP-Sil 5CB fused silica capillary column (25 m × 0.32 mm, Chrompack), using a temperature program of 120-240 °C at 4 °C/min, or with a CP-Sil 43CB fused silica capillary column (25 m × 0.32 mm, Chrompack) using a temperature program of 140-200 °C at 3 °C/min. GLC-MS analyses were carried out on a MD800/8060 system (Fisons instruments; electron energy, 70 eV), using a DB-1 fused silica capillary column (30 m × 0.32 mm, J&W Scientific) with a temperature program of 140-240 °C at 4 °C/min.

Monosaccharide analysis. — For monosaccharide analysis two procedures were followed: (I) Polysaccharides were hydrolyzed with 2 M CF_3COOH (2 h, 120 °C). After reduction of the monosaccharide mixtures with $NaBD_4$ in 0.5 M NH_4OH (1 h, room temperature), solutions were neutralized with HOAc and boric acid was removed by co-evaporation with MeOH. Alditol acetates, obtained by acetylation with acetic anhydride (3 h, 120 °C) were analyzed by GLC on CP-Sil 43CB. (II) Dry polysaccharides were subjected to methanolysis, followed by trimethylsilylation of the methyl glycoside mixtures and GLC analysis on CP-Sil 5CB as described [7,22,23]. Absolute configurations of monosaccharides were determined according to [24,25].

Methylation analysis. — Polysaccharides were permethylated as described [26]. After hydrolysis with 2 M CF_3COOH (2 h, 120 °C), the partially methylated monosaccharide mixtures were reduced and acetylated as in procedure I of the monosaccharide analysis. The obtained partially methylated alditol acetates were identified by GLC on CP-Sil 43CB and by GLC-MS on DB-1 [22,27].

NMR spectroscopy. — Prior to NMR-spectroscopic analysis, samples were exchanged twice in 99.9 atom% D_2O (Isotec) with intermediate lyophilization and finally dissolved in 99.96 atom% D_2O (Isotec). 1D ^1H and 2D NMR spectra were recorded on a Bruker AMX-500

spectrometer (Bijvoet Center, Department of NMR Spectroscopy) at a probe temperature of 80 °C for ^{1}H NMR experiments and 67 °C for heteronuclear NMR experiments. The HOD signal was suppressed either by applying a WEFT pulse sequence [28] in 1D ^{1}H NMR experiments, or by presaturation for 0.8-1 s in 2D experiments. Chemical shifts are expressed in ppm by reference to internal acetone (δ 2.225) for ^{1}H or to the α-anomeric signal of external [1-^{13}C]glucose ($\delta_{C\text{-}1}$ 92.9) for ^{13}C. Spectra were recorded with a spectral width of 4032 Hz and 16350 Hz for proton and carbon, respectively. Resolution enhancement of the spectra was performed by a Lorentzian-to-Gaussian transformation and when necessary, a fourth order polynomial baseline correction was performed.

The 2D DQF-COSY spectra were recorded according to ref. [29]. The 2D TOCSY spectra were recorded using a 'clean' MLEV-17 mixing sequence with an effective spin-lock time of 15-250 ms. The 2D NOESY experiments were performed with a mixing time of 150 ms. The natural abundance ^{13}C-^{1}H 2D HSQC experiment, the 2D gradient-enhanced ^{13}C-^{1}H HSQC-TOCSY experiment [30] with a mixing time of 80 ms, and the 2D gradient-enhanced ^{13}C-^{1}H HSQC-NOE experiment consisting of a gradient-enhanced ^{13}C-^{1}H HSQC building block continued by a ^{1}H NOE step of 80 ms, were recorded without decoupling during acquisition of the ^{1}H FID.

All NMR data were processed using TRITON (Bijvoet Center, Department of NMR Spectroscopy) or Bruker UXNMR software.

Acknowledgements

This study was supported by the PBTS Research Program with financial aid from the Ministry of Economic Affairs and by the Integral Structure Plan for the Northern Netherlands from the Dutch Development Company. The authors thank F. Kingma (NIZO food research, Ede, The Netherlands) for cultivation of the *S. thermophilus* strains and for HP-GPC analysis, and R. Tuinier (NIZO food research, Ede, The Netherlands) for molecular mass analyses.

References

[1] P.A. Sandford, J. Baird, in G.O. Aspinall (Ed.), *The Polysaccharides*, Vol. 2, Academic Press, New York, 1983, pp. 411-490.

[2] H. Nakajima, T. Hirota, T. Toba, T. Itoh, S. Adachi, *Carbohydr. Res.*, 224 (1992) 245-253.

[3] M. Gruter, B.R. Leeflang, J. Kuiper, J.P. Kamerling, J.F.G. Vliegenthart, *Carbohydr. Res.*, 231 (1992) 273-291.

[4] M. Gruter, B.R. Leeflang, J. Kuiper, J.P. Kamerling, J.F.G. Vliegenthart, *Carbohydr. Res.*, 239 (1993) 209-226.

[5] Y. Yamamoto, S. Murosaki, R. Yamauchi, K. Kato, Y. Sone, *Carbohydr. Res.*, 261 (1994) 67-78.

[6] Y. Yamamoto, T. Nunome, R. Yamauchi, K. Kato, Y. Sone, *Carbohydr. Res.*, 275 (1995) 319-332.

[7] G.W. Robijn, J.R. Thomas, H. Haas, D.J.C. van den Berg, J.P. Kamerling, J.F.G. Vliegenthart, *Carbohydr. Res.*, 276 (1995) 137-154.

[8] M. Staaf, G. Widmalm, Z. Yang, E. Huttunen, *Carbohydr. Res.*, 291 (1996) 155-164.

[9] F. Stingele, J. Lemoine, J.-R. Neeser, *Carbohydr. Res.*, 302 (1997) 197-202.

[10] G.W. Robijn, R. Gutiérrez Gallego, D.J.C. van den Berg, H. Haas, J.P. Kamerling, J.F.G. Vliegenthart, *Carbohydr. Res.*, 288 (1996) 203-218.

[11] G.W. Robijn, H.L.J. Wienk, D.J.C. van den Berg, H. Haas, J.P. Kamerling, J.F.G. Vliegenthart, *Carbohydr. Res.*, 285 (1996) 129-139.

[12] G.W. Robijn, D.J.C. van den Berg, H. Haas, J.P. Kamerling, J.F.G. Vliegenthart, *Carbohydr. Res.*, 276 (1995) 117-136.

[13] T. Doco, J.-M. Wieruszeski, B. Fournet, D. Carcano, P. Ramos, A. Loones, *Carbohydr. Res.*, 198 (1990) 313-321.

[14] W.A. Bubb, T. Urashima, R. Fujiwara, T. Shinnai, H. Ariga, *Carbohydr. Res.*, 301 (1997) 41-50.

[15] J. Lemoine, F. Chirat, J.-M. Wieruszeski, G. Strecker, N. Favre, J.-R. Neeser, *Appl. Environ. Microbiol.*, 63 (1997) 3512-3518.

[16] J. Cerning, C. Bouillanne, M.J. Desmazeaud, M. Landon, *Biotechnol. Lett.*, 10 (1988) 255-260.

[17] M.E. van Marle, P. Zoon, *Neth. Milk Dairy J.*, 49 (1995) 47-65.

[18] K. Bock, C. Pedersen, *J. Chem. Soc., Perkin Trans. 2*, (1974) 293-297.

[19] P.A.J. Gorin, M. Mazurek, *Can. J. Chem.*, 53 (1975) 1212-1223.

[20] G.M. Lipkind, A.S. Shashkov, S.S. Mamyan, N.K. Kochetkov, *Carbohydr. Res.*, 181 (1988) 1-12.

[21] B. Tinland, J. Mazet, M. Rinaudo, *Makromol. Chem.*, 9 (1988) 69-73.

[22] M.F. Chaplin, *Anal. Biochem.*, 123 (1982) 336-341.

[23] J.P. Kamerling, J.F.G. Vliegenthart, in A.M. Lawson (Ed.), *Clinical Biochemistry - Principles, Methods, Applications. Vol. 1, Mass Spectrometry*, Walter de Gruyter, Berlin, 1989, pp. 176-263.

[24] G.J. Gerwig, J.P. Kamerling, J.F.G. Vliegenthart, *Carbohydr. Res.*, 62 (1978) 349-357.

[25] G.J. Gerwig, J.P. Kamerling, J.F.G. Vliegenthart, *Carbohydr. Res.*, 77 (1979) 1-7.

[26] I. Ciucanu, F. Kerek, *Carbohydr. Res.*, 131 (1984) 209-217.

[27] P.-E. Jansson, L. Kenne, H. Liedgren, B. Lindberg, J. Lönngren, *Chem. Commun. Univ. Stockholm*, 8 (1976) 1-74.

[28] K. Hård, G. van Zadelhoff, P. Moonen, J.P. Kamerling, J.F.G. Vliegenthart, *Eur. J. Biochem.*, 209 (1992) 895-915.

[29] A.E. Derome, M.P. Williamson, *J. Magn. Reson.*, 88 (1990) 177-185.

[30] T. de Beer, C.W.E.M. van Zuylen, K. Hård, R. Boelens, R. Kaptein, J.P. Kamerling, J.F.G. Vliegenthart, *FEBS Lett.*, 348 (1994) 1-6.

Chapter 2

Structure of the exopolysaccharide produced by *Streptococcus thermophilus* S3

Elisabeth J. Faber, Mischa J. van den Haak, Johannis P. Kamerling, and Johannes F.G. Vliegenthart

Bijvoet Center, Department of Bio-Organic Chemistry, Utrecht University, PO Box 80.075, NL-3508 TB Utrecht, The Netherlands.

Abstract

The exopolysaccharide of *Streptococcus thermophilus* S3, produced in skimmed milk, is composed of D-galactose and L-rhamnose in a molar ratio of 2:1. The polysaccharide contains 0.4 equivalents of *O*-acetyl groups per repeating unit. Linkage analysis and 1D/2D NMR (^{1}H and ^{13}C) studies on native and de-*O*-acetylated EPS together with nanoES-CID tandem mass spectrometry studies on oligosaccharides generated by a periodate oxidation protocol, show the polysaccharide to have the following structure:

β-D-Gal*f* 2Ac$_{0.4}$
1
↓
6
→3)-β-D-Gal*p*-(1→3)-α-D-Gal*p*-(1→3)-α-L-Rha*p*-(1→2)-α-L-Rha*p*-(1→2)-α-D-Gal*p*-(1→

Elisabeth J. Faber, Mischa J. van den Haak, Johannis P. Kamerling, and Johannes F.G. Vliegenthart, *Carbohydr. Res.*, submitted.

2.1. Introduction

In the food industry, microbial exopolysaccharides (EPSs) are widely applied as thickening, gelling and stabilizing agents [1]. Lactic acid bacteria, which carry the GRAS (Generally Recognized as Safe) status, are excellent sources of such food grade exopolysaccharides. For example, when applied in food fermentation, the *in situ* production of exopolysaccharides will contribute to the texture of the product.

In order to initiate studies that may provide a better insight into the relationship between the structure of polysaccharides from lactic acid bacteria and the consistency of fermented products, detailed structural investigations have been performed on exopolysaccharides produced by different bacterial strains including *Lactobacillus acidophilus* [2], *Lb. delbrueckii* subsp. *bulgaricus* rr [3], *Lb. helveticus* [4-8], *Lb. paracasei* [9], *Lb. reuteri* [10], *Lb. rhamnosus* [11], *Lb. sake* [12], *Lactococcus lactis* subsp. *cremoris* [13,14], and *Streptococcus thermophilus* [15-18].

S. thermophilus strains in combination with *Lb. delbrueckii* subsp. *bulgaricus* strains are used as commercial yogurt starters. The structure of their exopolysaccharides, as well as the rheological properties of their subsequent yogurt gels, are studied in order to unravel the mechanisms by which the cultures and their exopolysaccharides influence the consistency of the yogurt [18].

Here, we report the structural determination of the exopolysaccharide produced by the highly ropy *S. thermophilus* S3 strain in skimmed milk.

2.2. Results and discussion

Isolation, purification, and composition of the exopolysaccharide

The exopolysaccharide produced by *S. thermophilus* S3 in pasteurized reconstituted skimmed milk was isolated, and purified via ethanol precipitation followed by acetone precipitation. The purity of the polysaccharide was confirmed by ^{1}H NMR spectroscopy (*vide infra*). From the *S. thermophilus* S3 culture 36 mg/L of polysaccharide with an average molecular mass of 5.9×10^{3} kDa was isolated.

Monosaccharide analysis of the native polysaccharide (n-EPS), including the determination of absolute configurations, revealed the presence of D-Gal and L-Rha in a molar ratio of 2:1. Methylation analysis of n-EPS (Table 1) demonstrated the presence of 2- and 3-substituted Rha*p*, 2-, 3-, and 3,6-substituted Gal*p* and terminal Gal*f* in equal molar

amounts, indicating a branched hexasaccharide repeating unit. To determine the position of the acid-labile terminal Gal*f* residue, methylation analysis was performed on partially hydrolyzed EPS (0.3 M trifluoroacetic acid, 20 min, 100 °C). A 70% conversion of 3,6-substituted Gal*p* into 3-substituted Gal*p*, together with a decrease in the amount of terminal Gal*f* (Table 1), demonstrated that in the native polysaccharide the terminal Gal*f* residue is attached to O-6 of the 3,6-substituted Gal*p* residue. The terminal Gal*p* derivative observed in the methylation analysis of the hydrolyzed sample originates from hydrolytically released Gal*f*.

Table 1. *Methylation analysis data of* S. thermophilus *S3 native EPS (n-EPS), de-*O*-acetylated EPS (dAc-EPS), and n-EPS after mild acid hydrolysis (hyd-EPS).*

Derivative	Molar amounts [a]		
	n-EPS	dAc-EPS	hyd-EPS
2,3,5,6-Gal [b]	0.9	0.9	0.4
2,3,4,6-Gal	-	-	0.7
3,4,6-Gal	1.0	1.0	1.0
2,4,6-Gal	1.0	1.0	1.7
2,4-Gal	1.0	1.0	0.3
3,4-Rha	1.0	1.0	1.0
2,4-Rha	1.0	1.1	0.9

[a] 3,4,6-Gal is taken as 1.0.
[b] 2,3,5,6-Gal = 1,4-di-*O*-acetyl-2,3,5,6-tetra-*O*-methyl-galactitol-*1-d*, *etc.*

Treatment of n-EPS with 5% (w/v) NH_4OH at room temperature resulted in complete de-*O*-acetylation of the polysaccharide (dAc-EPS), as determined by ^{1}H NMR spectroscopy (*vide infra*). Monosaccharide and methylation analysis (Table 1) indicated no additional changes of the de-*O*-acetylated polysaccharide.

The 1D ^{1}H NMR spectrum of n-EPS (Figure 1A) shows a complex signal pattern in terms of peak intensities in the anomeric region (δ 5.4 – 4.5) due to partial *O*-acetylation (*O*-acetyl, δ 2.148). After de-*O*-acetylation of the polysaccharide (dAc-EPS) the pattern changes into five anomeric signals (Figure 1B), of which the signal at δ ~5.16 represents two anomeric protons, indicating a hexasaccharide repeating unit. A distinction between the anomeric signal of residue **D** (δ 5.16) and residue **E** (δ 5.17) could be made in the TOCSY spectra (*vide infra*). Furthermore, high-field signals (δ ~1.3) are present, arising from the methyl groups of

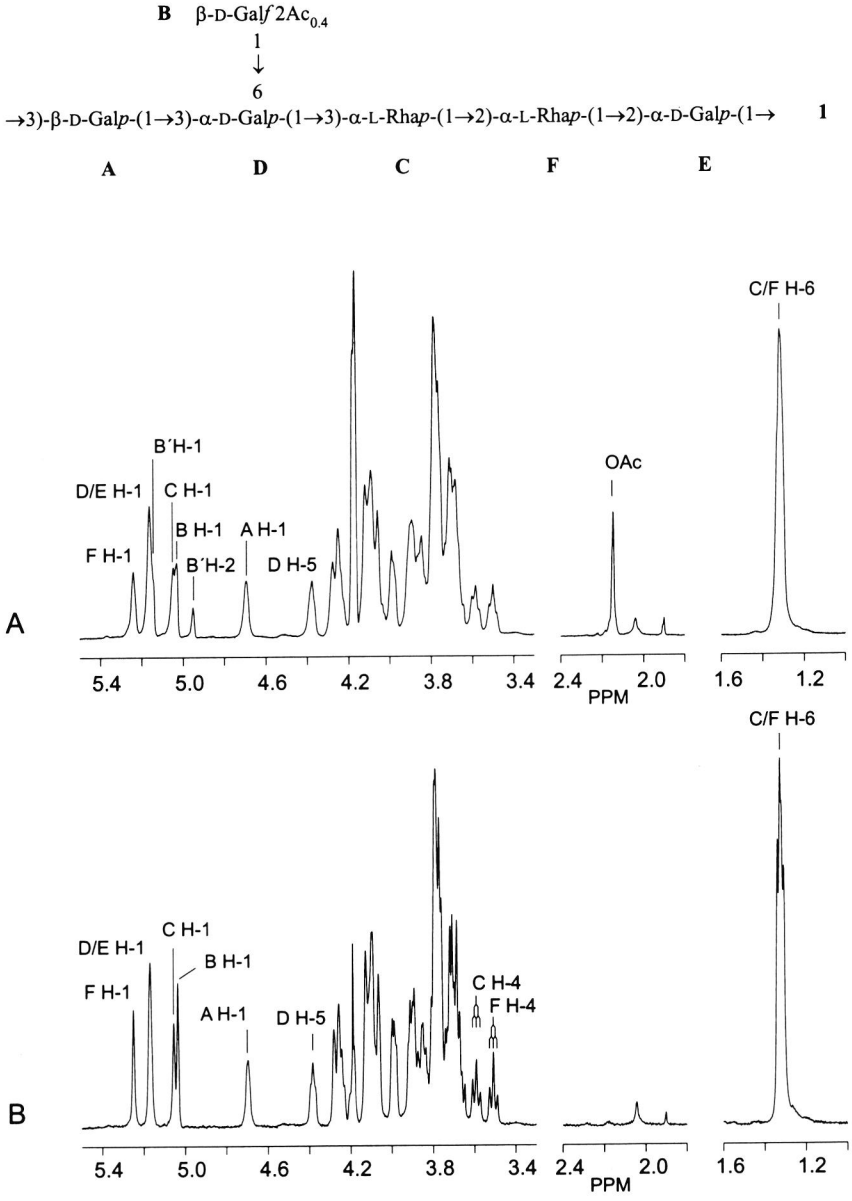

Figure 1. *500-MHz ^1H NMR spectra of n-EPS* ***1*** *(A), and dAc-EPS* ***2*** *(B) produced by* S. thermophilus *S3, recorded in D_2O at 80 °C.*

Rha*p* residues. The partial *O*-acetylation in n-EPS is reflected in the 1D ^{1}H NMR spectrum of n-EPS by an additional signal in the anomeric region at δ 4.958 for the proton at the *O*-acetylated carbon and a broadening of the anomeric signal at δ ~5.16 originating from a contribution of H-1 of the *O*-acetylated residue. Based on integration of the anomeric signals in the spectrum the extent of *O*-acetylation was determined to be 0.4 equivalents. However, it must be kept in mind that the procedure used for the isolation of the polysaccharide may have resulted in partial de-*O*-acetylation. The resolution of the dAc-EPS spectrum (Figure 1B) is higher than the resolution of the n-EPS spectrum (Figure 1A).

For the assignment of the acetylated hexasaccharide repeating unit the constituting residues are labeled **A-F** according to the increasing chemical shift values of the anomeric protons.

By making use of the 1D ^{1}H NMR spectrum, the 2D ^{13}C-^{1}H HSQC spectrum of dAc-EPS (*vide infra*) allowed the assignment of the chemical shifts of the corresponding anomeric carbon signals. The spectrum contains six anomeric signals at δ 96.0 (residue **E**, $^{1}J_{C\text{-}1,H\text{-}1}$ 176 Hz), δ 97.0 (residue **D**, $^{1}J_{C\text{-}1,H\text{-}1}$ 171 Hz), δ 100.9 (residue **F**, $^{1}J_{C\text{-}1,H\text{-}1}$ 177 Hz), δ 102.4 (residue **C**, $^{1}J_{C\text{-}1,H\text{-}1}$ 174 Hz), δ 104.8 (residue **A**, $^{1}J_{C\text{-}1,H\text{-}1}$ 163 Hz), and δ 108.1 (residue **B**, $^{1}J_{C\text{-}1,H\text{-}1}$ 177 Hz), respectively, confirming the proposed hexasaccharide repeating unit. Based on the observed $^{1}J_{C\text{-}1,H\text{-}1}$ values it could be deduced that residue **A** has β anomeric configuration, whereas residues **C**, **D**, **E** and **F** have α anomeric configurations. The relatively large $^{1}J_{C\text{-}1,H\text{-}1}$ values of residues **E** and **F** have been reported before for 2-substituted monosaccharides [18]. Since residue **B** is a Gal*f* residue (*vide infra*) $^{1}J_{C\text{-}1,H\text{-}1}$ will give no information about the anomeric configuration of the residue.

Periodate oxidation

The methylated material, obtained after periodate oxidation of n-EPS and subsequent reduction ($NaBH_4$), methylation (CH_3I), mild acid hydrolysis, reduction ($NaBD_4$), and methylation (CD_3I), was dissolved in a water/methanol mixture and analyzed by nanoES-CID tandem mass spectrometry. In the high-mass region of the ES mass spectrum an $[M+Na]^+$ ion at *m/z* 837 was detected, corresponding to a per-*O*-methylated alditol ($Hex_2Pen_1Deoxyhex_1$)-*1-d* containing three deuterated methyl groups. The tandem mass spectrum obtained on collision activation of *m/z* 837 (Figure 2) contains sodium-cationized $\mathbf{Y_n}$ fragments at *m/z* 252, 616, and 663 and sodium-cationized $\mathbf{C_n}$ fragments at *m/z* 215, 262 and 626. The $\mathbf{Y_1}$ ion at *m/z* 252 suggests the presence of a deoxyhexitol-*1-d* containing two deuterated methyl groups at the reducing end of the oligosaccharide. The signals at *m/z* 616 and 663, corresponding to the $\mathbf{Y_{2\alpha}}$

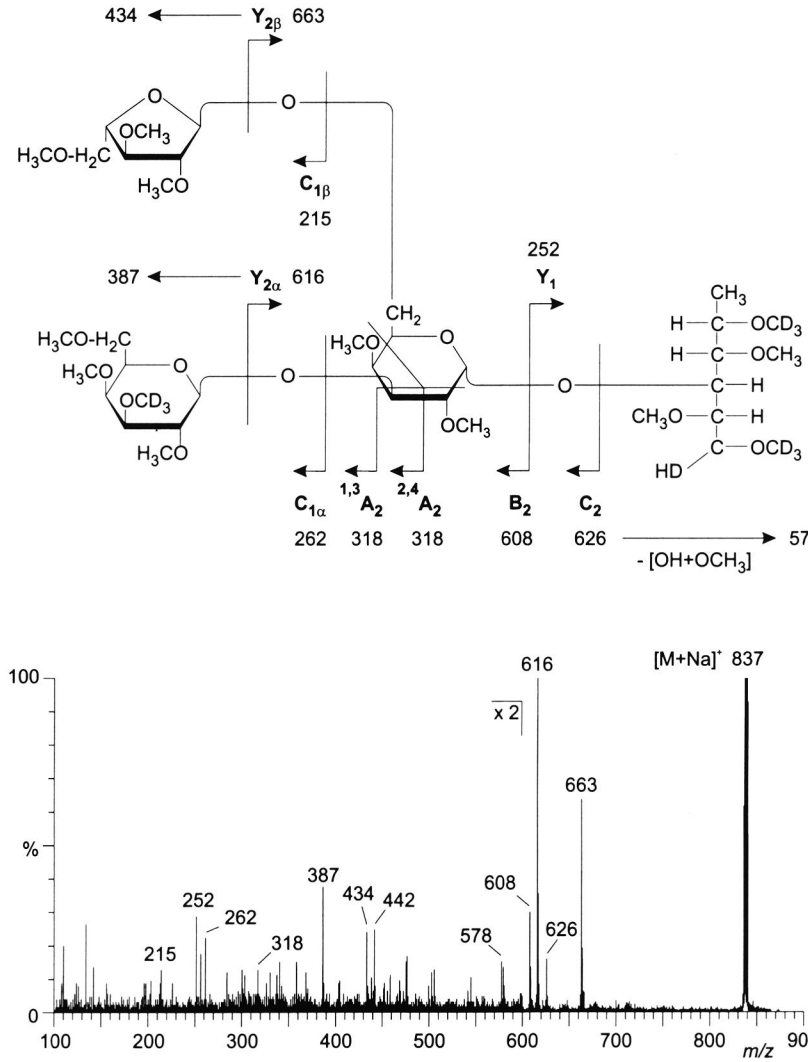

Figure 2. *Positive ion mode nanoES-CID tandem mass spectrum of sodiated ions of the tetrasaccharide product obtained by a periodate oxidation protocol.*

and $\mathbf{Y_{2\beta}}$ ions, respectively, are indicative of a disubstituted hexose linked to the deoxyhexitol-*1-d*, and thus reflect a branched structure. The $\mathbf{C_{1\alpha}}$ ion at *m/z* 262 corresponds to a terminal hexose containing one deuterated methyl group and the $\mathbf{C_{1\beta}}$ ion at *m/z* 215 corresponds to a

terminal pentose. In view of the monosaccharide and methylation analysis data (*vide supra*) the pentose has to originate from the Gal*f* residue since selective degradation of the side chain of Gal*f* by periodate oxidation followed by reduction results in the formation of Ara*f* [19]. Secondary fragment ions are observed at *m/z* 387, 434, and 442. The ion at *m/z* 387 results from the loss of (deutero)methylated deoxyhexitol-*1-d* from the $\mathbf{Y}_{2\alpha}$ ion (*m/z* 616 – 229), while the ion at *m/z* 434 results from the loss of (deutero)methylated deoxyhexitol-*1-d* from the $\mathbf{Y}_{2\beta}$ ion (*m/z* 663 – 229). The ion at *m/z* 442 is the result of the loss of terminal methylated pentose and terminal (deutero)methylated hexose from the pseudo-molecular ion (*m/z* 837 – 174 – 221). Furthermore, the ion at *m/z* 578 results from the loss of a hydroxy group at C-1 and an *O*-methyl group at C-2 forming a double bond between C-1 and C-2 at the reducing end of the $\mathbf{C}_2$ ion ($\mathbf{C}_2$ – [OH+OCH_3]) [20].

In addition to ions resulting from the cleavage of glycosidic linkages ($\mathbf{C}_n$ and $\mathbf{Y}_n$), $^{1,3}\mathbf{A}_2$ and $^{2,4}\mathbf{A}_2$ ions resulting from cross-ring cleavage, are observed at *m/z* 318. The number of ions obtained from cross-linkage cleavages in this spectrum is insufficient to assign linkage types. However, combining methylation analysis data (*vide supra*) and the knowledge that periodate oxidation causes cleavage of 1,2-diol groups in 2-linked residues, provides prove for the selective removal of the 2-linked residues, leaving three 3-linked residues and a 6-linked terminal Gal*f*.

The results obtained from the ES-MS/MS spectrum together with those from the monosaccharide and methylation analyses performed on n-EPS, allowed the partial structure to be formulated as:

D-Gal*f*
1
↓
6
→3)-D-Gal*p*-(1→3)-D-Gal*p*-(1→3)-L-Rha*p*-(1→

In view of the final structure (*vide infra*) one would expect the isolated tetrasaccharide to contain an additional glycerol group at the reducing end. The absence of this group is due to the hydrolysis of the labile rhamnosyl glyceraldehyde linkage in the reduced and per-*O*-methylated periodate-oxidized material.

In addition to the $[M+Na]^+$ ion at *m/z* 837 originating from the tetrasaccharide-alditol as illustrated above, the ES mass spectrum revealed amongst others also $[M+Na]^+$ ions at *m/z* 503, 506, 677, and 680. The tandem mass spectrum obtained from the $[M+Na]^+$ ion at *m/z* 677

contains sodium-cationized $\mathbf{Y_n}$ fragments at *m/z* 252 and 456 and sodium-cationized $\mathbf{C_n}$ fragments at *m/z* 262 and 466, indicating a per-*O*-methylated alditol ($Hex_2Deoxyhex_1$)-*1-d* containing three deuterated methyl groups. Furthermore, the tandem mass spectrum obtained from the $[M+Na]^+$ ion at *m/z* 680 reveals sodium-cationized $\mathbf{Y_n}$ fragments at *m/z* 252 and 459 and sodium-cationized $\mathbf{C_n}$ fragments at *m/z* 262 and 469, indicating a per-*O*-methylated alditol ($Hex_2Deoxyhex_1$)-*1-d* containing four deuterated methyl groups. Taking into account the tetrameric product generated by the periodate oxidation protocol (*vide supra*), the compound with a sodium-cationized ion at *m/z* 677 may result from the cleavage of the Sug*f*-(1→6)-Gal*p* (Sug = Gal or periodate-oxidized Gal) glycosidic linkage during periodate oxidation (pH ~4.0) and the subsequent addition of a methyl group at O-6 of the Gal*p* residue, whereas the compound having a $[M+Na]^+$ ion at *m/z* 680 may be formed by cleavage of the Ara*f* residue during the mild acid hydrolysis step and the subsequent addition of a deuterated methyl group.

The tandem mass spectrum obtained from the $[M+Na]^+$ ion at *m/z* 503 showed a sodium-cationized fragment $\mathbf{B_1}$ at *m/z* 244, $\mathbf{C_1}$ at *m/z* 262, and $\mathbf{Y_1}$ at *m/z* 282, corresponding to a per-*O*-methylated alditol (Hex_2)-*1-d* containing three deuterated methyl groups. Furthermore, the tandem mass spectrum obtained from the $[M+Na]^+$ ion at *m/z* 506 showed a sodium-cationized $\mathbf{B_1}$ fragment at *m/z* 244, a sodium-cationized $\mathbf{C_1}$ fragment at *m/z* 262, and an $\mathbf{Y_1}$ ion at *m/z* 285 indicating a per-*O*-methylated alditol (Hex_2)-*1-d* containing four deuterated methyl groups. The disaccharide fragments with $[M+Na]^+$ ions at *m/z* 503 and *m/z* 506 originate from the tetrameric product with additional cleavage of the 6-linked residue during the periodate oxidation or during the succeeding mild acid hydrolysis step, respectively, and with cleavage of the Rha residue at the reducing end during the mild acid hydrolysis step.

2D NMR spectroscopy

Assignments of the ^1H chemical shifts of n-EPS and dAc-EPS (Table 2) were performed by means of 2D TOCSY (mixing times 20, 75, and 150 ms) and 2D NOESY experiments. The TOCSY spectrum of dAc-EPS, with a mixing time of 150 ms, is illustrated in Figure 3A. Starting points for the interpretation of the spectra were the H-1 signals of residues **A**–**F** and the methyl signals of residues **C** and **F**. Comparison of TOCSY spectra with increasing mixing times allowed the assignment of the sequential order of the chemical shifts belonging to a single spin system.

In the TOCSY spectra, the **A** H-2,3,4 resonances could be assigned on the TOCSY **A** H-1 track (δ 4.696). The observation of an intraresidual connectivity **A** H-1,H-3 in the NOESY spectrum (*vide infra*) at 3.78 ppm confirmed the overlap of the **A** H-2 and **A** H-3 resonances.

Table 2. *^{1}H NMR [a] and ^{13}C NMR [b] chemical shifts of S3 native EPS (n-EPS) and de-O-acetylated EPS (dAc-EPS), recorded in D_2O at 80 °C for ^{1}H and at 67 °C for ^{13}C. $^{1}J_{C-1,H-1}$ values (Hz) are included in parentheses.*

Residue	Proton	1	2	Carbon	1	2
A	H-1	4.699	4.696	C-1	104.8 (164)	104.8 (163)
	H-2	3.79	3.77	C-2	70.2	70.3
	H-3	3.79	3.78	C-3	78.3	78.5
	H-4	4.13	4.11	C-4	66.1	66.1
	H-5	3.69	3.68	C-5	75.3	75.4
	H-6a	3.7-3.8 [c]	3.7-3.8 [c]	C-6	61.4	61.4
	H-6b	3.7-3.8 [c]	3.7-3.8 [c]			
B	H-1	5.04	5.031	C-1	108.1 (177)	108.1 (177)
	H-2	4.09	4.09	C-2	78.4	78.5
	H-3	4.06	4.06	C-3	77.5	77.5
	H-4	3.99	3.98	C-4	84.0	84.0
	H-5	3.84	3.84	C-5	71.5	71.6
	H-6a	3.73	3.71	C-6	63.3	63.4
	H-6b	3.66	3.66			
B´	H-1	5.151	-	C-1	105.5 (179)	-
	H-2	4.958	-	C-2	84.0	-
	H-3	4.22	-	C-3	75.9	-
	H-4	4.05	-	C-4	84.2	-
	H-5	3.86	-	C-5	71.0	-
	H-6a	3.74	-	C-6	63.0	-
	H-6b	3.67	-			
	O-Acetyl	2.148	-	*O*-Acetyl	20.5	-
C	H-1	5.05	5.051	C-1	102.3 (174)	102.4 (174)
	H-2	4.26	4.26	C-2	67.7	67.7
	H-3	3.86	3.85	C-3	77.3	77.2
	H-4	3.590	3.590	C-4	71.2	71.2
	H-5	3.78	3.77	C-5	69.7	69.6
	H-6	1.31	1.31	C-6	17.0	17.1
D	H-1	5.16	5.161	C-1	97.0 (172)	97.0 (171)
	H-2	4.09	4.09	C-2	67.9	68.0
	H-3	4.11	4.11	C-3	79.5	79.6
	H-4	4.28	4.28	C-4	69.6	69.7
	H-5	4.381	4.382	C-5	69.7	69.8
	H-6a	3.90	3.90	C-6	66.9	67.0
	H-6b	3.71	3.70			

Table 2. *Continued.*

E	H-1	5.17	5.17	C-1	96.0 (176)	96.0 (176)
	H-2	3.99	3.98	C-2	74.5	74.6
	H-3	4.10	4.11	C-3	69.8	69.8
	H-4	4.06	4.06	C-4	70.2	70.3
	H-5	4.24	4.24	C-5	71.5	71.6
	H-6a	3.76	3.76	C-6	61.4	61.4
	H-6b	3.76	3.76			
F	H-1	5.245	5.246	C-1	100.9 (177)	100.9 (177)
	H-2	4.10	4.09	C-2	81.6	81.7
	H-3	3.90	3.89	C-3	n.d.	70.8
	H-4	3.506	3.507	C-4	n.d.	72.9
	H-5	3.72	3.73	C-5	n.d.	69.8
	H-6a	1.33	1.323	C-6	17.0	17.1

[a] In ppm relative to the signal of internal acetone at δ 2.225.
[b] In ppm relative to the α-anomeric signal of external [1-^{13}C]glucose at δ 92.9.
[c] Assigned from ^{13}C-^{1}H HSQC spectra.

The intraresidual **A** H-1,H-5 contact in the NOESY spectrum allowed the assignment of **A** H-5. The resonances of **A** H-6a,6b were assigned via their correlation to the corresponding ^{13}C resonance in the ^{13}C-^{1}H HSQC spectrum (*vide infra*). The TOCSY **B** H-1 track (δ 5.031) contains the complete series of cross-peaks with **B** H-2,3,4,5,6a,6b. On the TOCSY **D** H-1 track (δ 5.16), cross-peaks with **D** H-2,3,4 were observed and the **D** H-5,6a,6b resonances were assigned through cross-peaks on the TOCSY **D** H-5 track (δ 4.382). All resonances of residue **E** (H-2,3,4,5,6a,6b) could be assigned on the TOCSY **E** H-1 track (δ 5.17). Beside it, the **E** (H-5,6a,6b) signals are clearly visible on the TOCSY **E** H-5 track (δ 4.24). The H-1,2,3,4,5 resonances of residues **C** and **F** could be assigned via their TOCSY C-6 track (**C** H-6 δ 1.31, **F** H-6 δ 1.33).

The assigned ^{1}H chemical shifts, in combination with the monosaccharide and methylation analysis data demonstrated **C** and **F** to be the Rha*p* residues; their H-6 signals are characteristic for 6-deoxy-hexose. Furthermore, the characteristic downfield chemical shifts of the H-4 signals of **A**, **D**, and **E** indicated these residues to represent Gal*p*, leaving residue **B** to be the Gal*f* residue.

Assignments of the ^{1}H chemical shifts of n-EPS (Table 2) were performed in essentially the same way as described for dAc-EPS. In addition, the **B´** H-1,3,4,5,6a,6b resonances of n-EPS (Figures 1 and 3B) could be assigned from the TOCSY **B´** H-2 track (δ 4.958). The

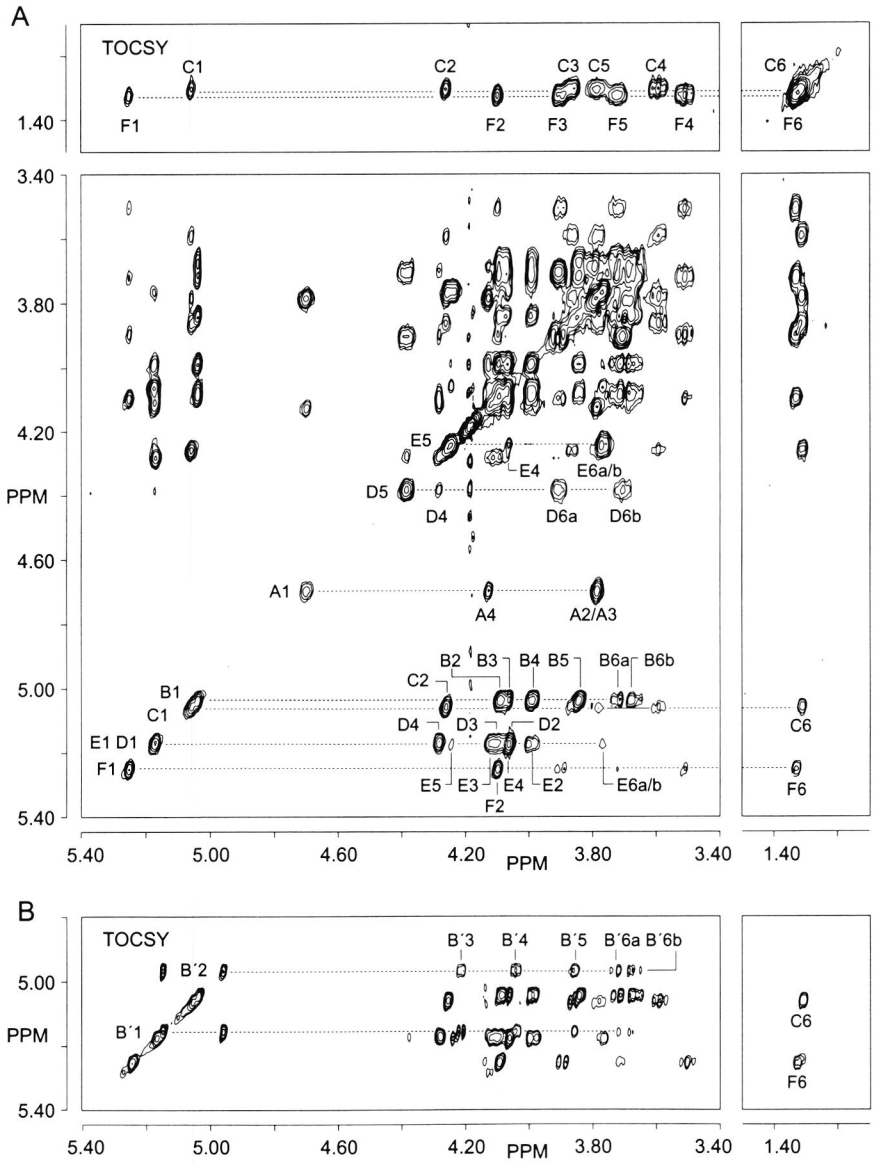

Figure 3. *500-MHz 2D TOCSY spectrum (mixing time 150 ms) of dAc-EPS (A), and n-EPS (B) recorded in D_2O at 80 °C. Diagonal peaks of the anomeric protons, of H-2 of residues **B´**, and of H-5 of residue **D** and **E** are indicated. Cross-peaks belonging to the same scalar-coupling network are indicated near a dotted line starting from the corresponding diagonal peak.*

differences in chemical shifts between **B** and **B´** H-1 ($\Delta\delta$ +0.12), **B** and **B´** H-2 ($\Delta\delta$ +0.87), and **B** and **B´** H-3 ($\Delta\delta$ +0.16), and the similarity of the chemical shifts of **B** and **B´** H-4,5,6a,6b (within $\Delta\delta$ 0.06) demonstrate that n-EPS is acetylated at O-2 of residue **B**.

The 2D ^{13}C-^{1}H HSQC spectra of both dAc-EPS (Fig. 4) and n-EPS (data not shown) allowed the assignment of the ^{13}C chemical shifts and coupling constants (Table 2). It should be noted that the intense signal at δ 61.4 reflects two C-atoms, namely **E** C-6 (deduced via **E** H-6a,6b and **A** C-6. Using the position of **A** C-6, the proton signals of **A** H-6a,b, which could not be allocated in the TOCSY and NOESY spectra, were assigned. By comparing the carbon chemical shifts of the polysaccharide with literature data of methyl aldosides [21], the linkage pattern of the individual residues was determined. In case of dAc-EPS, residue **A** could be assigned as the 3-substituted β-Gal*p* unit, since **A** C-3 (δ 78.5) has shifted downfield in comparison to β-D-Gal*p*1Me ($\delta_{C\text{-}3}$ 73.8). The upfield shift of **A** C-4 (δ 66.1) in comparison to β-D-Gal*p*1Me ($\delta_{C\text{-}4}$ 69.7) has been reported before for a 3-substituted β-D-Gal*p* glycoside [22]. Comparison of the ^{13}C chemical shifts of residue **B** with chemical shifts of α-D-Gal*f*1Me ($\delta_{C\text{-}1}$ 103.8, $\delta_{C\text{-}2}$ 78.2, $\delta_{C\text{-}3}$ 76.2, $\delta_{C\text{-}4}$ 83.1, $\delta_{C\text{-}5}$ 74.5, $\delta_{C\text{-}6}$ 64.1) and β-D-Gal*f*1Me ($\delta_{C\text{-}1}$ 109.9, $\delta_{C\text{-}2}$ 81.3, $\delta_{C\text{-}3}$ 78.4, $\delta_{C\text{-}4}$ 84.7, $\delta_{C\text{-}5}$ 71.7, $\delta_{C\text{-}6}$ 63.6) [21] showed this residue to be terminal β-Gal*f*. The downfield chemical shift of **E** C-2 (δ 74.6) demonstrated residue **E** to represent the 2-substituted α-Gal*p* residue (α-D-Gal*p*1Me, $\delta_{C\text{-}2}$ 69.2). The downfield chemical shifts for C-3 (δ 77.2) of residue **C** and C-2 (δ 81.7) of residue **F** indicate that these α-Rha*p* units are 3- and 2-substituted, respectively (α-L-Rha*p*1Me, $\delta_{C\text{-}2}$ 71.0, $\delta_{C\text{-}3}$ 71.3). Finally, residue **D** could be assigned as the 3,6-substituted α-Gal*p* unit, since the **D** C-3 and **D** C-6 signals ($\delta_{C\text{-}3}$ 79.6, $\delta_{C\text{-}6}$ 67.0) are shifted downfield in comparison to their methyl aldosides (α-D-Gal*p*1Me, $C_{C\text{-}3}$ δ 70.5, $C_{C\text{-}6}$ δ 62.2).

The sequence of the monosaccharides in the polysaccharide repeating unit was determined by means of a NOESY experiment (Figure 5). On the NOESY **C** H-1 track of dAc-EPS an interresidual connectivity with **F** H-2 was in accordance with the **C**(1→2)**F** sequence. A well-resolved NOE between **F** H-1 and **E** H-2 was observed, revealing a **F**(1→2)**E** linkage. The NOE between **F** H-1 and **C** H-5 reflects the closeness in space of these protons in the **C**(1→2)**F**(1→2)**E** sequence. The interresidual connectivity between **E** H-1 and **A** H-2,3 indicated an **E**(1→3)**A** linkage since carbon chemical shifts revealed residue **A** to be substituted at O-3. The NOE between **A** H-1 and **D** H-3 demonstrated an **A**(1→3)**D** linkage. Furthermore, an NOE between **D** H-1 and **C** H-2 was observed. This NOE represents a **D**(1→3)**C** linkage, since methylation analysis in combination with carbon chemical shifts demonstrated residue **C** to be 3-substituted. The observation of such non-glycosidic NOE cross-peaks has been reported previously for the α-D-Gal*p*-(1→3)-α-L-Rha*p* linkage in the

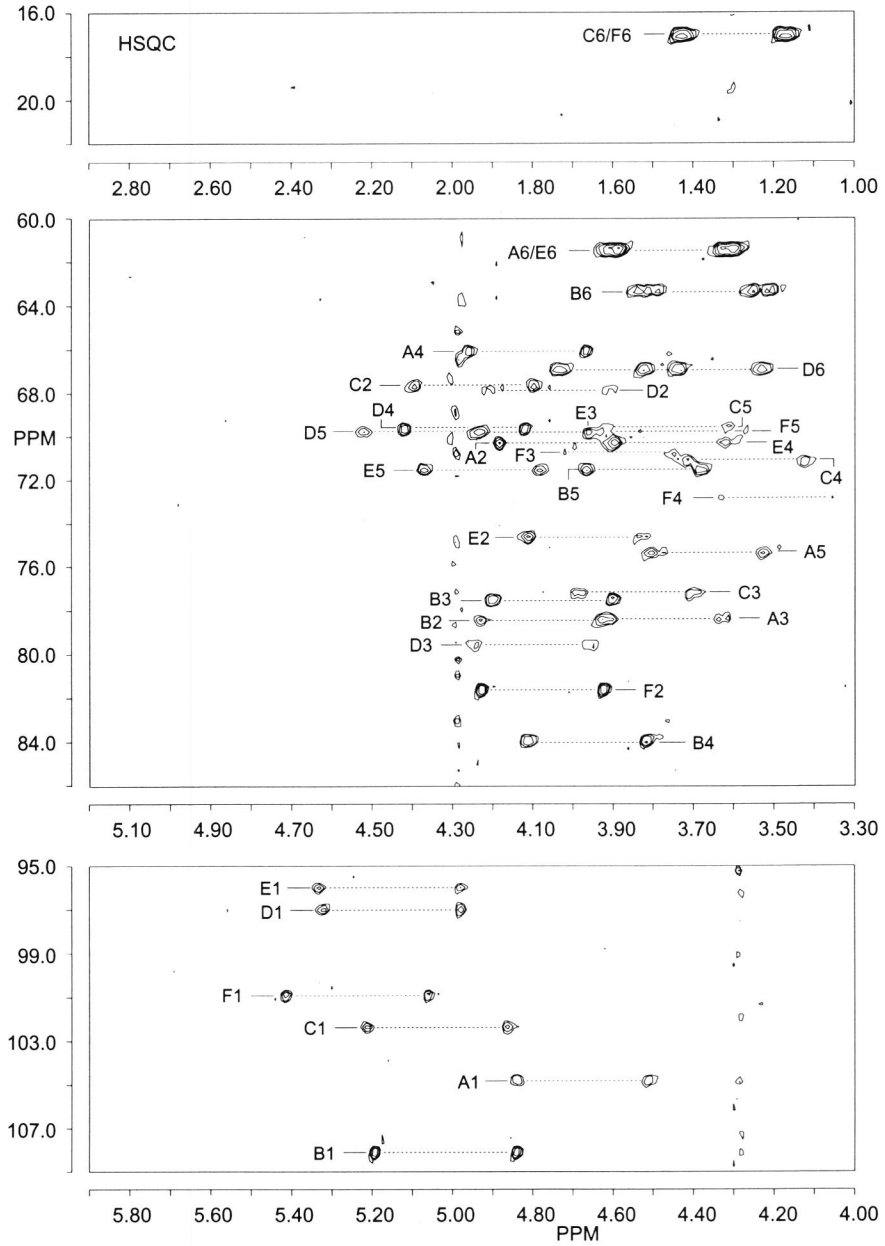

Figure 4. *500-MHz 2D ^{13}C–^{1}H undecoupled HSQC spectrum of dAc-EPS, recorded in D_2O at 67 °C. A1 stands for the set of cross-peaks between H-1 and C-1 of residue **A**, etc.*

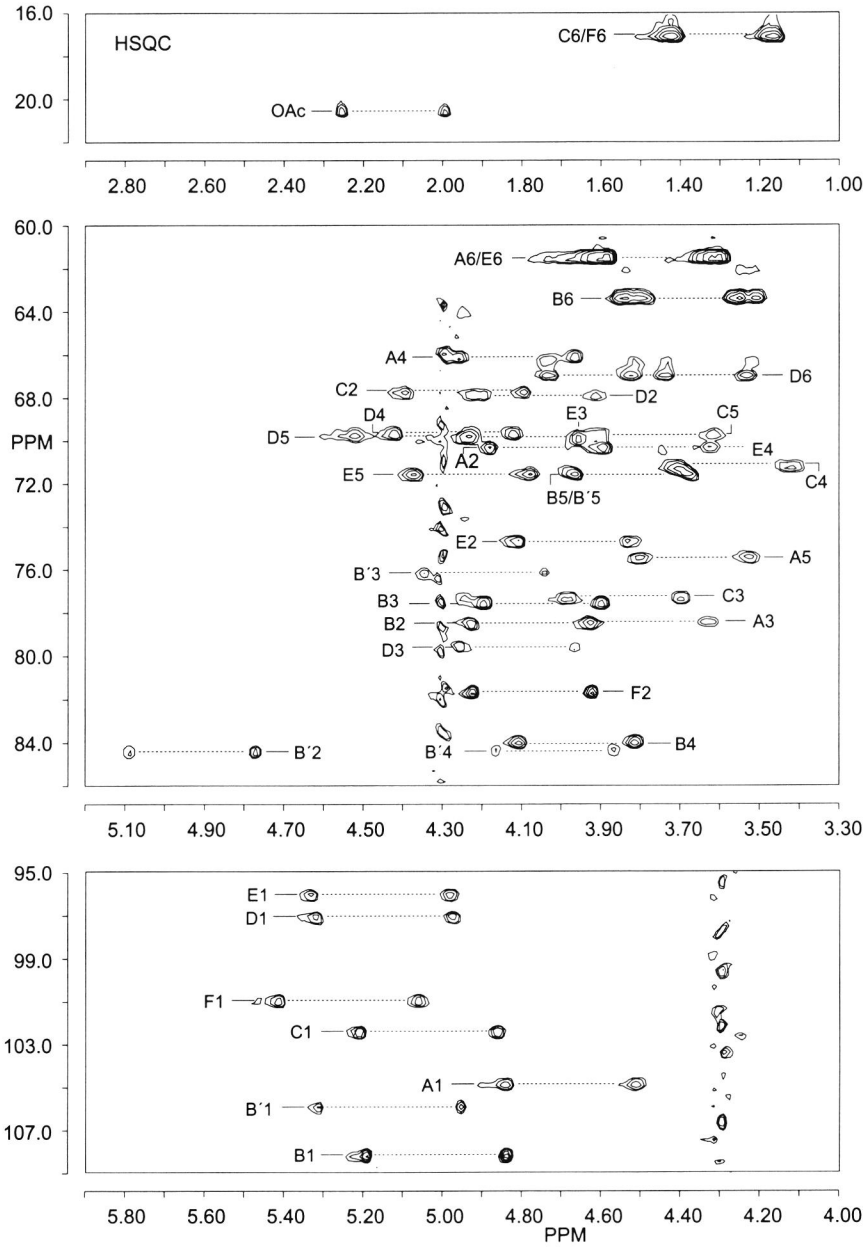

Figure 5. *500-MHz 2D ^{13}C–^{1}H undecoupled HSQC spectrum of n-EPS, recorded in D_2O at 67 °C. A1 stands for the set of cross-peaks between H-1 and C-1 of residue A, etc.*

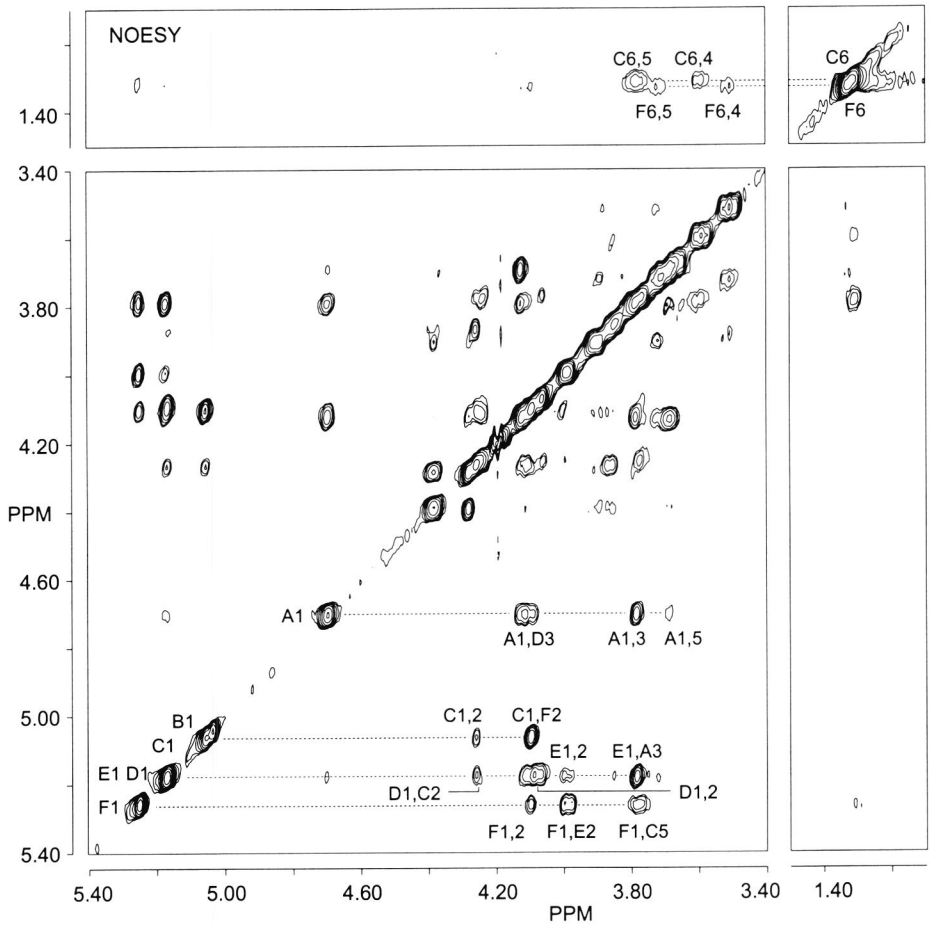

Figure 6. *500-MHz 2D NOESY spectrum (mixing time 200 ms) of dAc-EPS, recorded in D_2O at 80 °C. F1 corresponds to the diagonal peak belonging to residue* **F** *H-1; F1,2 refers to an intraresidual cross-peak between* **F** *H-1 and* **F** *H-2, and F1,E2 means an interresidual connectivity between* **F** *H-1 and* **E** *H-2, etc.*

EPS of *S. thermophilus* Rs and Sts [18]. The **B**(1→6)**D** linkage determined by partial acid hydrolysis and methylation analysis, could not be confirmed by the NOESY experiment.

The intraresidual connectivities in the NOESY spectrum confirm the anomeric configurations of the various monosaccharide residues in the polysaccharide.

By combining the various analytical data described above the structure of the repeating unit of the EPS produced by *S. thermophilus* S3 can be illustrated as:

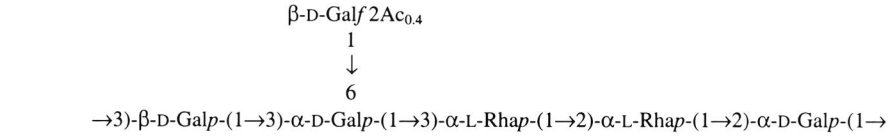

Concluding remarks

In this paper the complete elucidation of the structure of the EPS isolated from *S. thermophilus* S3 grown in skimmed milk is described. Several EPSs produced by strains of *S. thermophilus* have been isolated from yogurt, or related media, and their structures studied [15-18]. A number of the EPSs are structurally related polysaccharides and include the EPSs produced by *S. thermophilus* Sfi12 [17], OR 901 [16], Rs [18], Sts [18] and S3, of which the OR 901, Rs and Sts EPSs have identical repeating units. The EPSs are characterized by the presence of a pentameric backbone containing a →3)-α-D-Gal*p*-(1→3)-α-L-Rha*p*-(1→2)-α-L-Rha*p*-(1→2)-α-D-Gal*p*-(1→3)-Hex*p*-(1→ sequence, wherein the fifth residue differs by the presence of α-D-Glc*p* for Sfi12, α-D-Gal*p* for OR 901, Rs and Sts, and β-D-Gal*p* for the EPS produced by S3. Furthermore, the EPSs differ in the attachment site of the side chain, as well as in the composition of the side chain.

Although the EPSs produced by several *S. thermophilus* strains share structural features, strains producing EPS with only minor differences in the primary structure of the repeating unit (e.g. single monosaccharide replacement, molecular size) are excellent probes to obtain insight into the relationship between physical properties, such as ropiness, and the structure of the EPS. In this regard, research performed towards biosynthetic engineering techniques as well as genetic engineering techniques to tailor EPSs produced by lactic acid bacteria may assist in creating structural diversity in polysaccharides allowing the establishment of the structure-function relationship of EPS produced by lactic acid bacteria.

2.3. Experimental

Organism and culture conditions. — *S. thermophilus* S3 is a highly ropy strain obtained from NIZO food research (Ede, The Netherlands). The cultivation of *S. thermophilus* S3 was performed in pasteurized reconstituted skimmed milk as described [18].

Exopolysaccharide concentration. — The concentration of exopolysaccharide was determined by HP-GPC with RI-detection as previously described [18].

Isolation and purification of the exopolysaccharide. — To the milk culture, trichloroacetic acid was added to a final concentration of 4% (w/w). After stirring for 1 h, cells and precipitated proteins were removed by centrifugation (2 × 30 min at 16,300 *g*, 4 °C). EPS was precipitated from the supernatant by addition of two volumes of EtOH (4 °C). An aqueous solution of the precipitated material was extensively dialyzed against running tap water and after removal of insoluble material by centrifugation two volumes of EtOH were added. The precipitate formed was redissolved in water, and purified by a precipitation with 50% (v/v) acetone.

Molecular mass determination. — The average molecular mass of n-EPS was determined by using a combination of gel permeation chromatography, static light scattering, and differential refraction analysis, as described [23].

Gas-liquid chromatography and mass spectrometry. — GLC analyses were performed on a Chrompack CP9002 gas chromatograph equipped with a CP-Sil 5CB fused silica capillary column (25 m × 0.32 mm, Chrompack) or a CP-Sil 43CB fused silica capillary column (25 m × 0.25 mm, Chrompack). GLC–MS analyses were carried out on a MD800/8060 system (Fisons instruments; electron energy, 70 eV), using a CP-Sil 5CB fused silica capillary column (25 m × 0.25 mm, Chrompack). Both GLC and GLC–MS analyses were performed under conditions described previously [18]. Positive-ion mode nanoES-CID tandem mass spectra were obtained on a Micromass Q-TOF hybrid tandem mass spectrometer equipped with a nanospray ion source (Bijvoet Center, Department of Biomolecular Mass Spectrometry) essentially according to ref. [24]. Argon was used as collision gas with a collision energy of approximately 50 eV. Fragment ions were labeled according to the nomenclature of Domon and Costello [25].

Monosaccharide and methylation analysis. — For monosaccharide analysis, dry polysaccharide was subjected to methanolysis, followed by trimethylsilylation and GLC analysis as described [26,27]. The absolute configuration of the monosaccharides was determined according to [28,29]. For methylation analysis, polysaccharides were permethylated using CH_3I and solid NaOH in Me_2SO as described previously [30]. Subsequently, the methylated saccharides were hydrolyzed with 2 M CF_3COOH (2 h, 120 °C) and reduced with $NaBD_4$. After neutralization and removal of boric acid by coevaporation with MeOH, the mixtures of partially methylated alditols were acetylated with Ac_2O (3 h, 120 °C), and analyzed by GLC and GLC–MS [26,31].

Periodate oxidation. — To a solution of polysaccharide (30 mg) in 0.1 M NaOAC buffer (30 mL, pH 3.9), $NaIO_4$ was added to a final concentration of 50 mM, and the mixture was kept in the dark for 5 days at 4 °C. Excess of periodate was destroyed by the addition of ethylene glycol (2 mL) after which the solution was dialyzed against tap water. The oxidized polysaccharide was reduced with $NaBH_4$ (4 h, 20 °C), and permethylated as described above. The obtained permethylated material was subsequently hydrolyzed (0.5 M CF_3COOH, 75 min, 100 °C), reduced with $NaBD_4$ (4 h, 20 °C), and permethylated using CD_3I.

De-O-acetylation of the polysaccharide. — Native polysaccharide (30 mg) was de-*O*-acetylated by treatment with aq. 5% NH_4OH (30 mL) for 8 h at room temperature. The de-*O*-acetylated polysaccharide was recovered by lyophilization.

NMR spectroscopy. — Prior to NMR spectroscopic analysis, samples were exchanged twice in 99.9 atom% D_2O (Isotec) with intermediate lyophilization, and finally dissolved in 99.96 atom% D_2O (Isotec). The pH of the samples was adjusted to 7.0 using NaOD. 1D and 2D NMR spectra were recorded on a Bruker AMX-500 spectrometer (Bijvoet Center, Department of NMR Spectroscopy). The HOD signal was suppressed either by applying a WEFT pulse sequence [32] in 1D ^1H NMR experiments, or by presaturation for 0.8-1 s in 2D experiments. Chemical shifts are expressed in ppm by reference to internal acetone (δ 2.225) for ^1H or to the α-anomeric signal of external [1-^{13}C]glucose ($\delta_{C\text{-}1}$ 92.9) for ^{13}C. Homonuclear NMR experiments were recorded at a probe temperature of 80 °C and heteronuclear NMR experiments at a probe temperature of 67 °C, using a spectral width of 4032 Hz and 16350 Hz for ^1H and ^{13}C, respectively. Resolution enhancement of the spectra was performed by a Lorentzian-to-Gaussian transformation and when necessary, a fourth-order polynomial baseline correction was performed. 2D TOCSY spectra were recorded

using a 'clean' MLEV-17 mixing sequence with an effective spin-lock time of 20-150 ms. 2D NOESY experiments were performed with a mixing time of 200 ms, and the natural abundance ^{13}C-^{1}H 2D HSQC experiment was recorded without decoupling during acquisition of the ^{1}H FID. All NMR data were processed using TRITON (Bijvoet Center, Department of NMR Spectroscopy) or Bruker UXNMR software.

Acknowledgments

This study was supported by the PBTS Research Program with financial aid from the Ministry of Economic Affairs and by the Integral Structure Plan for the Northern Netherlands from the Dutch Development Company. The authors thank F. Kingma (NIZO food research, Ede, The Netherlands) for cultivation of *S. thermophilus* S3 and for HP-GPC analysis, R. Tuinier (NIZO food research, Ede, The Netherlands) for molecular mass analysis, and C. Versluis (Bijvoet Center, Department of Biomolecular Mass Spectrometry, Utrecht University, The Netherlands) for recording the ES-MS/MS spectra.

References

[1] I.W. Sutherland, *Trends Biotechnol.*, 16 (1998) 41-46.

[2] G.W. Robijn, R. Gutiérrez Gallego, D.J.C. van den Berg, H. Haas, J.P. Kamerling, J.F.G. Vliegenthart, *Carbohydr. Res.*, 288 (1996) 203-218.

[3] M. Gruter, B.R. Leeflang, J. Kuiper, J.P. Kamerling, J.F.G. Vliegenthart, *Carbohydr. Res.*, 239 (1993) 209-226.

[4] Y. Yamamoto, S. Murosaki, R. Yamauchi, K. Kato, Y. Sone, *Carbohydr. Res.*, 261 (1994) 67-78.

[5] Y. Yamamoto, T. Nunome, R. Yamauchi, K. Kato, Y. Sone, *Carbohydr. Res.*, 275 (1995) 319-332.

[6] G.W. Robijn, J.R. Thomas, H. Haas, D.J.C. van den Berg, J.P. Kamerling, J.F.G. Vliegenthart, *Carbohydr. Res.*, 276 (1995) 137-154.

[7] M. Staaf, G. Widmalm, Z. Yang, E. Huttunen, *Carbohydr. Res.*, 291 (1996) 155-164.

[8] F. Stingele, J. Lemoine, J.-R. Neeser, *Carbohydr. Res.*, 302 (1997) 197-202.

[9] G.W. Robijn, H.L.J. Wienk, D.J.C. van den Berg, H. Haas, J.P. Kamerling, J.F.G. Vliegenthart, *Carbohydr. Res.*, 285 (1996) 129-139.

[10] G.H. van Geel-Schutten, E.J. Faber, E. Smit, K. Bonting, M.R. Smith, B. ten Brink, J.P. Kamerling, J.F.G. Vliegenthart, L. Dijkhuizen, *Appl. Environ. Microbiol.* 65 (1999) 3008-3014.

[11] C. Vanhaverbeke, C. Bosso, P. Colin-Morel, C. Gey, L. Gamar-Nourani, K. Blondeau, J.-M. Simonet, A. Heyraud, *Carbohydr. Res.*, 314 (1998) 211-220.

[12] G.W. Robijn, D.J.C. van den Berg, H. Haas, J.P. Kamerling, J.F.G. Vliegenthart, *Carbohydr. Res.*, 276 (1995) 117-136.

[13] H. Nakajima, T. Hirota, T. Toba, T. Itoh, S. Adachi, *Carbohydr. Res.*, 224 (1992) 245-253.

[14] M. Gruter, B.R. Leeflang, J. Kuiper, J.P. Kamerling, J.F.G. Vliegenthart, *Carbohydr. Res.*, 231 (1992) 273-291.

[15] T. Doco, J.-M. Wieruszeski, B. Fournet, D. Carcano, P. Ramos, A. Loones, *Carbohydr. Res.*, 198 (1990) 313-321.

[16] W.A. Bubb, T. Urashima, R. Fujiwara, T. Shinnai, H. Ariga, *Carbohydr. Res.*, 301 (1997) 41-50.

[17] J. Lemoine, F. Chirat, J.-M. Wieruszeski, G. Strecker, N. Favre, J.-R. Neeser, *Appl. Environ. Microbiol.*, 63 (1997) 3512-3518.

[18] E.J. Faber, P. Zoon, J.P. Kamerling, J.F.G. Vliegenthart, *Carbohydr. Res.*, 310 (1998) 269-276.

[19] G.O. Aspinall, in G.O. Aspinall (Ed.), *The polysaccharides.* Vol. 1, Academic Press, New York, 1982, pp. 81-86.

[20] L.P. Brüll, V. Kovácik, J.E. Thomas-Oates, W. Heerma, J. Haverkamp, *Rapid Commun. Mass Spectrom.*, 12 (1998) 1520-1532.

[21] K. Bock, C. Pedersen, *Adv. Carbohydr. Chem. Biochem.*, 41 (1983) 27-66.

[22] O. Kol, J.-M. Wieruszeski, G. Strecker, B. Fournet, R. Zalisz, P. Smets, *Carbohydr. Res.*, 236 (1992) 339-344.

[23] B. Tinland, J. Mazet, M. Rinaudo, *Makromol. Chem.*, 9 (1988) 69-73.

[24] A.B. Samuelsen, E.H. Cohen, B.S. Paulsen, L.P. Brüll, J.E. Thomas-Oates, *Carbohydr. Res.*, 315 (1999) 312-318.

[25] B. Domon, C.E. Costello, *Glycoconjugate J.*, 5 (1988) 397-409.

[26] M.F. Chaplin, *Anal. Biochem.*, 123 (1982) 336-341.

[27] J.P. Kamerling, J.F.G. Vliegenthart, in A.M. Lawson (Ed.), *Clinical Biochemistry - Principles, Methods, Applications. Vol. 1, Mass Spectrometry*, Walter de Gruyter, Berlin, 1989, pp. 176-263.

[28] G.J. Gerwig, J.P. Kamerling, J.F.G. Vliegenthart, *Carbohydr. Res.*, 62 (1978) 349-357.

[29] G.J. Gerwig, J.P. Kamerling, J.F.G. Vliegenthart, *Carbohydr. Res.*, 77 (1979) 1-7.

[30] I. Ciucanu, F. Kerek, *Carbohydr. Res.*, 131 (1984) 209-217.

[31] P.-E. Jansson, L. Kenne, H. Liedgren, B. Lindberg, J. Lönngren, *Chem. Commun. Univ. Stockholm*, 8 (1976) 1-74.

[32] K. Hård, G. van Zadelhoff, P. Moonen, J.P. Kamerling, J.F.G. Vliegenthart, *Eur. J. Biochem.*, 209 (1992) 895-915.

Chapter 3

Structure of the extracellular polysaccharide produced by *Lactobacillus delbrueckii* subsp. *bulgaricus* 291

Elisabeth J. Faber, Johannis P. Kamerling, and Johannes F.G. Vliegenthart

Bijvoet Center, Department of Bio-Organic Chemistry, Utrecht University, PO Box 80.075, NL-3508 TB Utrecht, The Netherlands.

Abstract

The lactic acid bacteria *Lactobacillus delbrueckii* subsp. *bulgaricus* 291, when grown in skimmed milk, produced 80 mg/L exopolysaccharide with an average molecular mass of 1.4 $\times$ 10^3 kDa. Monosaccharide analysis, methylation analysis, MS, and 1D/2D NMR (^{1}H and ^{13}C) studies performed on the native polysaccharide, and on oligosaccharides obtained from a mild acid hydrolysate of the native polysaccharide, showed the polysaccharide to consist of branched pentasaccharide repeating units with the following structure:

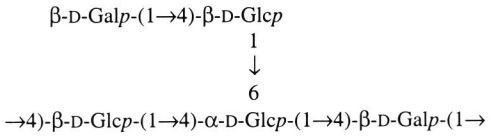

Elisabeth J. Faber, Johannis P. Kamerling, and Johannes F.G. Vliegenthart, *Carbohydr. Res.*, submitted.

3.1. Introduction

Microbial exopolysaccharides (EPSs) are employed as additives in a wide variety of food products, where they serve as viscosifying, stabilizing, emulsifying or gelling agents [1]. EPSs produced by lactic acid bacteria, which carry the GRAS (generally recognized as safe) status, are used to improve body and texture of dairy products [2]. To establish connections between EPS structure and rheological behavior, structural studies are performed on EPSs produced by various species of the *Lactobacillus*, *Lactococcus*, and *Streptococcus* genera [1,3]. More recent structural investigations have been performed on EPSs produced by *Lactobacillus reuteri* [4], *Lactococcus lactis* subsp. *cremoris* [5,6], *Streptococcus thermophilus* [7], and a *Lactobacillus* subsp. isolated from kefir grains [8].

S. thermophilus strains in combination with *Lb. delbrueckii* subsp. *bulgaricus* strains are used as commercial yoghurt starters. The EPSs produced by *Lb. delbrueckii* subsp. *bulgaricus* characterized so far are mainly composed of Glc and Gal [9,10] or of Glc, Gal and Rha [11-13]. A detailed structural study has been performed on the EPS produced by *Lb. delbrueckii* subsp. *bulgaricus* rr having a branched heptasaccharide repeating unit composed of Gal, Glc, and Rha in a molar ratio of 5:1:1 [13].

Here, we report on the structural elucidation of the EPS produced by *Lb. delbrueckii* subsp. *bulgaricus* 291 in skimmed milk, utilizing native and partially acid-hydrolyzed EPS, and applying monosaccharide analysis, methylation analysis, mass spectrometry, and NMR spectroscopy.

3.2. Results and discussion

Isolation, purification, and composition of the exopolysaccharide

The EPS produced by *Lb. delbrueckii* subsp. *bulgaricus* 291 in reconstructed skimmed milk, containing 0.35% peptone and 0.35% yeast extract, was isolated by ethanol precipitation of the protein free culture supernatant followed by gelfiltration using Sephacryl S-500. The purity of the EPS was confirmed by ^{1}H NMR spectroscopy (*vide infra*). From the *Lb. delbrueckii* subsp. *bulgaricus* 291 culture 80 mg/L of EPS with an average molecular mass of 1.4×10^3 kDa was isolated.

Quantitative monosaccharide analysis of the EPS, including the determination of absolute configurations, revealed a composition of D-Glc and D-Gal in a molar ratio of 3:2. Methylation analysis of the EPS (Table 1) demonstrated the presence of terminal Gal*p*,

4-substituted Gal*p*, 4-substituted Glc*p*, and 4,6-disubstituted Glc*p* (according to NMR experiments (*vide infra*) all residues are in the pyranose ring form) in a molar ratio of 1:1:2:1, indicating a branched pentasaccharide repeating unit.

Table 1. *Methylation analysis data of* Lb. delbrueckii *subsp.* bulgaricus *291 EPS.*

Derivative	Molar amounts [a]
2,3,4,6-Gal [b]	1.2
2,3,6-Gal	0.9
2,3,6-Glc	1.9
2,3-Glc	1.0

[a] 2,3-Glc is taken as 1.0.
[b] 2,3,4,6-Gal = 1,5-di-*O*-acetyl-2,3,4,6-tetra-*O*-methyl-D-galactitol-*1-d*, *etc*

The anomeric region (δ 4.4 – 5.0) of the 1D ^{1}H NMR spectrum (Figure 1) of EPS **1** contained three well-resolved signals and two overlapping signals corresponding with the suggested pentasaccharide repeating unit. The overlap of the anomeric doublets was confirmed by a ^{13}C-^{1}H HMQC experiment (*vide infra*). The five monosaccharide units were labeled **A-E** according to increasing chemical shift values of their anomeric protons. Based on observed $^{3}J_{1,2}$ values and chemical shifts, residues **A** ($^{3}J_{1,2}$ 7.9 Hz), **B** ($^{3}J_{1,2}$ ~8 Hz), **C** ($^{3}J_{1,2}$ ~8 Hz), and **D** ($^{3}J_{1,2}$ 7.3 Hz) were allocated the pyranose ring form and β anomeric configuration, and residue **E** ($^{3}J_{1,2}$ 3.4 Hz) was assigned the pyranose ring form and α anomeric configuration.

Partial acid hydrolysis

The complex mixture of oligosaccharides, obtained after partial acid hydrolysis of the EPS, was fractionated on Bio-Gel P-2, yielding fractions I to VI (Figure 2A). Fraction I contained the monosaccharides Glc and Gal, as demonstrated by GLC and ^{1}H NMR spectroscopy (data not shown). Fractions II to VI were subfractionated on CarboPac PA-1 (Figure 2B), and the resulting HPAEC-fractions **2-7** were reduced with $NaBD_4$ and desalted prior to analysis. A further fractionation of fractions **4-6** after reduction was performed on CarboPac PA-1, yielding subfractions **4a-6a** (Figure 2C).

Fractions 2 and 3. — The MALDI-TOF spectra of the components in fractions **2** and **3** showed $[M+Na]^{+}$ pseudomolecular ions at *m/z* 368, corresponding with HexHex-ol-*1-d*. According to monosaccharide analysis, methylation analysis, and 1D ^{1}H NMR spectroscopy,

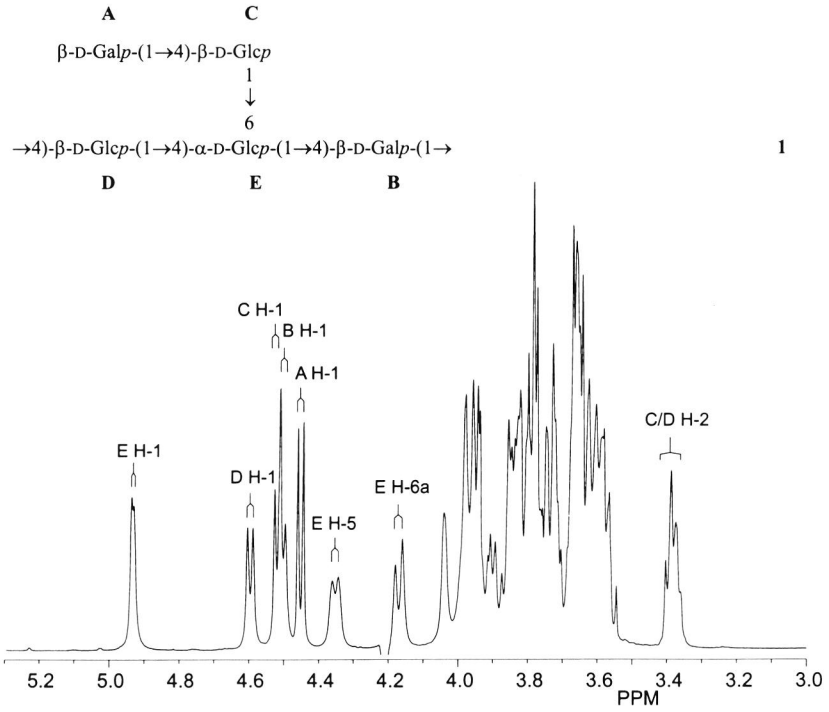

Figure 1. *500-MHz ^1H NMR spectrum of EPS **1** produced by* Lb. delbrueckii *subsp.* bulgaricus *291, recorded in D_2O at 80 °C.*

the disaccharide alditol-*1-d* in fraction **2** is lactitol and the alditols in fraction **3** are cellobiitol **3a** and gentiobiitol **3b**, respectively (Figure 3).

Fraction 4. — HPAEC of reduced fraction **4** resulted in the isolation of subfractions **4a** and **4b**. MALDI-TOF measurements of subfraction **4a** showed a $[M+Na]^+$ pseudomolecular ion at *m/z* 530, corresponding with Hex_2Hex-ol-*1-d*. Monosaccharide analysis in combination with methylation analysis of **4a** demonstrated the presence of terminal Gal*p*, 4-substituted Glc*p*, and 6-substituted Glc-ol-*1-d*, indicating a linear trisaccharide alditol. In the 1D ^1H NMR spectrum of **4a** (data not shown) anomeric signals were observed at δ 4.449 (residue **A**, $^3J_{1,2}$ 7.8 Hz), and at δ 4.529 (residue **C**, $^3J_{1,2}$ 7.8 Hz), suggesting two β-pyranose residues. Assignments of the ^1H chemical shifts and coupling constants of **4a** (Table 2) were performed by means of 2D TOCSY experiments (mixing times 25-250 ms), essentially as described for

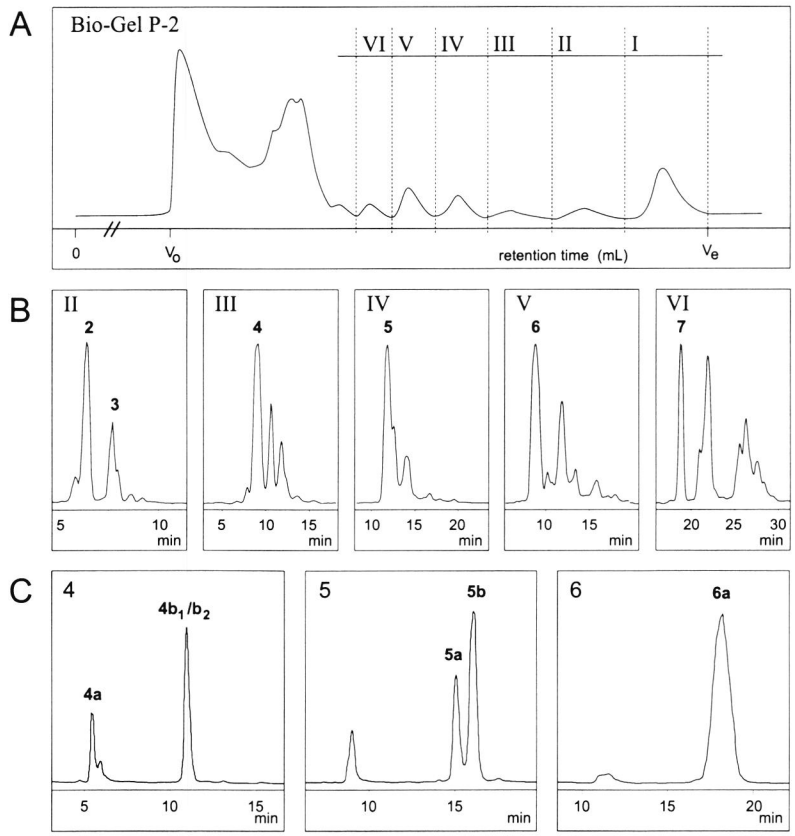

Figure 2. *(A) Bio-Gel P-2 elution profile of partially acid-hydrolyzed EPS; (B) HPAEC-PAD fractionation patterns of Bio-Gel P-2 fractions II-VI on CarboPac PA-1; (C) HPAEC-PAD fractionation patterns of fractions 4-6, after reduction with $NaBD_4$, on CarboPac PA-1.*

the ^{1}H assignment of EPS **1** (*vide infra*). In the 2D ROESY spectrum of **4a** an interresidual connectivity **C** H-1,**E**-ol H-6b was observed indicating the **C**(1→6)**E**-ol sequence. Furthermore, on the **A** H-1 ROESY track a cross-peak with a signal at δ 3.66 (**A** H-3, **C** H-3 and/or **C** H-4) was observed. Since methylation analysis of **4a** indicated the presence of a 4-substituted Glc*p*, it can be assumed that this cross-peak is partly derived from **A** H-1,**C** H-4, thereby supporting the **A**(1→4)**C** linkage. Based on the joint analytical data, the structure of the trisaccharide alditol **4a** can be formulated as illustrated in Figure 3.

β-D-Gal*p*-(1→4)-D-Glc-ol -*1-d* **2**

β-D-Glc*p*-(1→4)-D-Glc-ol -*1-d* **3a**

β-D-Glc*p*-(1→6)-D-Glc-ol -*1-d* **3b**

β-D-Gal*p*-(1→4)-β-D-Glc*p*-(1→6)-D-Glc-ol-*1-d* **4a**

A **C** **E**-ol

β-D-Glc*p*-(1→6)-α-D-Glc*p*-(1→4)-D-Gal-ol-*1-d* **4b$_1$**

C **E** **B**-ol

β-D-Glc*p*-(1→4)-α-D-Glc*p*-(1→4)-D-Gal-ol-*1-d* **4b$_2$**

D **E** **B**-ol

β-D-Gal*p*-(1→4)-β-D-Glc*p*-(1→6)-α-D-Glc*p*-(1→4)-D-Gal-ol-*1-d* **5a**

A **C** **E** **B**-ol

β-D-Glc*p* **C**
1
↓
6
β-D-Glc*p*-(1→4)-α-D-Glc*p*-(1→4)-D-Gal-ol-*1-d* **5b**

D **E** **B**-ol

A β-D-Gal*p*-(1→4)-β-D-Glc*p* **C**
1
↓
6
β-D-Glc*p*-(1→4)-α-D-Glc*p*-(1→4)-D-Gal-ol-*1-d* **6a**

D **E** **B**-ol

A β-D-Gal*p*-(1→4)-β-D-Glc*p* **C**
1
↓
6
β-D-Gal*p*-(1→4)-β-D-Glc*p*-(1→4)-α-D-Glc*p*-(1→4)-D-Gal-ol-*1-d* **7**

B **D** **E** **B**-ol

Figure 3. *Structures of oligosaccharide alditols* ***2-7*** *obtained from partially acid-hydrolyzed EPS.*

MALDI-TOF analysis of the major component of the reduced fraction **4**, subfraction **4b**, showed a $[M+Na]^+$ pseudomolecular ion at *m/z* 530, corresponding with Hex_2Hex-ol-*1-d*. Monosaccharide analysis revealed the presence of Glc and Gal-ol in a molar ratio of 2:1, and methylation analysis showed the presence of terminal Glc*p*, 4-substituted Glc*p*, 6-substituted Glc*p*, and 4-substituted Gal-ol-*1-d*, pointing to a mixture of two trisaccharide alditols differing in the substitution pattern of the internal residue. Taking into account the structures of the larger oligosaccharides (*vide infra*), the structures of the two trisaccharide alditols, $\mathbf{4b_1}$ and $\mathbf{4b_2}$, can be formulated as illustrated in Figure 3.

Fraction 5. — 1D ^{1}H NMR analysis of reduced fraction **5** suggested that it was composed of a mixture of oligosaccharide alditols. The MALDI-TOF spectra of the oligosaccharide alditols **5a** and **5b**, obtained after subfractionation of **5**, showed in each case a $[M+Na]^+$ pseudomolecular ion at *m/z* 692, corresponding with Hex_3Hex-ol-*1-d*. Monosaccharide analysis of **5a** revealed the presence of Gal, Glc, and Gal-ol in a molar ratio of 1:2:1. Methylation analysis showed terminal Gal*p*, 4-substituted Glc*p*, 6-substituted Glc*p*, and 4-substituted Gal-ol-*1-d*, indicating a linear tetrasaccharide alditol. The 1D ^{1}H NMR spectrum (Figure 4A) of **5a** contained three signals in the anomeric region (δ 4.3–5.2): δ 4.451 (residue **A**, $^3J_{1,2}$ 7.8 Hz; β-pyranose), δ 4.514 (residue **C**, $^3J_{1,2}$ 7.8 Hz; β-pyranose), and δ 5.082 (residue **E**, $^3J_{1,2}$ 3.9 Hz; α-pyranose). The ^{1}H assignments for residues **A**, **C**, **E**, and **B**-ol (Table 2) were performed by means of 2D TOCSY experiments (mixing times 25-250 ms), essentially as described for the ^{1}H assignment of EPS **1**. In the 2D ROESY spectrum of **5a** the interresidual connectivities **C** H-1,**E** H-6b and **E** H-1,**B**-ol H-4 indicated the **C**-(1→6)-**E**-(1→4)-**B**-ol sequence. Since methylation analysis of **5a** revealed the presence of a 4-substituted Glc*p*, the cross-peak on the **A** H-1 ROESY track at δ 3.66 can be partly derived from **A** H-1,**C** H-4 (Table 2), thereby supporting the **A**(1→4)**C** linkage. For a complete structure of **5a**, see Figure 3.

Monosaccharide analysis of component **5b** demonstrated the presence of Glc and Gal-ol in a molar ratio of 3:1. Methylation analysis showed the occurrence of terminal Glc*p*, 4,6-disubstituted Glc*p*, and 4-substituted Gal-ol-*1-d*, indicating a branched tetrasaccharide alditol. The 1D ^{1}H NMR spectrum of component **5b** (Figure 4B) contained three signals in the anomeric region (δ 4.3-5.2): δ 4.502 (residue **C**, $^3J_{1,2}$ 7.9 Hz; β-pyranose), δ 4.568 (residue **D**, $^3J_{1,2}$ 7.8 Hz; β-pyranose), and δ 5.084 (residue **E**, $^3J_{1,2}$ 3.9 Hz; α-pyranose). Most of the ^{1}H resonances of the four residues were determined (Table 2) essentially as described for the ^{1}H assignment of EPS **1**. In the 2D ROESY spectrum the interresidual connectivities **D** H-1,**E** H-4 and **E** H-1,**B**-ol H-4 demonstrated the **D**(1→4)**E**(1→4)**B**-ol sequence, whereas the interresidual connectivity **C** H-1,**E** H-6b proved the **C**(1→6)**E** branching. For a complete structure of **5b**, see Figure 3.

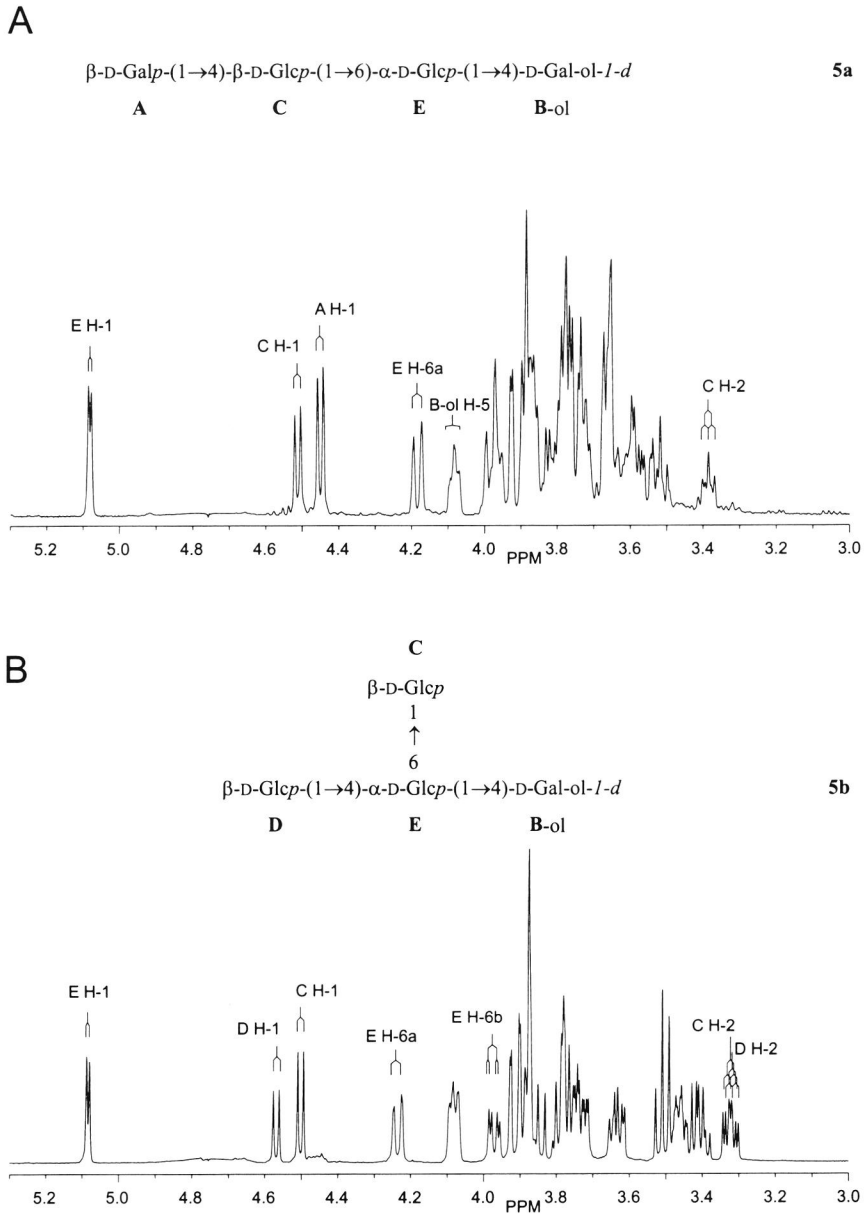

Figure 4. *500-MHz ^1H NMR spectra of (A) tetrasaccharide alditol* ***5a****, (B) tetrasaccharide alditol* ***5b****, (C) pentasaccharide alditol* ***6a****, and (D) hexasaccharide alditol* ***7****, recorded in D_2O at 27 °C.*

C

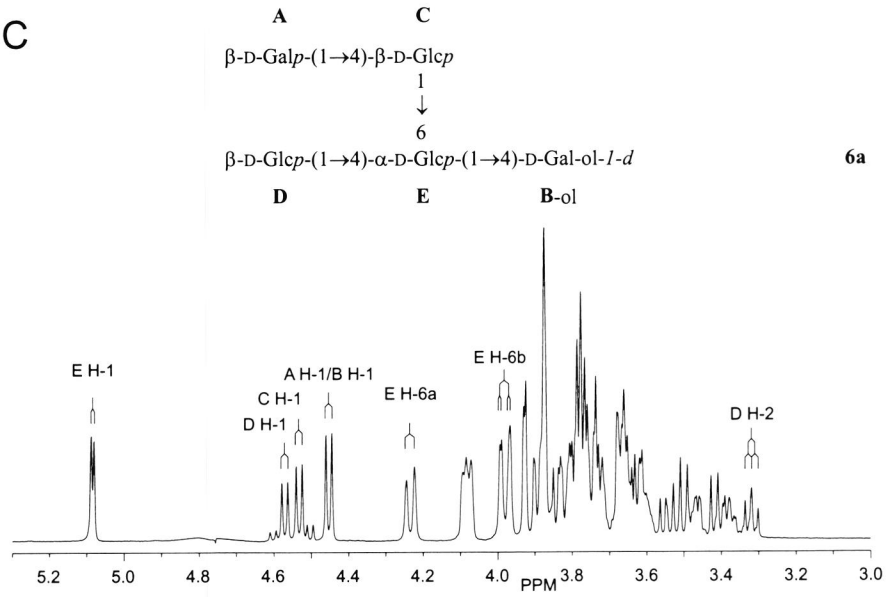

D

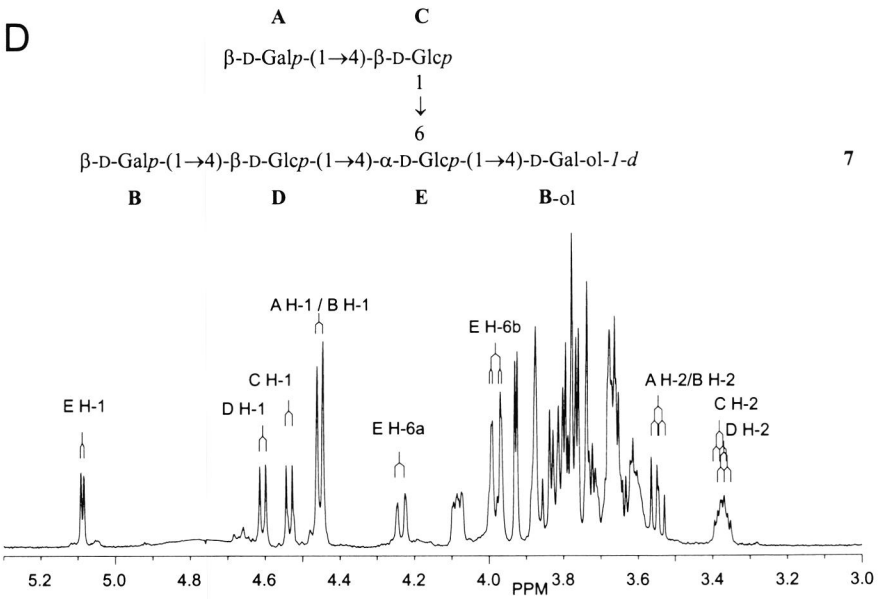

Figure 4. *Continued.*

Fraction **6**. — In the MALDI-TOF spectrum of oligosaccharide alditol **6a**, a $[M+Na]^+$ pseudomolecular ion at *m/z* 854 was detected corresponding with Hex_4Hex-ol-*1-d*. Monosaccharide analysis of **6a** showed the presence of Gal, Glc, and Gal-ol-*1-d* in a molar ratio of 1:3:1. Methylation analysis revealed terminal Gal*p*, terminal, 4-substituted and 4,6-disubstituted Glc*p*, and 4-substituted Gal-ol-*1-d*, defining a branched pentasaccharide alditol. 1D ^{1}H NMR analysis of **6a** (Figure 4C) revealed four anomeric signals at δ 4.453 (residue **A**, $^3J_{1,2}$ 7.9 Hz), δ 4.532 (residue **C**, $^3J_{1,2}$ 7.9 Hz), δ 4.571 (residue **D**, $^3J_{1,2}$ 8.3 Hz), and δ 5.084 (residue **E**, $^3J_{1,2}$ 3.9 Hz), respectively, and was consistent with the presence of a pentasaccharide alditol. The chemical shifts and coupling constants of residues **A**, **C**, and **D** indicated β-pyranoses and those of residue **E** an α-pyranose. The ^{1}H chemical shifts listed in Table 2, were assigned by means of 2D TOCSY experiments (mixing times 25-250 ms), essentially as described for the ^{1}H assignment of EPS **1**. In the 2D ROESY spectrum the interresidual connectivities **D** H-1,**E** H-4 and **E** H-1,**B**-ol H-4 proved the **D**(1→4)**E**(1→4)**B**-ol sequence. In the **A** H-1 ROESY track the cross-peak observed to the signal at δ 3.67 can originate from connectivities with **A** H-3, **C** H-3 and/or **C** H-4 (Table 2). The methylation analysis data of **6a** support that this cross-peak can be partly derived from **A** H1,**C** H-4; this, together with the interresidual connectivity **C** H-1,**E** H-6b reflects the **A**(1→4)**C**(1→6)**E** branch. Combining all data, a branched pentasaccharide alditol **6a** can be constructed, as given in Figure 3.

Fraction 7. — In the MALDI-TOF spectrum of oligosaccharide alditol **7**, a $[M+Na]^+$ pseudomolecular ion at *m/z* 1016 was detected, corresponding with Hex_5Hex-ol-*1-d*. Monosaccharide analysis of **7** showed the presence of Gal, Glc, and Gal-ol in a molar ratio of 2:3:1. Methylation analysis demonstrated the presence of terminal Gal*p*, 4-substituted Glc*p*, 4,6-disubstituted Glc*p*, and 4-substituted Gal-ol-*1-d*. Taking together these data, a branched hexasaccharide alditol is suggested. In the 1D ^{1}H NMR spectrum of **7** (Figure 4D) two overlapping anomeric signals were present at δ 4.452 (residue **A** and **B**, $^3J_{1,2}$ 7.8 Hz), and three fully resolved anomeric signals at δ 4.534 (residue **C**, $^3J_{1,2}$ 7.8 Hz), δ 4.605 (residue **D**, $^3J_{1,2}$ 7.8 Hz), and δ 5.086 (residue **E**, $^3J_{1,2}$ 4.0 Hz), respectively. The chemical shifts and coupling constants of residues **A**, **B**, **C**, and **D** illustrated β-pyranoses and those of residue **E** an α-pyranose. The ^{1}H assignments for residues **A**, **B**, **C**, **D**, and **E** (Table 2) are based on cross-peaks observed in the 2D TOCSY spectra (mixing times 25-250 ms), using the strategy essentially as described for the ^{1}H assignment of EPS **1.** The monosaccharide sequence was determined by means of a 2D ROESY experiment. The spectrum revealed the well-resolved interresidual connectivities **D** H-1,**E** H-4 and **E** H-1,**B**-ol H-4 indicating the **D**(1→4)**E**(1→4)**B**-ol sequence. The interresidual connectivity **C** H-1,**E** H-6b specified the

C(1→6)**E** branch. Furthermore, cross-peaks are observed from the overlapping anomeric proton signals of residues **A** and **B** to signals at δ ~3.66, which can have different origins including **A** H-1,**C** H-4 and **B** H-1,**D** H-4 (Table 2). Taking into account the monosaccharide sequences of the oligosaccharide alditols **4a**, **5a**, and **6a**, and the methylation analysis data of alditol **7**, the glycosidic linkages were assigned **A**(1→4)**C** and **B**(1→4)**D**. The derived structure of alditol **7** is given in Figure 3.

Table 2. *^{1}H NMR chemical shifts[a] of EPS (**1**), recorded in D_2O at 80 °C and oligosaccharide alditols **4**-**7**, recorded in D_2O at 27 °C. Coupling constants are included in parentheses.*

Residue	Proton	**1**	**4a**	**5a**	**5b**	**6a**	**7**
A	H-1	4.456 (7.9)	4.449 (7.8)	4.451 (7.8)	-	4.453 (7.9)	4.452 (7.8)
	H-2	3.56	3.546	3.55	-	3.55	3.544 [c]
	H-3	3.66	3.66	3.66	-	3.67	3.66
	H-4	3.94	3.93	3.93	-	3.93	3.93
	H-5	3.72	3.72	3.72	-	3.72	3.73
	H-6a	3.79	n.d. [b]	3.77	-	3.77	3.77
	H-6b	3.79	n.d.	3.77	-	3.77	3.77
B	H-1	4.510 (~8)	-	-	-	-	4.452 (7.8)
	H-2	3.59	-	-	-	-	3.548 [c]
	H-3	3.74	-	-	-	-	3.66
	H-4	4.041	-	-	-	-	3.93
	H-5	3.79	-	-	-	-	3.73
	H-6a	3.91	-	-	-	-	3.77
	H-6b	3.78	-	-	-	-	3.77
C	H-1	4.525 (~8)	4.529 (7.8)	4.514 (7.8)	4.502 (7.9)	4.532 (7.9)	4.534 (7.8)
	H-2	3.39	3.377	3.385	3.327	3.38	3.374
	H-3	3.67	3.66	3.66	3.50	3.67	3.67
	H-4	3.65	3.66	3.66	3.40	3.67	3.66
	H-5	3.59	3.61	3.60	3.45	3.60	3.60
	H-6a	3.97	3.986 (12.7)	3.99	3.92	3.98	3.97
	H-6b	3.81	3.81	3.81	3.73	3.82	3.82
D	H-1	4.605 (7.3)	-	-	4.568 (7.8)	4.571 (8.3)	4.605 (7.8)
	H-2	3.38	-	-	3.320	3.318	3.368
	H-3	3.67	-	-	3.50	3.51	3.67
	H-4	3.66	-	-	3.42	3.42	3.67
	H-5	3.62	-	-	3.47	3.47	3.61
	H-6a	3.98	-	-	3.92	3.91	3.97
	H-6b	3.83	-	-	3.73	3.74	3.82

Table 2. *Continued.*

E	H-1	4.935 (3.4)	-	5.082 (3.9)	5.084 (3.9)	5.084 (3.9)	5.086 (4.0)
	H-2	3.62	-	3.58	3.62	3.63	3.63
	H-3	3.86	-	3.73	3.84	3.85	3.85
	H-4	3.76	-	3.52	3.79	3.80	3.79
	H-5	4.37	-	3.97	4.08	4.08	4.08
	H-6a	4.17	-	4.184 (10.8)	4.235 (10.3)	4.234 (10.3)	4.234 (9.8)
	H-6b	3.98	-	3.86	3.971	3.979	3.980
B-ol	H-4	-	-	3.88	3.88	3.88	3.88
	H-5	-	-	4.084	4.08	4.08	4.08
	H-6a	-	-	3.78	3.77	3.77	3.78
	H-6b	-	-	3.78	3.77	3.77	3.78
E-ol	H-1a	-	3.64	-	-	-	-
	H-1b	-	3.72	-	-	-	-
	H-2	-	3.83	-	-	-	-
	H-3	-	3.84	-	-	-	-
	H-4	-	3.73	-	-	-	-
	H-5	-	3.92	-	-	-	-
	H-6a	-	4.145 (10.8)	-	-	-	-
	H-6b	-	3.82	-	-	-	-

[a] In ppm relative to the signal of internal acetone at δ 2.225
[b] n.d., not determined.
[c] Signals may have to be interchanged.

2D NMR spectroscopy of the native polysaccharide

The ^{1}H chemical shifts of the EPS (Table 2) were assigned by means of 2D TOCSY (mixing times 10-200 ms) and 2D NOESY experiments (mixing time 200 ms). The TOCSY spectrum with a mixing time of 120 ms is depicted in Figure 5. Starting points for the interpretation of the spectra were the anomeric signals of residues **A**-**E**. Comparison of TOCSY spectra with increasing mixing times allowed the assignment of the sequential order of the chemical shifts belonging to a single spin system.

The TOCSY **A** H-1 track (δ 4.456) showed cross-peaks with **A** H-2,3,4. Via the **A** H-4 signal the **A** H-5 TOCSY track (δ 3.724) was found, and on this track cross-peaks with **A** H-4,6a,6b were observed. The **B** H-1 TOCSY track (δ 4.510) showed a cross-peak with **B** H-4. The **B** H-2,3 chemical shifts, which could not be assigned accurately on the **B** H-1 track due to overlap with cross-peaks on the **C** H-1 track (δ 4.525), were assigned on the **B** H-4

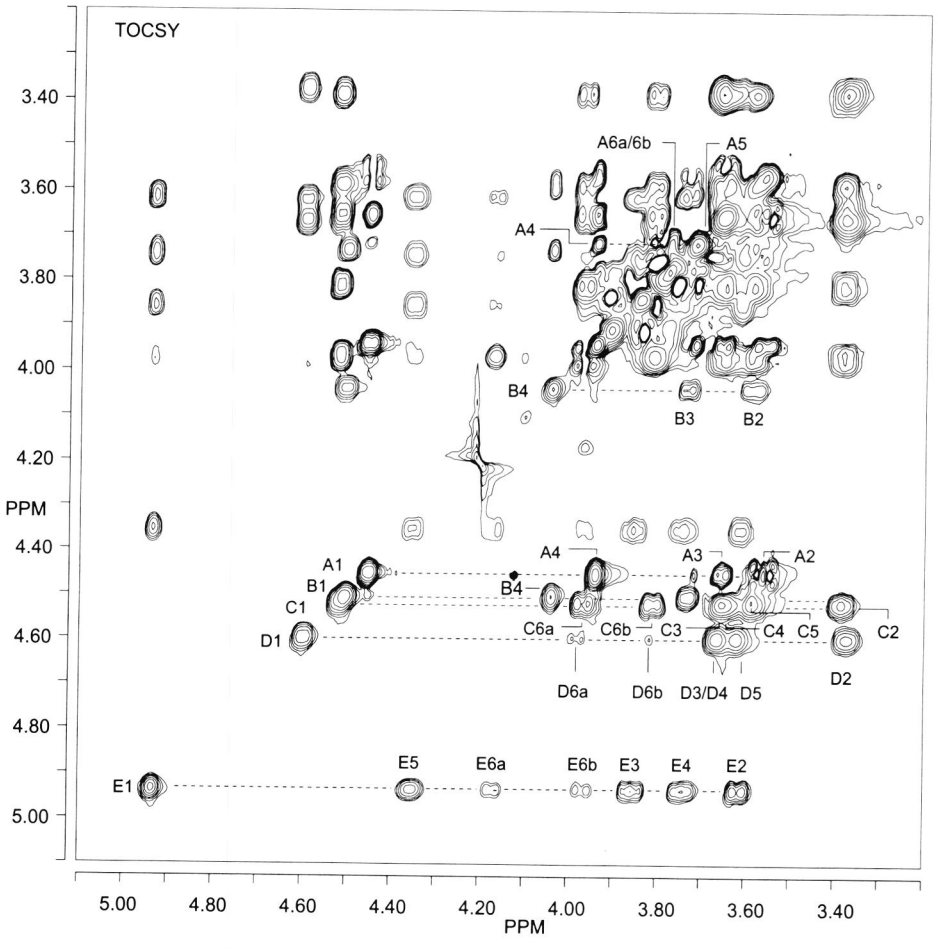

Figure 5. *500-MHz 2D TOCSY spectrum (mixing time 200 ms) of EPS **1**, recorded in D_2O at 80 °C. Diagonal peaks of the anomeric protons, of H-4 of residue **B**, and of H-5 of residue **A** are indicated. Cross-peaks belonging to the same scalar-coupling network are indicated near a dotted line starting from the corresponding diagonal peak. A1 means **A** H-1, etc.*

TOCSY track (δ 4.041). The resonance for **B** H-5 was found via an intraresidual cross-peak between **B** H-1 and **B** H-5 in the NOESY spectrum (*vide infra*). The chemical shifts of **B** H-6a,6b were derived from NOEs on the **E** H-1 track in the NOESY spectrum, since residue **E** is linked to residue **B** (*vide infra*). On the TOCSY **C** H-1 track (δ 4.525) the complete series

of cross-peaks with **C** H-2,3,4,5,6a,6b were observed. The H-2,3,4,5,6a,6b resonances of residue **D** were identified on the basis of cross-peaks on the **D** H-1 TOCSY track (δ 4.605) and the complete series of the well-resolved **E** H-2,3,4,5,6a,6b connectivities were found on the **E** H-1 TOCSY track (δ 4.935).

The assigned ^{1}H chemical shifts demonstrated residue **A** and **B** to be β-Gal*p* since they show spin systems typical of Gal*p* residues. Furthermore, residues **C** and **D** could be assigned as β-Glc*p* by the characteristic upfield shift of their H-2 resonances [14], leaving residue **E** to be α-Glc*p*.

Table 3. *^{13}C NMR chemical shifts[a] of EPS (**1**), as determined from a 2D ^{13}C-^{1}H HMQC spectrum, recorded at 80 °C. $^{1}J_{C\text{-}1,H\text{-}1}$ Values are included in parentheses.*

Residue	C-1	C-2	C-3	C-4	C-5	C-6
A	103.6 (162)	71.9	73.6	69.5	76.1	61.9
B	104.0 (161)	71.9	73.1	78.4	76.2	61.2
C	103.1 (161)	73.9	75.2	79.7	75.6	61.2
D	102.9 (163)	73.9	75.2	79.8	75.6	61.1
E	100.5 (173)	72.4	72.2	79.3	70.6	68.3

[a] In ppm relative to the α-anomeric signal of external [1-^{13}C]glucose at δ 92.9.

All ^{13}C resonances of the EPS (Table 3) could be assigned using a 2D ^{13}C-^{1}H HMQC spectrum (Figure 6). The $^{1}J_{C\text{-}1,H\text{-}1}$ values of the anomeric ^{13}C atoms of residues **A** ($^{1}J_{C\text{-}1,H\text{-}1}$162 Hz), **B** ($^{1}J_{C\text{-}1,H\text{-}1}$161 Hz), **C** ($^{1}J_{C\text{-}1,H\text{-}1}$161 Hz), and **D** ($^{1}J_{C\text{-}1,H\text{-}1}$ 163 Hz) are in agreement with β anomeric configurations, and that of residue **E** ($^{1}J_{C\text{-}1,H\text{-}1}$ 173 Hz) with α anomeric configuration [15].

Combining the ^{13}C NMR data and the methylation analysis data of the EPS, taking into account published ^{13}C chemical shift data of methyl aldosides [16], demonstrated residue **A** to be terminal β-D-Gal*p* and residue **B** to be 4-substituted β-D-Gal*p* (**B** C-4 δ 78.4; β-D-Gal*p*1Me, $\delta_{C\text{-}4}$ 69.7). The downfield chemical shifts of **C** C-4 (δ 79.7) and **D** C-4 (δ 79.8) indicated that residues **C** and **D** accord with 4-substituted β-D-Glc*p* units (β-D-Glc*p*1Me, $\delta_{C\text{-}4}$ 70.6). The remaining residue **E** could be assigned as 4,6-disubstituted α-D-Glc*p*, since **E** C-4 (δ 79.3) and **E** C-6 (δ 68.3) are shifted downfield (β-D-Glc*p*1Me, $\delta_{C\text{-}4}$ 70.6, $\delta_{C\text{-}6}$ 61.6).

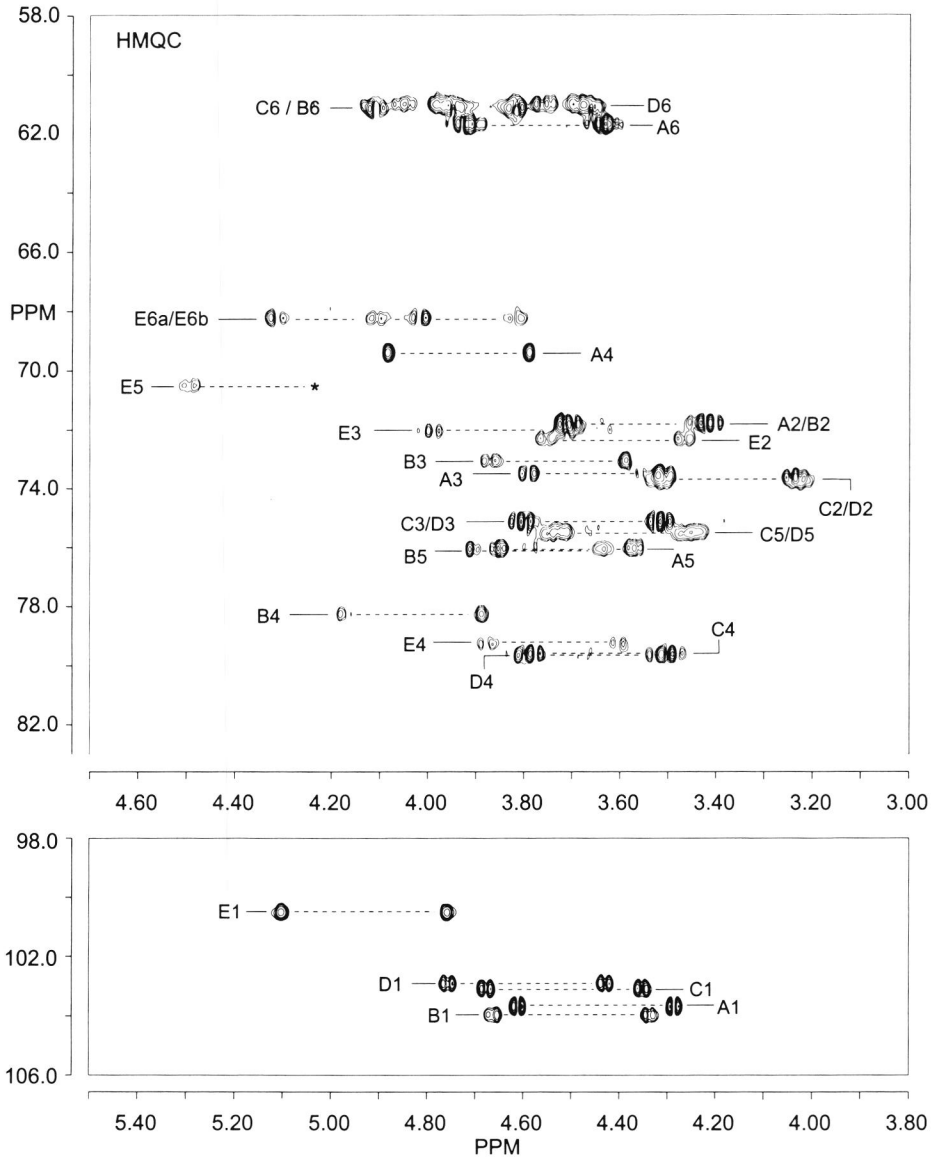

Figure 6. *500-MHz 2D ^{13}C-^{1}H undecoupled HMQC spectrum of EPS* ***1****, recorded in D_2O at 80 °C. A1 stands for the set of cross-peaks between H-1 and C-1 of residue* ***A****, etc. The asterisk (*) indicates the right-hand side of the E5 doublet, which is lost due to HOD suppression.*

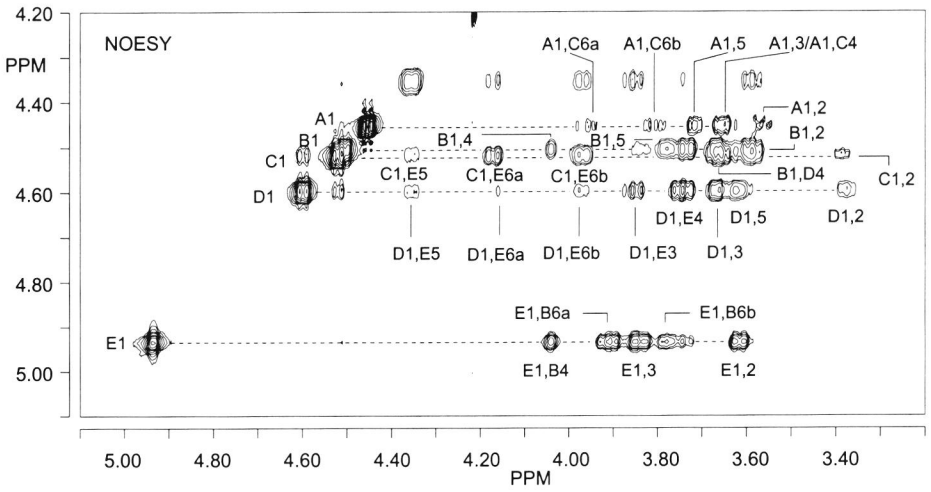

Figure 7. *Partial 500-MHz 2D NOESY spectrum (mixing time 200 ms) of EPS* ***1****, recorded in D_2O at 80 °C. E1 corresponds to the diagonal peak belonging to residue* ***E*** *H-1; E1,2 refers to an intraresidual cross-peak between* ***E*** *H-1 and* ***E*** *H-2, and E1,B4 means an interresidual connectivity between* ***E*** *H-1 and* ***B*** *H-4, etc.*

The assignment of interresidual cross-peaks in the 2D NOESY spectrum (Figure 7) and of long-range couplings in the HMBC spectrum (Figure 8) allowed the determination of the sequence and the linkage positions of the residues within the repeating unit of the EPS. On the NOESY **C** H-1 track strong NOEs with **E** H-6a,6b were observed, suggesting a **C**(1→6)**E** linkage. This linkage was confirmed by a long-range ^{1}H-^{13}C coupling between **C** H-1 and **E** C-6, observed in the HMBC spectrum. The interresidual connectivities **D** H-1,**E** H-3,4,5,6a,6b indicated a linkage between residue **D** and **E**. Taking into account the (1→6) linkage between residue **C** and **E** and the substitution pattern of residue **E** (*vide supra*), the NOE between **D** H-1 and **E** H-4 must reflect the **D**(1→4)**E** linkage. The additional NOEs between residues **D** and **E** were brought about by spin diffusion. Besides the **C**(1→6)**E** linkage, also the **D**(1→4)**E** linkage was confirmed by a long-range ^{1}H-^{13}C coupling in the HMBC spectrum. Interresidual connectivities between **E** H-1 and **B** H-4,6a,6b in the NOESY spectrum together with a long-range ^{1}H-^{13}C coupling between **E** H-1 and **B** C-4 in the HMBC spectrum indicated a **E**(1→4)**B** linkage. On the **A** H-1 NOESY track cross-peaks with **C** H-6a,6b were observed. Since the chemical shifts of both **A** H-3 (δ 3.66) and **C** H-4 (δ 3.65) were nearly identical, the NOE between **A** H-1 and **C** H-4 could not be distinguished

from the intraresidual connectivity **A** H-1,**A** H-3. As residue **C** is 4-substituted β-Glc*p* (*vide supra*), the **A**(1→4)**C** linkage is supported. Finally, the interresidual NOESY connectivity between **B** H-1 and a signal at δ ~3.65 established the **B**(1→4)**D** linkage. In the HMBC spectrum the long-range ^{1}H-^{13}C couplings **A** H-1,**C** C-4 and **B** H-1,**D** C-4 confirmed the **A**(1→4)**C** and **B**(1→4)**D** linkages, respectively.

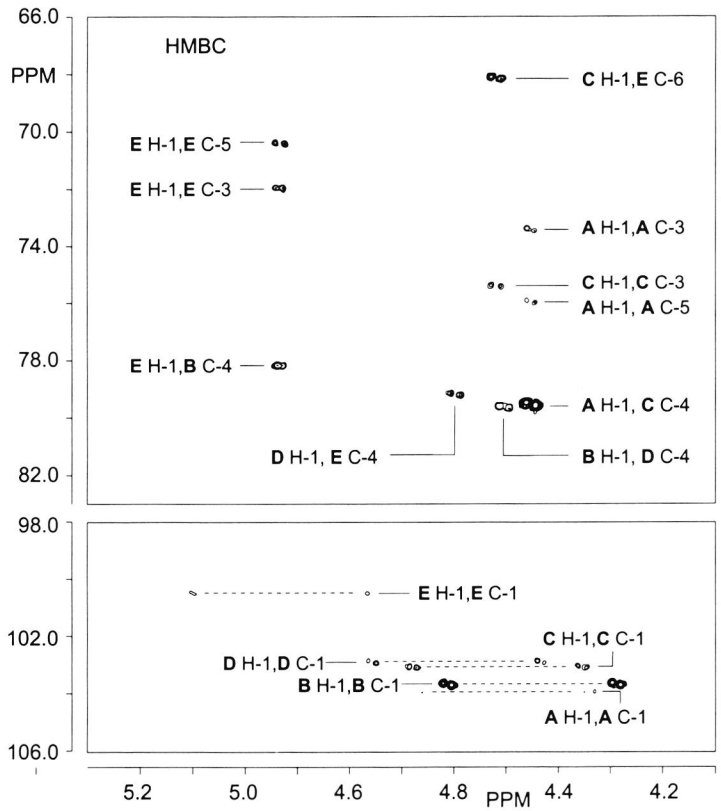

Figure 8. *Partial 500-MHz 2D ^{13}C–^{1}H undecoupled HMBC spectrum of EPS* ***1****, recorded in D_2O at 80 °C.* ***E*** *H-1,****B*** *C-4 corresponds to a cross-peak between* ***E*** *H-1 and* ***B*** *C-4, etc.*

Concluding remarks

Based on monosaccharide analysis, methylation analysis, and MS and 1D/2D NMR studies on EPS **1** and on oligosaccharides obtained from a partial acid hydrolysate of the

EPS, the primary structure of the EPS produced by *Lb. delbrueckii* subsp. *bulgaricus* 291 was shown to be built up from the following pentasaccharide repeating units:

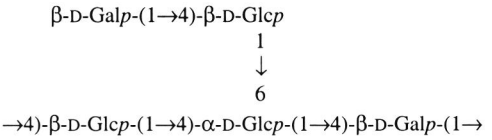

1

It is remarkable that the oligosaccharides isolated from the partial acid hydrolysate of EPS **1** do not give complete evidence for the repeating unit of the EPS. Even though, the structure of oligosaccharide **7** suggests a full elucidation of the repeating unit, it must be kept in mind that residues **A** and **B** in this oligosaccharide are chemically equivalent, leaving the accurate determination of the **A**-(1→4)-**C** and **B**-(1→4)-**D** fragments within the EPS **1** to be essential for the correct determination of the primary structure of the EPS.

The repeating unit of the EPS produced by *Lb. delbrueckii* subsp. *bulgaricus* 291 consists of a trimeric main chain, containing one Gal and two Glc residues, and carrying a lactosyl side chain. This type of side chain has been reported before for the EPSs produced by several strains of *Lb. helveticus* [17-19] and *L. lactis* subsp. *cremoris* [5,6] and may confer these EPSs specific biological properties [19]. Surprisingly, the repeating unit of the EPS produced by *Lb. delbrueckii* subsp. *bulgaricus* 291 was found to be identical to the de-*O*-acetylated repeating unit of the EPS produced by *L. lactis* subsp. *cremoris* B891 [6]. Repeating units, only differing in the presence or absence of *O*-acetyl groups have been reported before for capsular polysaccharides produced by *S. pneumoniae* strains belonging to the same serotype [20]. However, the absence of *O*-acetylation in the repeating unit of the *Lb. delbrueckii* subsp. *bulgaricus* 291 EPS as compared to the *L. lactis* subsp. *cremoris* B891 EPS can also be the result of differences in culturing conditions, as known for xanthan, produced by *Xanthamonas campestris* [21]. Furthermore, it must be kept in mind that differences in the procedure used for the isolation of the *Lb. delbrueckii* subsp. *bulgaricus* 291 EPS might have resulted in de-*O*-acetylation of the EPS.

To our knowledge there are no reports on the appearance of identical hetero-polysaccharide repeating units produced by different genera of lactic acid bacteria. Therefore, the production of an identical EPS by *Lb. delbrueckii* subsp. *bulgaricus* 291 and *L. lactis* subsp. *cremoris* B891 is remarkable.

3.3. Experimental

Culture conditions of microorganism and isolation of polysaccharide. — *Lb. delbrueckii* subsp. *bulgaricus* 291 (WISBY, Niebüll, Germany) was inoculated into skimmed milk containing 0.35% peptone and 0.35% yeast extract. After incubation (22 h, 37 °C), trichloroacetic acid was added to a final concentration of 8% (v/v), and the culture was stirred for 45 min. Cells and precipitated coagulated proteins were removed by centrifugation (20 min, 8,300 *g*, 4 °C). The pH of the supernatant was adjusted to 3.7 using 10 M NaOH. EPS in the supernatant was precipitated with 1.65 vols of EtOH during 16 h at 4 °C. Precipitated material was collected through centrifugation (20 min, 8,300 *g*, 4 °C), re-dissolved in water and dialyzed for 24 h against running water. The EPS was recovered by lyophilization and further purified on a Sephacryl S-500 gel filtration column as described [14].

Molecular mass determination. — The average molecular mass of the polysaccharide was determined using a modified method combining gel permeation chromatography, static light scattering, and differential refraction analysis, as described [22].

Gas-liquid chromatography and mass spectrometry. — GLC analyses were performed on a Chrompack CP9002 gas chromatograph equipped with a CP-Sil 5CB fused silica capillary column (25 m × 0.32 mm, Chrompack). GLC–MS analyses were carried out on a MD800/8060 system (Fisons instruments; electron energy, 70 eV), using a CP-Sil 5CB fused silica capillary column (25 m × 0.25 mm, Chrompack) or an AT-1 fused silica capillary column (30 m × 0.25 mm, Alltech). Both GLC and GLC-MS analyses were performed using conditions as described previously [23]. Matrix-assisted laser desorption ionization time-of-flight mass spectrometry (MALDI-TOF-MS) experiments were performed using a Voyager-DE mass spectrometer equipped with a nitrogen laser. Samples were prepared by mixing directly on the target 1 µl oligosaccharide-alditol solution with 2 µl aqueous 10% 2,5-dihydroxybenzoic acid as matrix solution.

Monosaccharide and methylation analysis. — For monosaccharide analysis, samples were methanolysed followed by trimethylsilylation and GLC analysis as described [24-26]. The absolute configuration of the monosaccharides was determined by GLC analysis of their trimethylsilylated (-)-2-butyl glycosides [27,28]. For methylation analysis, the polysaccharide and isolated oligosaccharide alditols were subsequently permethylated, hydrolyzed, reduced,

and acetylated, as described previously [23]. The obtained partially methylated alditol acetates were identified by GLC and by GLC–MS [26,29].

Partial acid hydrolysis. — Exopolysaccharide (15 mg) was treated with 0.3 M trifluoroacetic acid (15 mL) for 1 h at 100 °C. After lyophilization, the residue was fractionated on a Bio-Gel P-2 column (200–400 mesh, 100 × 1.6 cm, Bio-Rad), eluted with 5 mM NH_4HCO_3 at a rate of 0.5 mL/min at 57 °C, monitored by differential refractive index detection (LKB Bromma). Collected fractions were subfractionated by high-pH anion-exchange chromatography with pulsed amperometric detection (HPAEC-PAD) on a CarboPac PA-1 pellicular anion-exchange column (25 cm × 9 mm, Dionex). The column was eluted with a gradient of NaOAc in 0.1 M NaOH at a flow rate of 4 mL/min. Gradients were optimized for each fraction. PAD-detection was carried out with a gold working electrode and triple-pulse amperometry (pulse potentials and durations: E_1 0.05 V, 300 ms; E_2 0.65 V, 60 ms; E_3 –0.95 V, 180 ms) was used. Collected fractions were desalted on graphitized carbon according to [30], and reduced with $NaBD_4$ in 1 M NH_4OH prior to analysis. In the cases of oligosaccharide alditol mixtures, a further fractionation was carried out on CarboPac PA-1 using the same conditions as described above, and prior to analysis the collected fractions were desalted on graphitized carbon.

NMR spectroscopy. — Prior to NMR-spectroscopic analysis, samples were exchanged twice in 99.9 atom% D_2O (Cambridge Isotope Laboratories Inc.) with intermediate lyophilization and finally dissolved in 99.96 atom% D_2O (Isotec Inc.). NMR spectra were recorded on a Bruker AMX-500 spectrometer (Bijvoet Center, Department of NMR Spectroscopy) at a probe temperature of 80 °C for the EPS and 27 °C for the oligosaccharide alditols. The HOD signal was suppressed either by applying a WEFT pulse sequence [31] in 1D ^1H NMR experiments, or by presaturation for 0.8-1 s in 2D experiments. When necessary, the remaining HOD signal was eliminated by convolution of low frequency contributions in the FID by a first order phase correction [32]. Chemical shifts were referenced to internal acetone (δ 2.225) for ^1H or to the α-anomeric signal of external [1-^{13}C]glucose ($\delta_{C\text{-}1}$ 92.9) for ^{13}C. Spectra were recorded using a spectral width of 4032 Hz and 16350 Hz for ^1H and ^{13}C, respectively. Resolution enhancement of the spectra was performed by a Lorentzian-to-Gaussian transformation or by multiplication with a squared-bell function phase shifted by π/(2.3), and when necessary, a fifth-order polynomial baseline correction was performed. 2D TOCSY spectra were recorded using a 'clean' MLEV-17 mixing sequence with an effective spin-lock time of 10-200 ms. 512 experiments of 1024 points were acquired with 16 or 32

scans per increment. 2D NOESY experiments were performed with a mixing time of 200 ms and 2D off-resonance ROESY spectra were obtained with a mixing time of 300 ms; both NOESY and ROESY spectra were acquired with 512 experiments of 1024 points with 16 to 32 scans per increment. Both natural abundance ^{13}C-^{1}H 2D HMQC and ^{13}C-^{1}H 2D HMBC experiments were recorded without decoupling during acquisition of the ^{1}H FID. 512 free induction decays of 1024 data points were acquired using 140 or 400 scans per decay. The ^{13}C-^{1}H 2D HMBC spectrum was recorded using a delay of 50 ms for the evolution of the long range coupling.

All NMR data were processed using TRITON (Bijvoet Center, Department of NMR Spectroscopy) software.

Acknowledgements

This study was supported by the PBTS Research Program with financial aid from the Ministry of Economic Affairs and by the Integral Structure Plan for the Northern Netherlands from the Dutch Development Company. The authors thank Dr. A.M. Ledeboer (Unilever Research, Vlaardingen, The Netherlands) for cultivation and isolation of the EPS.

References

[1] L. De Vuyst, B. Degeest, *FEMS Microbiol. Rev.*, 23 (1999) 153-177.
[2] J. Cerning, C. Bouillanne, M.J. Desmazeaud, M. Landon, *Biotechnol. Lett.*, 10 (1988) 255-260.
[3] J. Sikkema, T. Oba, *Snow Brand R&D Reports*, 107 (1998) 1-31.
[4] G.H. van Geel-Schutten, E.J. Faber, E. Smit, K. Bonting, M.R. Smith, B. ten Brink, J.P. Kamerling, J.F.G. Vliegenthart, L. Dijkhuizen, *Appl. Environ. Microbiol.*, 65 (1999) 3008-3014.
[5] W.H.M. van Casteren, C. Dijkema, H.A. Schols, G. Beldman, A.G.J. Voragen, *Carbohydr. Res.*, 324 (2000) 170-181.
[6] W.H.M. van Casteren, P. de Waard, C. Dijkema, H.A. Schols, A.G.J. Voragen, *Carbohydr. Res.*, 327 (2000) 411-422.
[7] E.J. Faber, M.J. van den Haak, J.P. Kamerling, J.F.G. Vliegenthart, *Carbohydr. Res.*, (2000) Submitted.
[8] L. Micheli, D. Uccelletti, C. Palleschi, V. Crescenzi, *Appl. Microbiol. Biotechnol.*, 53 (1999) 69-74.
[9] J. Uemura, T. Itoh, T. Kaneko, K. Noda, *Milchwissenschaft*, 53 (1998) 443-446.
[10] G.J. Grobben, M.R. Smith, J. Sikkema, J.A.M. de Bont, *Appl. Microbiol. Biotechnol.*, 46 (1996) 279-284.
[11] J. Cerning, C. Bouillanne, M.J. Desmazeaud, M. Landon, *Biotechnol. Lett.*, 8 (1986) 625-628.
[12] G.J. Grobben, J. Sikkema, M.R. Smith, J.A.M. de Bont, *J. Appl. Bacteriol.*, 79 (1995) 103-107.
[13] M. Gruter, B.R. Leeflang, J. Kuiper, J.P. Kamerling, J.F.G. Vliegenthart, *Carbohydr. Res.*, 239 (1993) 209-226.
[14] G.W. Robijn, D.J.C. van den Berg, H. Haas, J.P. Kamerling, J.F.G. Vliegenthart, *Carbohydr. Res.*, 276 (1995) 117-136.
[15] K. Bock, C. Pedersen, *J. Chem. Soc., Perkin Trans. 2*, (1974) 293-297.
[16] K. Bock, C. Pedersen, *Adv. Carbohydr. Chem. Biochem.*, 41 (1983) 27-66.
[17] Y. Yamamoto, S. Murosaki, R. Yamauchi, K. Kato, Y. Sone, *Carbohydr. Res.*, 261 (1994) 67-78.
[18] Y. Yamamoto, T. Nunome, R. Yamauchi, K. Kato, Y. Sone, *Carbohydr. Res.*, 275 (1995) 319-332.
[19] F. Stingele, J. Lemoine, J.-R. Neeser, *Carbohydr. Res.*, 302 (1997) 197-202.
[20] J.P. Kamerling, in A. Tomasz (Ed.), *Streptococcus pneumoniae – Molecular Biology & Mechanisms of Disease*, Mary Ann Liebert Inc., Larchmont, 2000, pp. 81-114.
[21] A. Becker, F. Katzer, A. Pühler, L. Ielpi, *Appl. Microbiol. Biotechnol.*, 50 (1998) 145-152.

[22] B. Tinland, J. Mazet, M. Rinaudo, *Makromol. Chem.*, 9 (1988) 69-73.

[23] E.J. Faber, P. Zoon, J.P. Kamerling, J.F.G. Vliegenthart, *Carbohydr. Res.*, 310 (1998) 269-276.

[24] G.W. Robijn, J.R. Thomas, H. Haas, D.J.C. van den Berg, J.P. Kamerling, J.F.G. Vliegenthart, *Carbohydr. Res.*, 276 (1995) 137-154.

[25] M.F. Chaplin, *Anal. Biochem.*, 123 (1982) 336-341.

[26] J.P. Kamerling, J.F.G. Vliegenthart, in A.M. Lawson (Ed.), *Clinical Biochemistry - Principles, Methods, Applications. Vol. 1, Mass Spectrometry*, Walter de Gruyter, Berlin, 1989, pp. 176-263.

[27] G.J. Gerwig, J.P. Kamerling, J.F.G. Vliegenthart, *Carbohydr. Res.*, 62 (1978) 349-357.

[28] G.J. Gerwig, J.P. Kamerling, J.F.G. Vliegenthart, *Carbohydr. Res.*, 77 (1979) 1-7.

[29] P.-E. Jansson, L. Kenne, H. Liedgren, B. Lindberg, J. Lönngren, *Chem. Commun. Univ. Stockholm*, 8 (1976) 1-74.

[30] N.H. Packer, M.A. Lawson, D.R. Jardine, J.W. Redmond, *Glycoconjugate J.*, 15 (1998) 737-747.

[31] K. Hård, G. van Zadelhoff, P. Moonen, J.P. Kamerling, J.F.G. Vliegenthart, *Eur. J. Biochem.*, 209 (1992) 895-915.

[32] D. Marion, M. Ikura, A. Bax, *J. Magn. Reson.*, 84 (1989) 425-430.

Chapter 4

The exopolysaccharide produced by *Streptococcus thermophilus* 8S contains a novel open chain nononic acid

Elisabeth J. Faber, J. Albert van Kuik, Johannis P. Kamerling, and Johannes F.G. Vliegenthart

Bijvoet Center, Department of Bio-Organic Chemistry, Utrecht University, PO Box 80.075, NL-3508 TB Utrecht, The Netherlands.

Abstract

A novel sugar constituent was isolated from the heteropolysaccharide excreted by *Streptococcus thermophilus* 8S when grown in skimmed milk. The structure was determined by means of chemical analysis, mass spectrometry, NMR spectroscopy, along with molecular dynamics simulations, and shown to be 6-*O*-(3′,9′-dideoxy-D-*threo*-D-*altro*-nononic acid-2′-yl)-D-glucopyranose.

Elisabeth J. Faber, J. Albert van Kuik, Johannis P. Kamerling, and Johannes F.G. Vliegenthart, *Manuscript in preparation.*

4.1. Introduction

The exopolysaccharides (EPSs) produced by lactic acid bacteria are promising to constitute a new generation of food thickeners because of their physical properties in combination with their GRAS (Generally Recognized as Save) status. For that reason, detailed structural studies have been performed on the EPSs produced by various species of the *Lactobacillus*, *Lactococcus*, and *Streptococcus* genera ([1], and references cited therein). The EPSs characterized so far consist mainly of combinations of glucose, galactose and/or rhamnose, and to a minor extent of *N*-acetylglucosamine, *N*-acetylgalactosamine, or glucuronic acid. In some cases non-carbohydrate substituents such as phosphate and acetyl functions, and glycerol groups are present.

Here, we report on the structural elucidation of a novel sugar constituent found in the EPS excreted by the lactic acid bacterium *Streptococcus thermophilus* 8S when grown in skimmed milk.

4.2. Results and discussion

Isolation, purification, and composition of the exopolysaccharide

The EPS produced by *S. thermophilus* 8S in pasteurized reconstituted skimmed milk was isolated, and purified via ethanol precipitation followed by acetone precipitation and gelfiltration using Sephacryl S-500. Monosaccharide analysis of the native EPS (n-EPS), including the determination of absolute configurations, demonstrated the occurrence of D-Gal, D-Glc, D-GalNAc, and D-Rib in a molar ratio of 2:1:1:1, as well as an unknown sugar component in a molar ratio of 0.7 in terms of peak areas compared to Glc. Methylation analysis of n-EPS revealed, besides the presence of 4-substituted Gal*p*, 4-substituted Glc*p*, 4-substituted Gal*p*NAc, and 2-substituted Rib*f* (molar ratio of 2:1:1:1), the occurrence of an unknown sugar component. However, no conclusive structural information could be deduced from the alditol-*1-d* mass spectrum. In order to test if the problems in the identification might be caused by the presence of a carboxyl-group, n-EPS was subjected to a carboxyl-reduction ($NaBD_4$; cr-EPS) prior to methylation analysis. EIMS of the partially methylated alditol-*1-d* acetate originating from the unknown sugar component in cr-EPS revealed a fragmentation pattern in accordance with a polyhydroxy C_9-chain linked at C-2′ via an ether bond to C-6 of a Hex-ol-*1-d* residue (Figure 1). The *O*-acetyl groups at C-1 and C-5 of Hex-ol-*1-d* indicated a pyranose ring for the Hex part of the unknown sugar component, whereas the *O*-acetyl

group at C-7′ suggested a glycosylation site for an adjacent monosaccharide residue. The doubly deuterium-labeled C-1′ atom might indeed reflect the presence of a native carboxyl-group. Furthermore, the fragmentation pattern indicated deoxygenation at C-3′ and C-9′, giving rise to a dideoxy sugar. To determine the identity of the Hex residue, the carboxyl-reduced component was isolated from a hydrolyzate of cr-EPS and subjected to treatment with BBr_3 in order to cleave the ether bond between C-2′ and C-6. Monosaccharide analysis of the obtained material, including absolute configuration determination, indicated the Hex residue to be D-Glc. Based on the foregoing, the unknown sugar component can be hypothesized as a 6-*O*-(3′,9′-dideoxy-nononic acid-2′-yl)-D-glucopyranose.

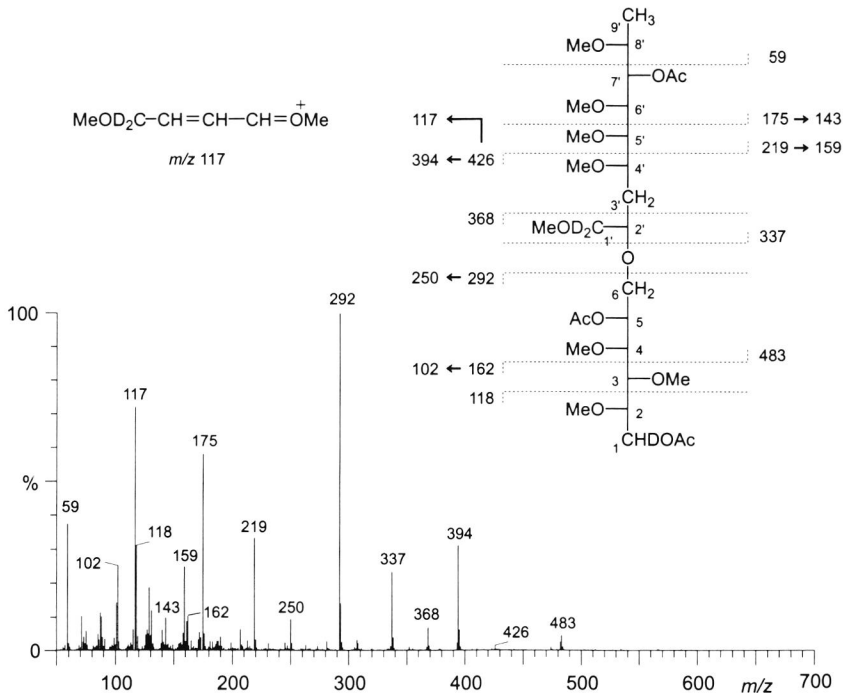

Figure 1. *EIMS spectrum of the partially methylated alditol-1-d acetate of the novel sugar constituent isolated from cr-EPS.*

Identification of the unknown sugar component

For the structural characterization of the unknown exopolysaccharide constituent, the non-derivatized and the carboxyl-reduced ($NaBH_4$) unknown sugar components were isolated

from acid hydrolyzates of n-EPS and cr-EPS, respectively, by using graphitized carbon. MALDI-TOF analysis of the compound isolated from n-EPS revealed a $[M+Na]^+$ pseudomolecular ion at *m/z* 421, corresponding with the mass of structure **1**, having a lactone ring in the nononic acid (C_9) part (Scheme 1).

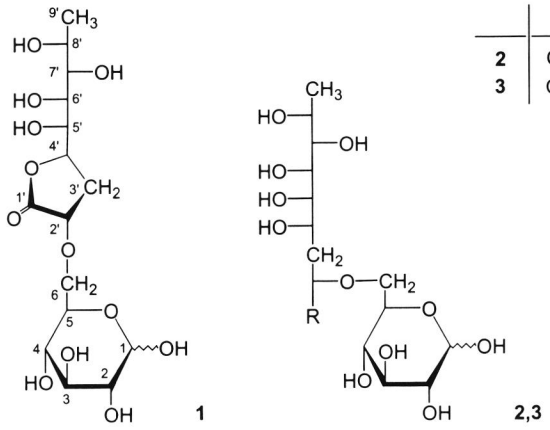

Scheme 1.

In the anomeric region (δ 4.4 - 5.4) of the 1D ^{1}H NMR spectrum of **1** (Figure 2A) doublets were observed at δ 5.205 ($^3J_{1,2}$ 3.8 Hz; α-pyranose) and δ 4.629 ($^3J_{1,2}$ 7.9 Hz; β-pyranose), indicating the two anomers of the Glc part of **1**. Furthermore, methylene (δ ~2.71, δ ~2.23) and methyl (δ 1.180) protons were observed, originating from the C_9 part of **1**. Comparison of the 2D TOCSY spectra of **1** with increasing mixing times (25→250 ms) allowed the assignment of the ^{1}H signals belonging to each of the spin systems (Table 1). The α H-1 and β H-1 TOCSY tracks showed spin systems characteristic of α- and β-Glc*p*, respectively, and the H-3′pro*R*, H-3′pro*S*, and H-9′ TOCSY tracks revealed the complete spin system of the C_9 part (Figure 3). Stereospecific assignments of Glc H-6pro*R* and H-6pro*S* were performed by analogy with ^{1}H NMR studies of stereospecifically deuterated D-Glc*p* [2], and are in agreement with the assignments of H-6pro*R* and H-6pro*S* of 6-substituted D-Glc*p* in gentiobiose [3]. The methylene protons of the C_9 part were assigned as pro*R* and pro*S* in accordance with the configuration of the C_9 part of compound **1** (*vide infra*). The 2D ^{13}C-^{1}H HMQC spectra of **1** (Figure 4) allowed the assignment of the ^{13}C signals (Table 1). The downfield chemical shift values of α C-6 (δ 70.0) and β C-6 (δ 70.4) in comparison with NMR data of Glc*p* (α-D-Glc*p*, $\delta_{C\text{-}6}$ 61.6; β-D-Glc*p*, $\delta_{C\text{-}6}$ 61.7 [4]) confirmed the 6-substitution of the Glc*p* part of **1**.

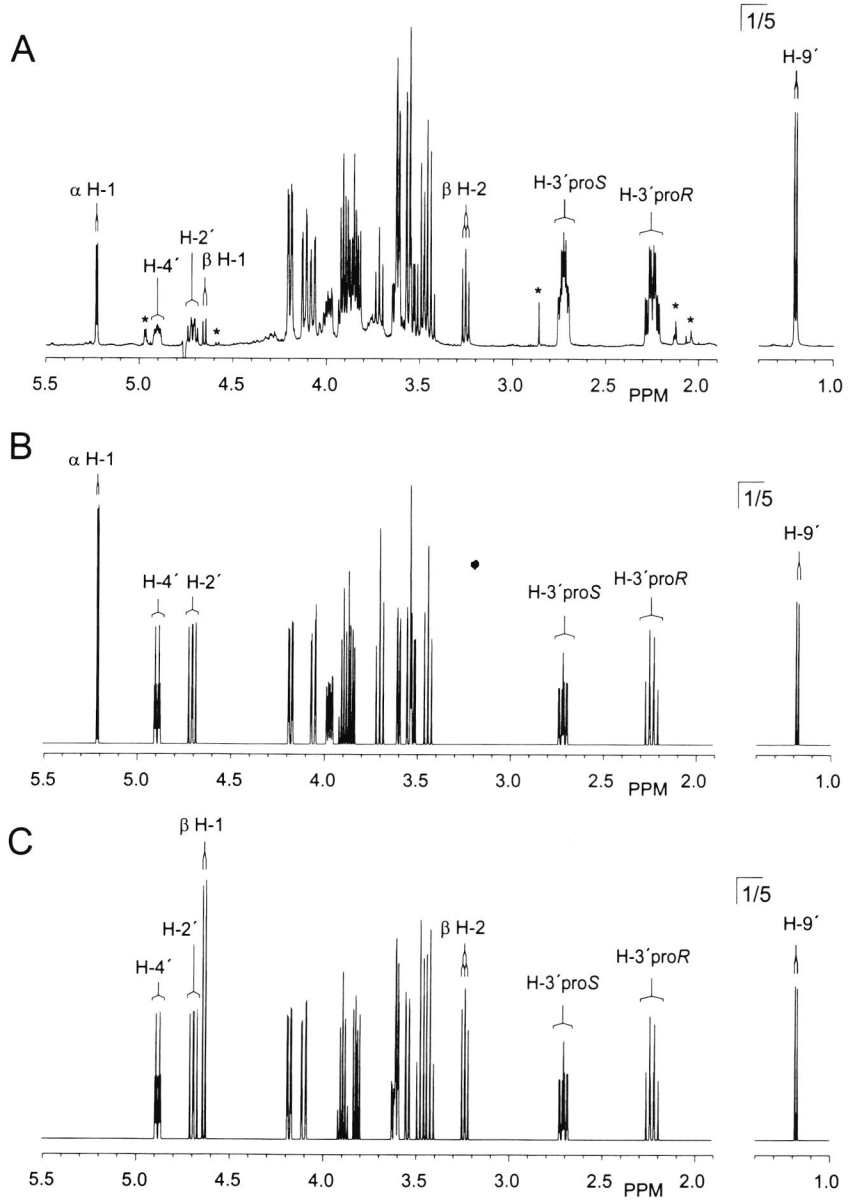

Figure 2. *1D ^{1}H NMR spectrum of (A)* ***1****, recorded at 500 MHz and 27 °C, and simulated spectra of* ***1*** *having (B) α and (C) β configurations of the Glc part, respectively. Asterisks (*) in spectrum A indicate impurities.*

Table 1. *^{1}H NMR chemical shifts[a] of **1**, **2**, and **3**, and ^{13}C NMR chemical shifts[b] of **1**, recorded in D_2O at 27 °C. Coupling constants are included in parentheses.*

	Proton		**1**[c]		**2**	**3**	Carbon	**1**
α-D-Glc*p*	H-1		5.205	($J_{1,2}$ 3.8)	5.296	5.224	C-1	92.9
	H-2		3.518	($J_{2,3}$ 9.8)	3.345	3.50	C-2	72.2
	H-3		3.694	($J_{3,4}$ 9.3)	n.d.[d]	3.70	C-3	73.6
	H-4		3.437	($J_{4,5}$ 10.0)	n.d.	3.52	C-4	70.3
	H-5		3.964	($J_{5,6proS}$ 2.0)	n.d.	3.93	C-5	71.0
	H-6pro*S*		4.051	($J_{5,6proR}$ 5.1)	n.d.	3.98	C-6	70.0
	H-6pro*R*		3.846	($J_{6proS,6proR}$ -11.0)	n.d.	3.78		
β-D-Glc*p*	H-1		4.629	($J_{1,2}$ 7.9)	4.685	4.643	C-1	96.8
	H-2		3.231	($J_{2,3}$ 9.5)	3.065	3.24	C-2	74.9
	H-3		3.468	($J_{3,4}$ 9.3)	n.d.	3.47	C-3	76.5
	H-4		3.420	($J_{4,5}$ 10.0)	n.d.	3.47	C-4	70.3
	H-5		3.606	($J_{5,6proS}$ 1.9)	n.d.	3.56	C-5	75.4
	H-6pro*S*		4.095	($J_{5,6proR}$ 6.0)	n.d.	4.03	C-6	70.4
	H-6pro*R*		3.812	($J_{6proS,6proR}$ -11.2)	n.d.	3.74		
C_9 part	H-2′	α	4.699	($J_{2',3'proS}$ 8.7)	3.971	3.77	C-2′	76.5
		β	4.686	($J_{2',3'proR}$ 10.7)				
	H-3′pro*S*	α	2.710	($J_{3'proS,3'proR}$ -12.3)	1.90	1.77	C-3′	28.0
		β	2.699	($J_{3'proS,4}$ 2.7)				
	H-3′pro*R*	α	2.233	($J_{3'proR,4}$ 10.3)	1.79	1.60		
		β	2.223					
	H-4′	α	4.886	($J_{4',5'}$ 2.6)	4.07	4.12	C-4′	79.5
		β	4.876					
	H-5′		4.173	($J_{5',6'}$ 9.3)	3.68	3.82	C-5′	69.3
	H-6′		3.539	($J_{6',7'}$ 1.4)	3.66	3.60	C-6′	71.0
	H-7′		3.594	($J_{7',8'}$ 7.1)	3.58	3.62	C-7′	74.5
	H-8′		3.887	($J_{8',9'}$ 6.5)	3.90	3.91	C-8′	69.4
	H-9′		1.180		1.179	1.200	C-9′	18.9

[a] In ppm relative to the signal of internal acetone at δ 2.225.
[b] In ppm relative to the α-anomeric signal of external [1-^{13}C]glucose at δ 92.9.
[c] Data were refined by simulation of the 1D ^{1}H NMR spectrum.
[d] n.d., not determined.

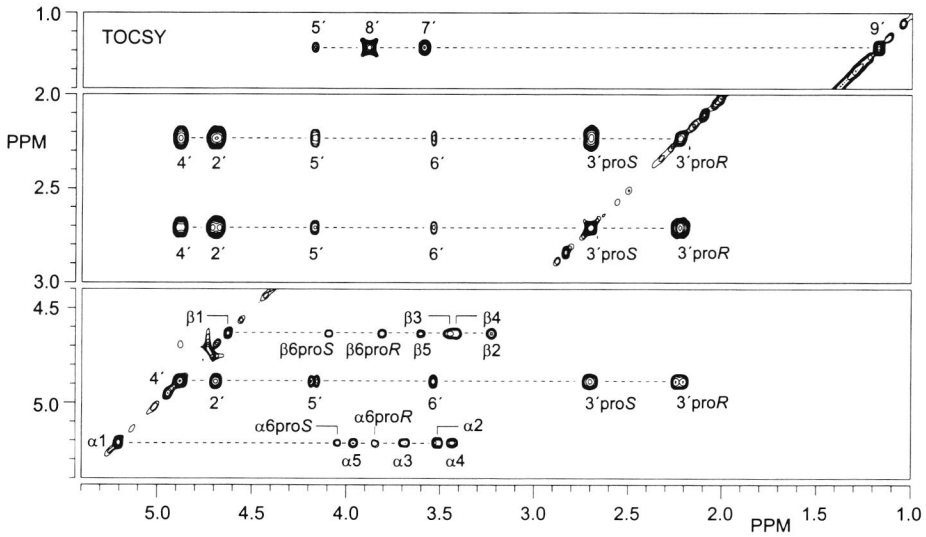

Figure 3. *Parts of the 500 MHz 2D TOCSY spectrum of* ***1****, recorded in* D_2O *at 27 °C. Diagonal peaks of the anomeric protons of the Glc*p *part, and of H-3′proR,3′proS,4′,9′ of the* C_9 *part are indicated. Labels near cross-peaks refer to the protons of the scalar-coupling network belonging to the diagonal peak. The absence of the H-2′ track in F2 is caused by HOD suppression.*

As indicated by NMR and MS analysis of **1**, it was released as an 1′,4′-lactone by hydrolysis of n-EPS. An aliquot of **1** was de-lactonized (→**2**) by adding NaOD prior to NMR analysis. The H-1,2 signals of the Glc*p* part and all the ^{1}H resonances of the C_9 part of **2** were assigned by means of TOCSY experiments (mixing times 25 → 250 ms), consistent with structure **2** depicted in Scheme 1. In addition, the ^{1}H signals of the component isolated from cr-EPS were assigned essentially as described for **1** (Table 1), indicating structure **3** (Scheme 1).

^{1}H-^{1}H coupling constants of compound **1** (Table 1) were determined by simulation of ^{1}H sub-spectra for the α- and β-anomers of **1** (Figures 2B and 2C). Two sets of chemical shifts are observed for H-2′,3′pro*R*,3′pro*S*,4′, induced by the two anomeric configurations of Glc*p*. The vicinal coupling constants $J_{4',5'}$ (2.6 Hz), $J_{5',6'}$ (9.3 Hz), $J_{6',7'}$ (1.4 Hz), and $J_{7',8'}$ (7.1 Hz) in the C_9 part indicate that the dihedral angles χ^1 (H-4′–C-4′–C-5′–H-5′), χ^2 (H-5′–C-5′–C-6′–H-6′), χ^3 (H-6′–C-6′–C-7′–H-7′), and χ^4 (H-7′–C-7′–C-8′–H-8′) are in the regions of ±60°, 180°, ±60°, and 180°, respectively [5].

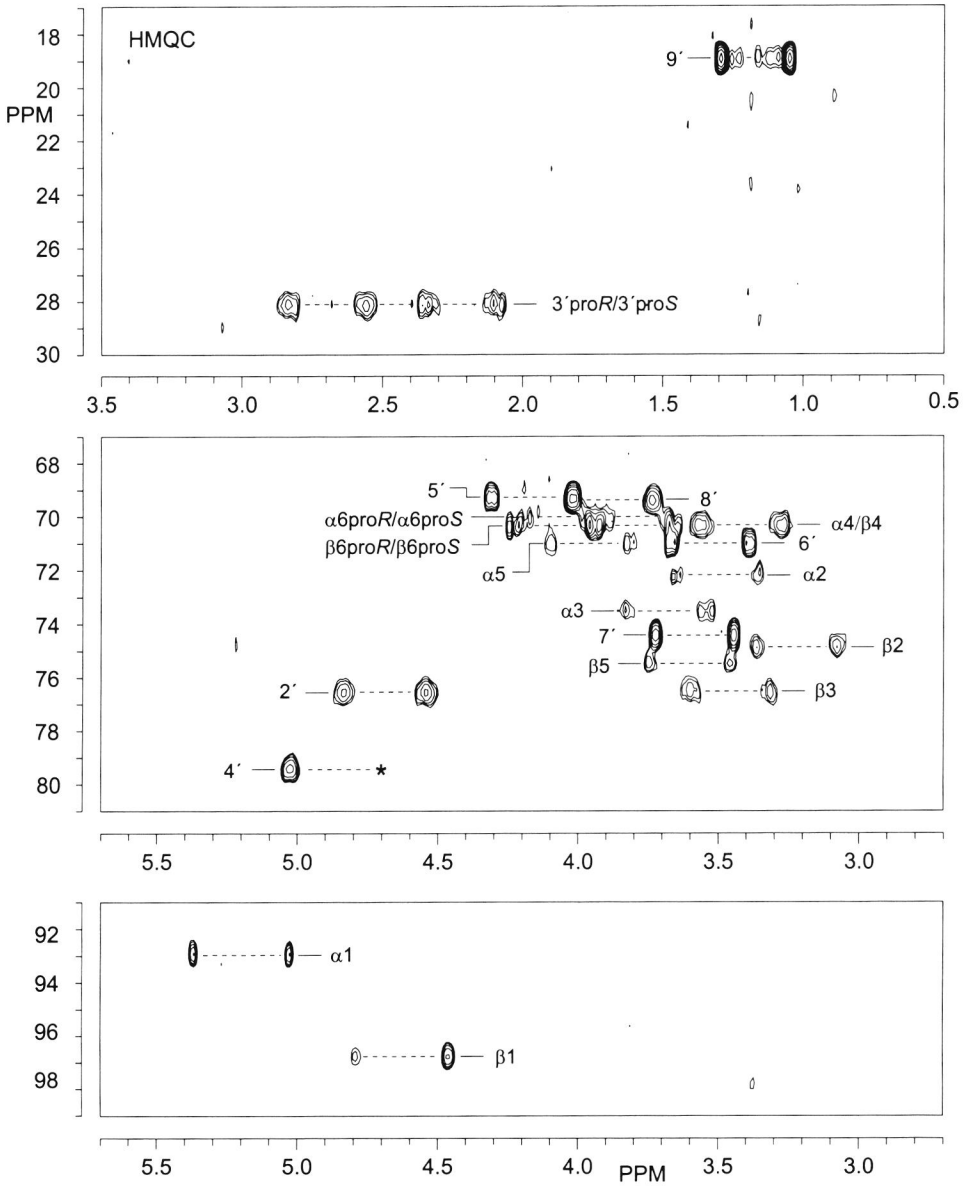

Figure 4. *Part of the 500 MHz ^{13}C-^{1}H HMQC spectrum of* ***1****, recorded in D_2O at 27 °C. α1 stands for the set of cross-peaks between H-1 and C-1 of the α-D-Glcp part, etc. The asterisk (*) indicates a signal lost by HOD suppression.*

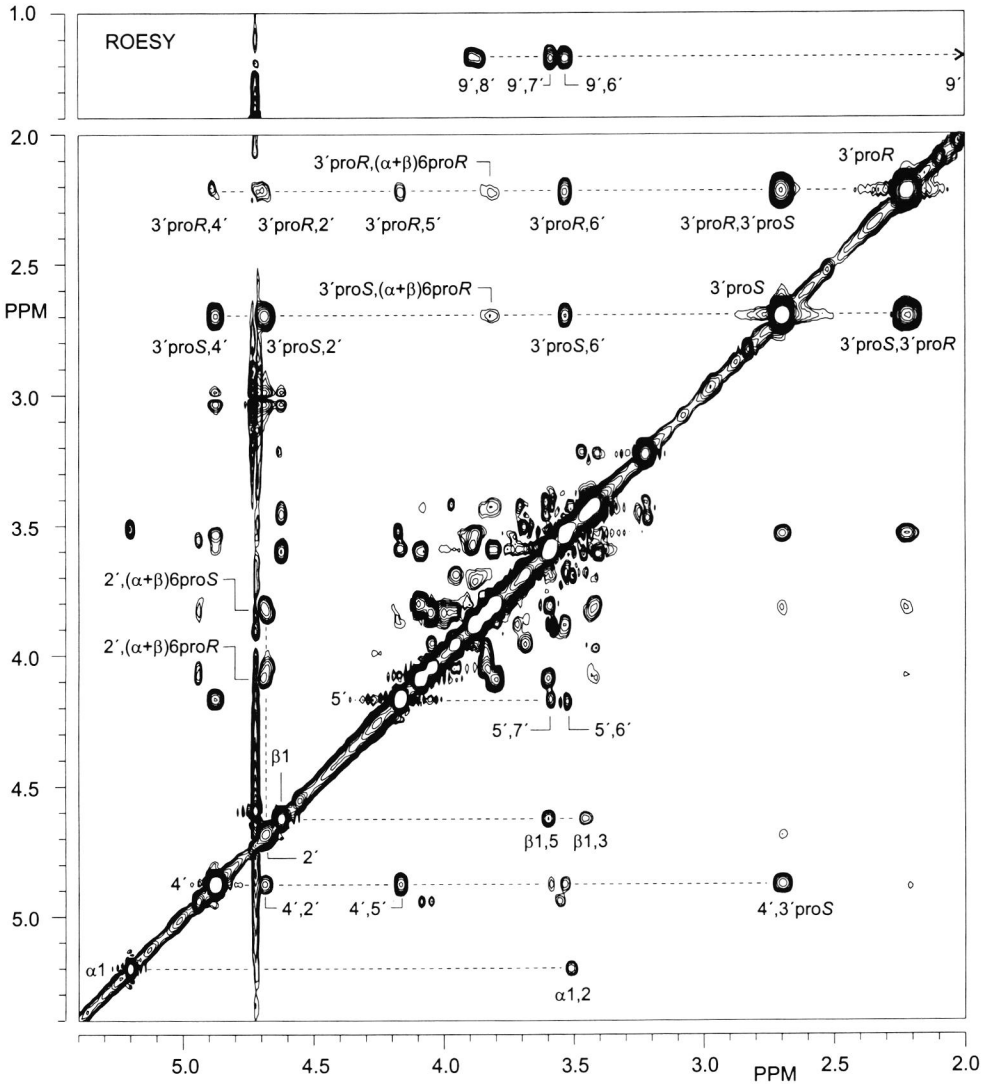

Figure 5. *500 MHz 2D ROESY spectrum of **1**, recorded in D_2O at 27 °C. α1 corresponds to the diagonal peak belonging to residue α H-1; α 1,2 refers to an intraresidual cross-peak between α H-1 and α H-2, and 3´proS,(α+β)6proR means an interresidual connectivity from H-3´proS to α H-6proR and β H-6proR, etc. The absence of the H-2´track in F2 is caused by HOD suppression.*

For the determination of the *R/S*-configurations at the chiral C-2′,4′ atoms, distance information for the intraresidual protons of **1** turned out to be essential. In the 2D ROESY spectrum (Figure 5) H-3′pro*S* showed strong cross-peaks with H-2′ and H-4′, whereas H-3′pro*R* showed weak cross-peaks with H-2′ and H-4′, proving H-2′,3′pro*S*,4′ to be located at the same side of the lactone ring. This observation excludes the 2′*S*,4′*R*- and 2′*R*,4′*S*-configurations. Cross-peaks of identical intensity observed on the H-2′ ROESY track to the H-6pro*R* and H-6pro*S* signals indicated an extended planar conformation for the C-5–C-6-O–C-2′ bonds from the Glc*p* to the C_9 part. This conformation allows for the determination of the absolute configuration of the chiral atoms in the lactone ring of the C_9 part of **1**. In the 2′*R*,4′*R*-configuration the methylene protons would be directed towards H-6pro*S* and in the 2′*S*,4′*S*-configuration towards H-6pro*R*. The cross-peaks observed on the H-3′pro*R* and H-3′pro*S* ROESY tracks to the H-6pro*R* signal show that these methylene protons are in the proximity of H-6pro*R*. These findings prove the *S*-configuration (2′*S*,4′*S*) at both chiral atoms in the lactone ring.

To determine the *R/S*-configurations at the chiral C-5′,6′,7′,8′ atoms, model structures with all possible chiral combinations for these atoms were computer-generated and investigated. The model structures were created with $\chi^1 = \pm 60°$, $\chi^2 = 180°$, $\chi^3 = \pm 60°$, and $\chi^4 = 180°$, in agreement with the vicinal coupling constants, resulting in 64 structures. The structures were labeled according to the configurations of the chiral C-5′,6′,7′,8′ atoms as follows: $\mathbf{C}_{RRRS}$ = model structure with 5′*R*,6′*R*,7′*R*,8′*S*-configuration, etc., taking into account that each label represents four conformers differing in χ^1 and χ^3.

The cross-peaks in the ROESY spectrum of **1**, originating from atoms separated by more than four bonds (H-3′pro*R*,H-6′, H-3′pro*S*,H-6′ and H-6′,9′), were used to check the 64 structures for violations of ^{1}H-^{1}H distances. To compensate for idealized dihedral angle values in the model structures, the upper proton distance was set to 3.6 Å, which is approximately 1 Å larger then the distances of H-3′pro*R*,H-6′, H-3′pro*S*,H-6′, and H-6′,9′, calculated from the ROE intensities. This resulted in eight possible configurations: $\mathbf{C}_{RRRS}$, $\mathbf{C}_{RRSR}$, $\mathbf{C}_{RSRS}$, $\mathbf{C}_{RSSR}$, $\mathbf{C}_{SRRS}$, $\mathbf{C}_{SRSR}$, $\mathbf{C}_{SSRS}$, and $\mathbf{C}_{SSSR}$. Evaluation of the computer-generated structures having the 5′*S*-configuration showed that due to significant differences in distances of H-3′pro*R*,H-6′ (~2.6 Å) and H-3′pro*S*,H-6′ (~3.6 Å) within these structures, the ROESY cross-peak H-3′pro*S*,H-6′ is expected to be much weaker than the cross-peak H-3′pro*R*,H-6′. This in contrast to the computer-generated structures with 5′*R*-configuration, where the two cross-peaks are expected to have the same intensity. The cross-peaks, observed in the ROESY spectrum (Figure 5), have equal intensity and therefore prove the 5′*R*-configuration. This reasoning left four possible configurations for the C-5′–C-8′ fragment: $\mathbf{C}_{RRRS}$, $\mathbf{C}_{RRSR}$,

$\mathbf{C}_{RSRS}$, and $\mathbf{C}_{RSSR}$. The use of additional ROESY cross-peaks did not further reduce the number of allowed model structures. Therefore, the conformational stability of the four remaining structures was examined by investigating the probabilities of relevant dihedral angles with the method of adaptive umbrella sampling of the potential-of-mean-force [6]. Free energy differences between conformers, obtained by sampling of the individual dihedral angles, were translated into rotamer population distributions (Table 2).

Table 2. *Probability distributions*[a] *of relevant dihedral angles of different configurations of the chiral C-5′–C-8′ part of* ***1****, and calculated and experimentally obtained coupling constants.*

Configuration	Dihedral angles[b] and vicinal coupling constants					
	χ^1	$J_{4',5'}$	χ^2	$J_{5',6'}$	χ^3	$J_{6',7'}$
$\mathbf{C}_{RRRS}$[c]	180 (65), -75 (24)	5.9	180 (>90)	8.5	-175 (>90)	7.5
$\mathbf{C}_{RRSR}$	-75 (47), -175 (35)	3.7	180 (>90)	8.5	60 (>90)	2.2
$\mathbf{C}_{RSRS}$	175 (>90)	8.4	65 (>90)	1.7	n.d.[d]	n.d.
$\mathbf{C}_{RSSR}$	175 (>90)	8.4	65 (>90)	1.7	n.d.	n.d.
Experimental ^3J		2.6		9.3		1.4

[a] Probability distributions for χ values (degrees) are given in parentheses in %; conformations contributing for less than 10% are not listed.

[b] χ^1 = H-4′–C-4′–C-5′–H-5′, χ^2 = H-5′–C-5′–C-6′–H-6′, and χ^3 = H-6′–C-6′–C-7′–H-7′.

[c] $\mathbf{C}_{RRRS}$ = model structure with 5′*R*,6′*R*,7′*R*,8′*S*-configuration etc.

[d] n.d., not determined.

From the obtained dihedral angles, coupling constants were calculated using a modified Karplus equation [5]. For conformations with multiple dihedral angles, weighted-average coupling constants were calculated. From these calculated coupling constants (Table 2) the computer-generated structures with 5′*R*,6′*S*-configuration could easily be excluded. This was confirmed by comparison of experimentally obtained ^{1}H chemical shifts and vicinal coupling constants of the C_9 part of compound **1** with those of NMR data of deoxyalditols [7] (Table 3). The vicinal coupling constants of 1-deoxy-L-Gal-ol, in which the C-5–C-1 fragment has the same configuration as the C-5′–C-9′ fragment of $\mathbf{C}_{RSSR}$, do not resemble the

corresponding coupling constants of the novel nononic acid. In a similar way, the vicinal coupling constants of 1-deoxy-D-Xyl-ol, in which the C-4–C-1 fragment has the same configuration as the C-6′–C-9′ fragment of $\mathbf{C}_{RSRS}$, are not in agreement with the vicinal coupling constants of **1**. This leaves two configurations to be examined: $\mathbf{C}_{RRRS}$ and $\mathbf{C}_{RRSR}$. Evaluation of the probability distribution of χ^3 of these conformations indicated preferences for $\chi^3 = -175°$ and $\chi^3 = 60°$, in $\mathbf{C}_{RRRS}$ and $\mathbf{C}_{RRSR}$, respectively. Based on comparison of the coupling constants calculated from the preferred dihedral angles ($\mathbf{C}_{RRRS}$ $J_{6',7'} = 7.5$ Hz and $\mathbf{C}_{RRSR}$ $J_{6',7'} = 2.2$ Hz), with the experimental coupling constant of **1** ($J_{6',7'} = 1.4$ Hz), $\mathbf{C}_{RRRS}$ was rejected. This was confirmed by comparison of vicinal coupling constants of the C-4–C-1 fragment of 1-deoxy-D-Ara-ol and 1-deoxy-L-Gal-ol [7], which is the mirror image of the C-6′–C-9′ fragment of $\mathbf{C}_{RRRS}$, with the coupling constants of **1**. Finally, comparison of the vicinal coupling constants of the C-5′–C-9′ fragment of $\mathbf{C}_{RRSR}$ with those of the C-5–C-1 fragment of 1-deoxy-D-Glc-ol, which is the mirror image of the C-5′–C-9′ fragment of $\mathbf{C}_{RRSR}$, confirmed $\mathbf{C}_{RRSR}$ to represent the correct configuration.

Table 3. *^1H NMR chemical shifts and ^1H-^1H coupling constants of deoxyalditols [7] and the C-5′–C-9′ fragment of compound **1**, in D_2O.*

Compound	H-1 ($J_{1,2}$)	H-2 ($J_{2,3}$)	H-3 ($J_{3,4}$)	H-4 ($J_{4,5}$)	H-5	H-6
1-deoxy-D-Ara-ol	1.25 (6.6)	4.04 (3.0)	3.40 (7.5)	3.74 (3.0)	3.83/3.66	-
1-deoxy-D-Xyl-ol	1.24 (6.5)	3.93 (5.8)	3.42 (3.5)	3.81 (4.6)	3.72/3.66	-
1-deoxy-L-Gal-ol	1.24 (6.7)	4.09 (1.9)	3.47 (9.1)	3.63 (1.7)	3.96	3.68/3.67
1-deoxy-D-Glc-ol	1.23 (6.5)	3.94 (7.2)	3.63 (1.8)	3.66 (8.5)	3.79	3.86/3.68
	H-9′ ($J_{8',9'}$)	H-8′ ($J_{7',8'}$)	H-7′ ($J_{6',7'}$)	H-6′ ($J_{5',6'}$)	H-5′	
1	1.180 (6.5)	3.887 (7.1)	3.594 (1.4)	3.539 (9.3)	4.173	

In conclusion, the absolute configurations at the chiral centers in the C_9 part of **1** are determined to be 2′*S*,4′*S*,5′*R*,6′*R*,7′*S*,8′*R*. To get an impression of the three dimensional time-average structure of compound **1**, a short molecular dynamics (MD) simulation starting from the calculated favorite conformation was performed. A snap shot of the simulated methyl glycoside of **1**, together with intraresidual ROEs, is presented in Figure 6.

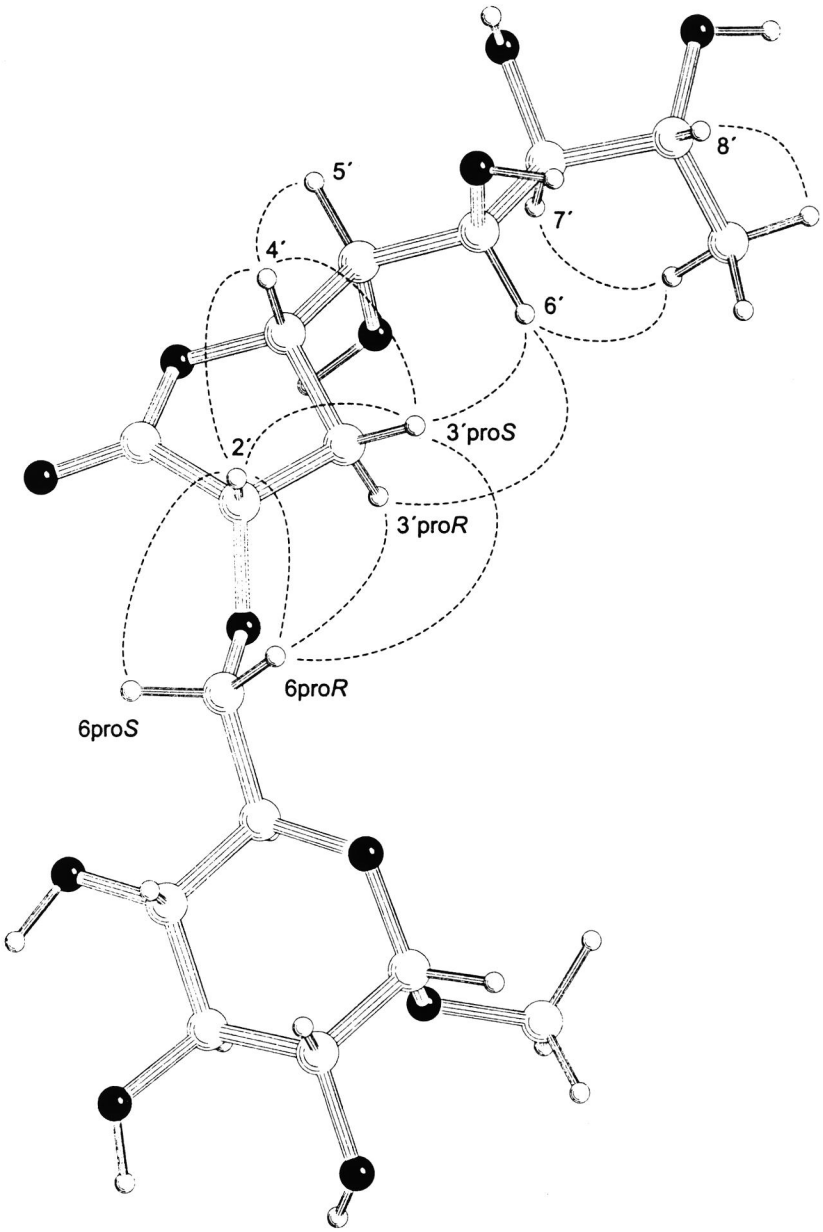

Figure 6. *Snap shot from the MD simulation of the methyl α-glycoside of compound* ***1****. Dotted lines indicate ROEs observed in the 2D ROESY spectrum. Aliphatic protons were re-attached.*

Concluding remarks

In this study, NMR spectroscopy supplemented with MD simulations were found to be extremely useful for the determination of the absolute configurations of the chiral centers in the C_9 part of **1**. Especially where ROESY data were insufficient, coupling constants calculated from population distributions obtained from adaptive umbrella sampling of the potential-of-mean-force, could be used to determine the configurations of the chiral atoms. The combined results obtained by chemical analyses, mass spectrometry, NMR spectroscopy, and MD simulations, demonstrated that the structure of **2** is 6-*O*-(3′,9′-dideoxy-D-*threo*-D-*altro*-nononic acid-2′-yl)-D-Glc. In this compound acid-catalyzed lactonization affords an 1′,4′-lactone. The lactone-containing C_9 part of **1** has predominantly an extended planar conformation. The repulsive 1,3-parallel interaction of oxygen within the lactone ring and O-6′ results in a 'bent' or 'sickle' conformation of C-3′,4′,5′,6′. These conformation characteristics are in agreement with results obtained from studies performed on solution conformations of alditols [8]. They showed a predominantly extended planar arrangement for the alditols, and indicated the presence of bent conformations in order to avoid 1,3-parallel interactions between oxygen atoms.

The nononic acid linked via an ether-bond to a monosaccharide presents a novel constituent of naturally occurring polysaccharides. Detailed analysis of the complete EPS repeating unit will be reported elsewhere.

4.3. Experimental

Culture conditions of microorganism and isolation of exopolysaccharide. — *S. thermophilus* 8S, obtained from NIZO food research (Ede, The Netherlands), was cultivated in reconstituted skimmed milk, and the EPS was isolated and purified as described [1].

Isolation of the unknown sugar component. — The exopolysaccharide (5 mg) was hydrolyzed using 2 M trifluoroacetic acid (2 h, 100 °C), and the obtained mixture lyophilized. The residue was dissolved in water and fractionated on graphitized carbon [9]. The unknown component, eluted with 40% acetonitrile containing 0.05% trifluoroacetic acid, was lyophilized prior to analysis. A similar protocol was followed for the carboxyl-reduced ($NaBH_4$) polysaccharide.

Carboxyl reduction. — Carboxyl reduction of the EPS was performed as described [10]. A solution of polysaccharide (2 mg) in 2-(4-morpholino)-ethanesulfonic acid (0.2 M, 1 mL, pH 4.75), containing *N*-ethyl-*N*-(3-dimethylaminopropyl)-carbodiimidehydrochloride (30 mg), was stirred for 90 min at room temperature. After reduction with $NaBD_4$ (10 mg, 1 h), the obtained material was neutralized with 1.5 M HCl, desalted on graphitized carbon, and lyophilized prior to analysis. To obtain a complete carboxyl reduction the procedure was repeated twice.

Ether bond cleavage. — To a cooled solution of polysaccharide in dry dichloromethane (1 mg/mL, -80 °C), freshly distilled BBr_3 was added. The mixture was kept at -80 °C for 30 min, then slowly brought to room temperature. After 18 h the excess of reagent was decomposed with water, the solution evaporated to dryness, and boric acid removed by coevaporation with methanol.

Monosaccharide and methylation analysis. — Monosaccharide analysis, including the determination of the absolute configurations, and methylation analysis were performed as described previously [1]. Obtained derivatives were analyzed by GLC and GLC–EIMS as described [1].

Mass spectrometry. — Matrix-assisted laser desorption ionization time-of-flight mass spectrometry (MALDI-TOF-MS) experiments were performed as described previously [1].

NMR spectroscopy. — 1D and 2D NMR spectra were recorded in D_2O on a Bruker AMX-500 spectrometer (Bijvoet Center, Department of NMR Spectroscopy). NMR spectra were recorded and processed as described [1]. Spectral simulations were performed using in-house written software based on the LAOCOON program [11]. Vicinal and geminal coupling constants were taken positively and negatively, respectively. Proton distances were estimated from cross-peak intensities in the 2D ROESY spectrum and were calibrated to distances on the basis of distances of the geminal methylene protons H-6pro*R*,H-6pro*S* and H-3′pro*R*,H-3′pro*S* (1.8 Å).

Adaptive umbrella sampling of the potential-of-mean-force. — Potential-of-mean-force (PMF) calculations [6] were performed on theoretical *R*/*S*-configurations of the C_9 part of compound **1**; to this end the Glc residue was replaced by an *O*-methyl group. For the calculations the GROMOS program [12] with the standard force field for carbohydrates [13] was used. All simulations were divided into jobs of 10 ps. Dihedral angle values were partitioned into 72 classes, each having a width of 5°. The derivative of the PMF was evaluated as a 12-term Fourier series. Each system was simulated for 1.0-5.0 ns, and the final PMF for each system was used to obtain the rotamer population distributions of the sampled dihedral angle.

Molecular dynamics simulations. — An MD simulation in water was performed using the GROMOS program [12] with the standard force field for carbohydrates [13]. The molecule was placed in a truncated octahedron with periodic boundary conditions containing approximately 500 water molecules using the SPC/E model [14]. All bond lengths were kept fixed using the SHAKE procedure [15]. Simulations were performed at constant temperature (300K) and pressure (1 atm.) with relaxation times of 0.1 and 0.5 ps, respectively. For the simulations a cut-off radius of 0.8 nm, a time step of 2 fs and a total simulation time of 5 ns were used.

Acknowledgements

This work was supported by the PBTS Research Program with financial aid from the Ministry of Economic Affairs and by the Integral Structure Plan for the Northern Netherlands from the Dutch Development Company. The authors thank F. Kingma (NIZO food research, Ede, The Netherlands) for cultivation of *S. thermophilus* 8S, and Drs. S.R. Haseley and B.R. Leeflang for stimulating discussions.

References

[1] E.J. Faber, J.P. Kamerling, J.F.G. Vliegenthart, *Carbohydr. Res.*, 2000, Submitted.
[2] Y. Nishida, H. Ohrui, H. Meguro, *Tetrahedron Lett.*, 25 (1984) 1575-1578.
[3] L. Poppe, *J. Am. Chem. Soc.*, 115 (1993) 8421-8426.
[4] K. Bock, C. Pedersen, *Adv. Carbohydr. Chem. Biochem.*, 41 (1983) 27-66.
[5] C.A.G. Haasnoot, F.A.A.M. de Leeuw, C. Altona, *Tetrahedron*, 36 (1980) 2783-2792.
[6] R.W.W. Hooft, B.P. van Eijck, J. Kroon, *J. Chem. Phys.*, 97 (1992) 6690-6694.
[7] D.G. Gillies, D. Lewis, *J. Chem. Soc., Perkin Trans. 2*, (1985) 1155-1159.
[8] S.J. Angyal, *Pure Appl. Chem.*, 59 (1987) 1521-1528.
[9] N.H. Packer, M.A. Lawson, D.R. Jardine, J.W. Remond, *Glycoconjugate J.*, 15 (1998) 737-747.
[10] R.L. Taylor, H.E. Conrad, *Biochemistry*, 11 (1972) 1383-1388.
[11] S. Castellano, A.A. Bothner-By, *J. Chem. Phys.*, 41 (1964) 3863-3869.
[12] W.F. van Gunsteren, 'GROMOS, Groningen Molecular Simulation Package', University of Groningen, The Netherlands, 1987.
[13] S.A.H. Spieser, J.A. van Kuik, L.M.J. Kroon-Batenburg, J. Kroon, *Carbohydr. Res.*, 322 (1999) 264-273.
[14] H.J.C. Berendsen, J.P.M. Postma, W.F. van Gunsteren, J. Hermans, in B. Pullman (Ed.), *Intermolecular Forces*, Reidel, Dordrecht, 1981, pp. 331-342.
[15] J.-P. Ryckaert, G. Ciccotti, H.J.C. Berendsen, *J. Comput. Phys.*, 23 (1977) 327-341.

Chapter 5

Characterization of the exopolysaccharide produced by *Streptococcus thermophilus* 8S containing an open chain nononic acid

Elisabeth J. Faber, Daan J. van Haaster, Johannis P. Kamerling, and Johannes F.G. Vliegenthart

Bijvoet Center, Department of Bio-Organic Chemistry, Utrecht University, PO Box 80.075, NL-3508 TB Utrecht, The Netherlands.

Abstract

The exopolysaccharide produced by *Streptococcus thermophilus* 8S in reconstituted skimmed milk is a heteropolysaccharide containing D-galactose, D-glucose, D-ribose, and *N*-acetyl-D-galactosamine in a molar ratio of 2:1:1:1. Furthermore, the polysaccharide contains 1 equivalent of a novel open chain nononic acid constituent, 3,9-dideoxy-D-*threo*-D-*altro*-nononic acid, ether-linked via C-2 to C-6 of an additional D-glucose per repeating unit. Methylation analysis and 1D/2D NMR studies (^{1}H and ^{13}C) performed on the native polysaccharide, and mass spectrometric and NMR analyses of the oligosaccharide obtained from the polysaccharide by de-*N*-acetylation followed by deamination and reduction demonstrated the "hepta"saccharide repeating unit to be:

→4)-α-D-Gal*p*-(1→2)-β-D-Rib*f*-(1→4)-β-D-Gal*p*-(1→4)-β-D-Glc*p*-(1→7′)-Sug-(1→4)-β-D-Gal*p*NAc-(1→

in which Sug is 6-*O*-(3′,9′-dideoxy-D-*threo*-D-*altro*-nononic acid-2′-yl)-α-D-glucopyranose.

Elisabeth J. Faber, Daan J. van Haaster, Johannis P. Kamerling, and Johannes F.G. Vliegenthart, *Manuscript in preparation.*

5.1. Introduction

Microbial exopolysaccharides (EPSs) are employed in the food industry as viscosifying, stabilizing, emulsifying and gelling agents [1]. The texturizing properties of EPSs in fermented dairy products [2] in combination with the GRAS (Generally Recognized as Safe) status of EPS-producing lactic acid bacteria, make these EPSs of interest for the food industry. To understand the relationship between the structure of EPSs and their physical properties, structural studies have been performed on EPSs produced by various species of the *Lactobacillus*, *Lactococcus*, and *Streptococcus* genera ([3], and references cited therein).

The lactic acid bacterium *Streptococcus thermophilus* is used in combination with other lactic acid bacteria like *Lactobacillus delbrueckii* subsp. *bulgaricus* as starter culture for fermentations in dairy industry. In the last decade, the primary structure of the EPSs secreted by seven *S. thermophilus* strains [4-8] were elucidated. A number of the EPSs are structurally related polysaccharides and include the EPSs produced by *S. thermophilus* Sfi12 [5], OR 901 [6], Rs [7], Sts [7], and S3 [8], of which the OR 901, Rs and Sts EPSs have identical repeating units. These EPSs are characterized by the presence of a repeating pentameric backbone containing the →3)-α-D-Gal*p*-(1→3)-α-L-Rha*p*-(1→2)-α-L-Rha*p*-(1→2)-α-D-Gal*p*-(1→3)-Hex*p*-(1→ sequence, wherein the fifth residue is α-D-Glc*p* for Sfi12, α-D-Gal*p* for OR 901, Rs and Sts, and β-D-Gal*p* for S3. Furthermore, the EPSs differ in the attachment site of the side chain, as well as in the composition of the side chain.

Recently [9], we reported for the EPS produced by *S. thermophilus* 8S the occurrence of a Glc residue etherified at O-6 with a novel open chain nononic acid, i.e. 6-*O*-(3′,9′-dideoxy-D-*threo*-D-*altro*-nononic acid-2′-yl)-D-glucopyranose. Here, we report the complete structure of this EPS.

5.2. Results and discussion

Isolation, purification, and composition of the exopolysaccharide

The EPS produced by *S. thermophilus* 8S in reconstituted skimmed milk was isolated as an ethanol precipitate from the protein-free supernatant. The EPS was purified by fractionated acetone precipitation, followed by gel filtration of the 30 and 40% acetone-precipitated fractions on Sephacryl S-500. The purity of the isolated EPS was confirmed by 1D ^{1}H NMR spectroscopy.

GLC monosaccharide analysis, including absolute configuration determination, of the native EPS (n-EPS) showed the presence of D-Gal, D-Glc, D-Rib, and D-GalNAc in a molar ratio of 2:1:1:1. In addition, GLC peaks were observed originating from a novel constituent, 6-*O*-(3′,9′-dideoxy-D-*threo*-D-*altro*-nononic acid-2′-yl)-D-glucopyranose [9]. The molar ratio of this constituent in terms of peak areas was 0.7 compared to Glc. Methylation analysis of n-EPS revealed, besides the occurrence of a product stemming from the novel constituent, the presence of 4-substituted Glc*p*, 4-substituted Gal*p*, 4-substituted Gal*p*NAc, and 2-substituted Rib*f* (for a proof of the pyranose ring forms, see NMR analysis) in a molar ratio of 1.0:1.7:0.6:0.7. Methylation analysis of n-EPS after carboxyl-reduction (cr-EPS) yielded also the substitution pattern of the novel constituent: 7′-substituted 6-*O*-(3′,9′-dideoxy-nonitol-2′-yl)-Glc*p* [9]. Based on these results, a linear heteropolysaccharide is indicated.

The 1D ^{1}H NMR spectrum of n-EPS (Figure 1A) contained six well-resolved anomeric signals, labeled **A** to **F** following increasing anomeric proton chemical shift values. The anomeric signal data of the residues **A** (δ 4.473, $^{3}J_{1,2}$ 7.9 Hz), **B** (4.621, $^{3}J_{1,2}$ 8.0 Hz), and **C** (δ 4.766, $^{3}J_{1,2}$ 7.9 Hz) demonstrated β-pyranose ring forms, and those of residues **D** (δ 4.952, $^{3}J_{1,2}$ 3.7 Hz) and **E** (δ 5.178, $^{3}J_{1,2}$ 3.1 Hz) α-pyranose ring forms. In addition, the H-1 signal data of residue **F** (δ 5.358, $^{3}J_{1,2}$ <2 Hz) suggested a furanose ring form. Methyl and methylene signals were detected at δ 1.224 and δ 1.88, respectively, originating from the nononic acid part in residue **D**, being the novel constituent 6-*O*-(3′,9′-dideoxy-D-*threo*-D-*altro*-nononic acid-2′-yl)-α-D-glucopyranose (Sug, *vide infra*). Furthermore, a characteristic signal at δ 2.057 was observed, originating from the *N*-acetyl group of Gal*p*NAc.

De-*N*-acetylation and deamination of the native polysaccharide

Owing to the presence of GalNAc in the linear polysaccharide chain (*vide supra*), n-EPS could be subjected to de-*N*-acetylation followed by deamination in order to generate an oligosaccharide repeating unit fragment. After reduction with $NaBD_4$, the obtained material was fractionated on CarboPac PA-1 yielding one major fraction, having the monosaccharide composition of Gal, Rib, and Glc in the molar ratio of 2:1:1 (GLC analysis), with the deamination product of Gal*p*NAc (2,5-anhydro-Tal-ol-*1-d*) in a molar ratio of 1 in terms of peak areas compared to Glc, and with traces of product stemming from Sug. Methylation analysis of the oligosaccharide demonstrated the presence of terminal Gal*p*, 4-substituted Gal*p*, 4-substituted Glc*p*, 2-substituted Rib*f*, and 4-substituted 2,5-anhydro-Tal-ol-*1-d* in a molar ratio of 1.1:0.9:1.0:0.8:0.8 (based on peak areas).

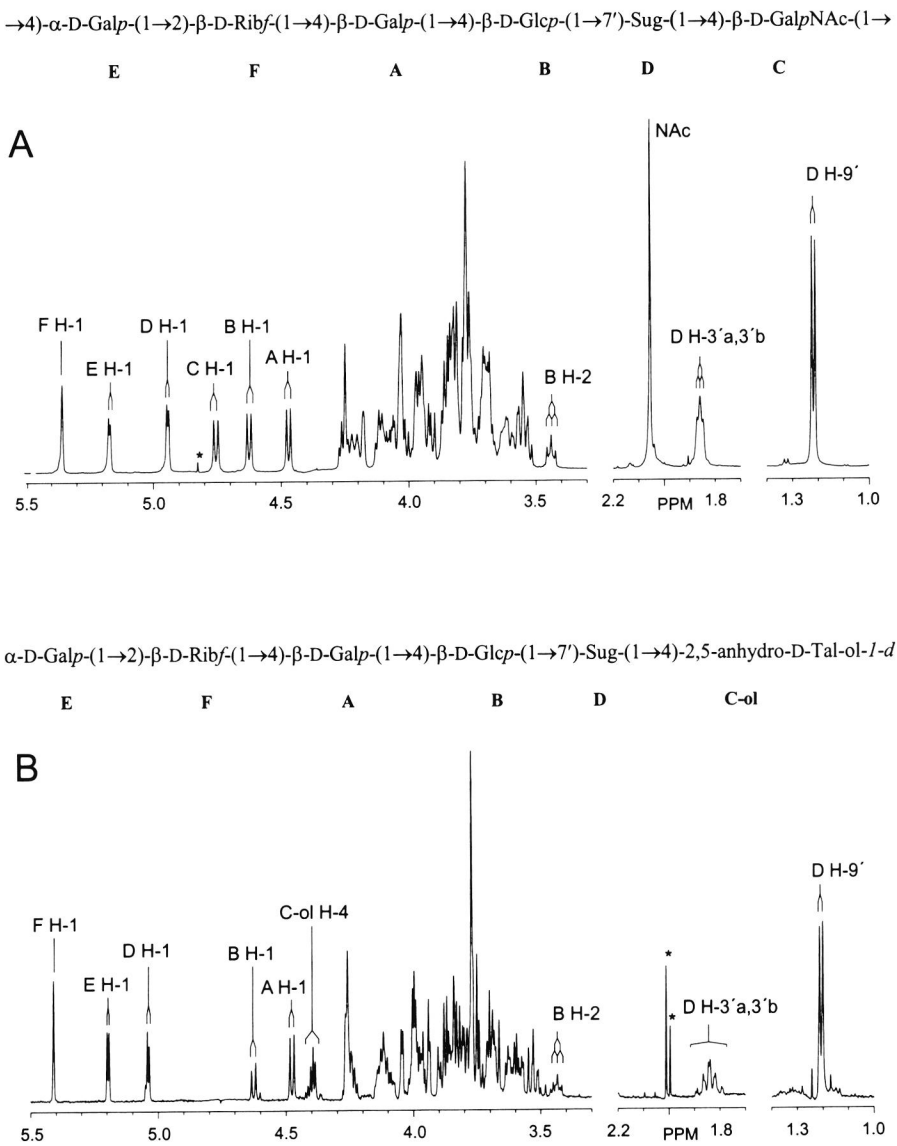

Figure 1. *500-MHz ^1H NMR spectrum of (A) n-EPS produced by* S. thermophilus *8S, recorded in D_2O at 64 ℃, and of (B) the oligosaccharide-alditol generated by de-*N*-acetylation/ deamination/reduction of n-EPS, recorded in D_2O at 27 ℃. Signals marked with an asterisk (*) stem from impurities. Sug = 6-*O*-(3′,9′-dideoxy-D-*threo*-D-*altro*-nononic acid-2′-yl)-α-D-glucopyranose.*

In order to obtain information on the sequence of the monosaccharides, the isolated oligosaccharide was analyzed by nanoES-CID tandem mass spectrometry. The obtained fragment ions were labeled according to the nomenclature of Domon and Costello [10]. In the ES spectrum a sodium-cationized $[M+Na]^+$ pseudomolecular ion was observed at *m/z* 1204 corresponding to $Hex_3Pent_1Sug_1anhydroHex_1$-ol-*1-d*. Furthermore, a $[M+Na]^+$ ion was present at *m/z* 1186, arising from the loss of water due to the formation of an intraresidual lactone in the nononic acid part of Sug [9]. The tandem mass spectrum obtained on collision activation of the pseudomolecular ion at *m/z* 1204 (Figure 2) contained a series of sodium-cationized $\mathbf{B_n}$ and Yn sequence ions at *m/z* 479, 641, 877, 1039, and *m/z* 586, 748, 910, 1042, respectively, consistent with a linear "hepta"saccharide Hex→Pent→Hex→Hex→Sug→anhydro-Hex-ol-*1-d*. In addition to the $\mathbf{B_n}$ and $\mathbf{Y_n}$ ions, a secondary fragment ion was observed at *m/z* 421 originating from the loss of anhydro-Hex-ol-*1-d* from the $\mathbf{Y_2}$ ion (586 – 165).

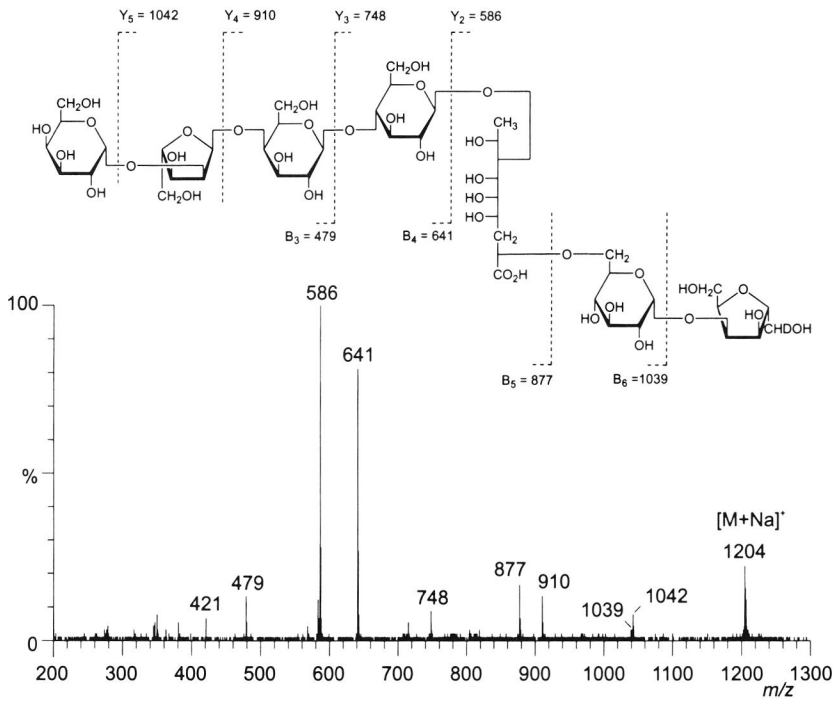

Figure 2. *Positive-ion mode nanoES-CID tandem mass spectrum of m/z 1204 ($[M+Na]^+$) of the oligosaccharide-alditol generated by de-*N*-acetylation/deamination/ reduction of n-EPS.*

In the 1D ^{1}H NMR spectrum of the isolated oligosaccharide (Figure 1B) five anomeric signals were observed at δ 4.475 (residue **A**, $^{3}J_{1,2}$ 7.9 Hz; β-pyranose), δ 4.625 (residue **B**, $^{3}J_{1,2}$ 7.8 Hz; β-pyranose), δ 5.037 (residue **D**, $^{3}J_{1,2}$ 3.9 Hz; α-pyranose), δ 5.194 (residue **E**, $^{3}J_{1,2}$ 3.4 Hz; α-pyranose), and δ 5.408 (residue **F**, $^{3}J_{1,2} < 2$ Hz; furanose), respectively. The absence of signals under the HOD signal (δ 4.76) was confirmed by a 1D ^{1}H NMR experiment at 64 °C (data not shown). In addition to signals in the anomeric region (δ 4.4 – 5.5), well-resolved signals were observed at δ 1.205 (CH_3) and δ ~1.83 (CH_2), originating from the nononic acid part in residue **D**. Comparison of the ^{1}H NMR spectrum of the oligosaccharide with that of n-EPS revealed **C** to be the Gal*p*NAc residue, since the anomeric signal of **C** is absent in the spectrum of the oligosaccharide. The ^{1}H resonances listed in Table 1, were assigned essentially as described for n-EPS (*vide infra*). The signal at δ 4.40, assigned to **C**-ol H-4 by comparison with 2,5-anhydro-D-Tal-ol [11], was used as starting point for the assignment of the **C**-ol H-2,3,5,6a,6b resonances. Interresidual connectivities deduced from a 2D ROESY spectrum, yielded evidence for the **E**-(1→2)-**F**-(1→4)-**A**-(1→4)-**B**-(1→7′)-**D**-(1→4)-**C**-ol sequence. The combined results from chemical analysis, mass spectrometry, and NMR studies allowed the oligosaccharide to be formulated as a "hepta"saccharide with the following structure:

α-D-Gal*p*-(1→2)-β-D-Rib*f*-(1→4)-β-D-Gal*p*-(1→4)-β-D-Glc*p*-(1→7′)-Sug-(1→4)-2,5-anhydro-D-Tal-ol-*1-d*

E **F** **A** **B** **D** **C**-ol

2D NMR spectroscopy of the native polysaccharide

By means of 2D TOCSY, 2D NOESY, and ^{13}C-^{1}H HMQC experiments most of the ^{1}H chemical shifts for n-EPS could be assigned (Table 1). As an example, the TOCSY spectrum with a mixing time of 300 ms is presented in Figure 3.

The ^{1}H resonances of **A** H-2,3,4, **B** H-2,3,4,5,6a,6b, **C** H-2,3,4,5, **D** H-2,3,4,5, **E** H-2,3,4,5, and **F** H-2,3,4,5a,5b were assigned via connectivities with the corresponding anomeric signals in the TOCSY spectra using increasing mixing times. The **A** H-5 resonance was determined on the **A** H-4 track in the TOCSY spectrum. The overlap of **A** H-3 and **A** H-5 was confirmed in the ^{13}C-^{1}H HMQC spectrum (Figure 4). The resonances of **A** H-6a,6b were assigned via their correlation to the corresponding ^{13}C resonance in the ^{13}C-^{1}H HMQC spectrum. The H-6 signal of residue **C** could be assigned via the **C** H-4 TOCSY track. The

Table 1. *^{1}H NMR chemical shifts[a] and ^{13}C NMR chemical shifts[b] of native EPS (n-EPS) recorded in D_2O at 64 °C and of the isolated oligosaccharide alditol (oligo) recorded in D_2O at 27 °C. Coupling constants are given in parentheses.*

Residue	Proton	n-EPS	oligo	*Carbon*	n-EPS
A	H-1	4.473 (7.9)	4.475 (7.9)	C-1	103.6 (160)
	H-2	3.54	3.53	C-2	70.8
	H-3	3.77	3.79	C-3	73.7
	H-4	4.03	4.04	C-4	77.2
	H-5	3.76	3.77	C-5	75.4
	H-6a	~3.77	n.d.[c]	C-6	61.8
	H-6b	~3.77	n.d.		
B	H-1	4.621 (8.0)	4.625 (7.8)	C-1	103.9 (161)
	H-2	3.44	3.43	C-2	74.1
	H-3	3.71	3.69	C-3	75.0
	H-4	3.70	3.69	C-4	79.5
	H-5	3.64	3.61	C-5	75.5
	H-6a[d]	3.96	3.95	C-6	60.3
	H-6b[d]	3.83	3.84		
C	H-1	4.766 (7.9)	-	C-1	103.5 (162)
	H-2	3.93	-	C-2	53.8
	H-3	3.85	-	C-3	71.5
	H-4	4.03	-	C-4	77.2
	H-5	3.72	-	C-5	76.0
	H-6a	3.77	-	C-6	61.8
	H-6b	3.77	-		
	NAc	2.057	-	$CO\mathit{C}H_3$	22.7
				$\mathit{C}OCH_3$	178.6
C-ol	H-1	-	n.d.	C-1	-
	H-2	-	3.99	C-2	-
	H-3	-	4.24	C-3	-
	H-4	-	4.40	C-4	-
	H-5	-	4.24	C-5	-
	H-6a[d]	-	3.88	C-6	-
	H-6b[d]	-	3.83		
D	H-1	4.952 (3.7)	5.037 (3.9)	C-1	100.7 (171)
	H-2	3.58	3.59	C-2	72.7

Table 1. *Continued.*

	H-3	3.83	3.79	C-3	73.4
	H-4	3.56	3.53	C-4	72.2
	H-5	4.20	4.13	C-5	71.8
	H-6a	3.87	3.89	C-6	69.0
	H-6b	3.63	3.60		
	H-2′	4.10	4.12	C-2′	69.8
	H-3′a	1.88	1.83	C-3′	34.9
	H-3′b	1.88	1.84		
	H-4′	3.96	3.99	C-4′	79.8
	H-5′	3.93	3.97	C-5′	73.6
	H-6′	3.71	3.68	C-6′	71.6
	H-7′	3.82	3.81	C-7′	85.1
	H-8′	4.02	4.00	C-8′	68.5
CH₃	H-9′	1.224 (6.7)	1.205 (6.4)	C-9′	18.0
E	H-1	5.178 (3.1)	5.194 (3.4)	C-1	98.5 (172)
	H-2	3.78	3.86	C-2	69.2
	H-3	4.04	3.94	C-3	70.4
	H-4	4.18	4.00	C-4	78.3
	H-5	4.11	4.11	C-5	71.6
	H-6a	3.74	n.d.	C-6	60.3
	H-6b	3.74	n.d.		
F	H-1	5.358 (<2)	5.408 (<2)	C-1	107.7 (176)
	H-2	4.25	4.26	C-2	80.7
	H-3	4.26	4.26	C-3	71.0
	H-4	4.06	4.09	C-4	83.9
	H-5a[d]	3.82	3.83	C-5	63.4
	H-5b[d]	3.69	3.68		

[a] In ppm relative to the signal of internal acetone at δ 2.225.

[b] In ppm relative to the α-anomeric signal of external [1-^{13}C]glucose at δ 92.9.

[c] n.d., not determined.

[d] Proton signals belonging to the same CH_2OH group are assigned a and b following increasing proton chemical shift.

D H-6a,6b resonances were determined in the ^{13}C-^{1}H HMQC spectrum, taking into account that residue **D** is substituted at O-6, resulting in a characteristic track in this spectrum. Furthermore, the chemical shifts of **E** H-6a,6b could be assigned via the **E** H-5 TOCSY track.

From the methyl group in **D** (**D** H-9′, δ 1.224) the resonances of **D** H-5′,6′,7′,8′, and from the methylene group in **D** (**D** H-3a′,3b′, δ 1.88) the resonances of **D** H-2′,4′,5′,6′ could be observed.

From the assigned ^{1}H chemical shifts it was clear that **A**, **C** and **E** are Gal*p*(NAc) residues since their downfield chemical shift of H-4 are characteristic for *galacto*-hexopyranose residues [7]. Residue **B** was assigned as Glc*p* by the characteristic upfield chemical shift of **B** H-2 [12], and residue **D** as Sug [9]. Finally, residue **F** could be assigned as the Rib*f* residue by its spin system, which is characteristic for this pentose residue [13].

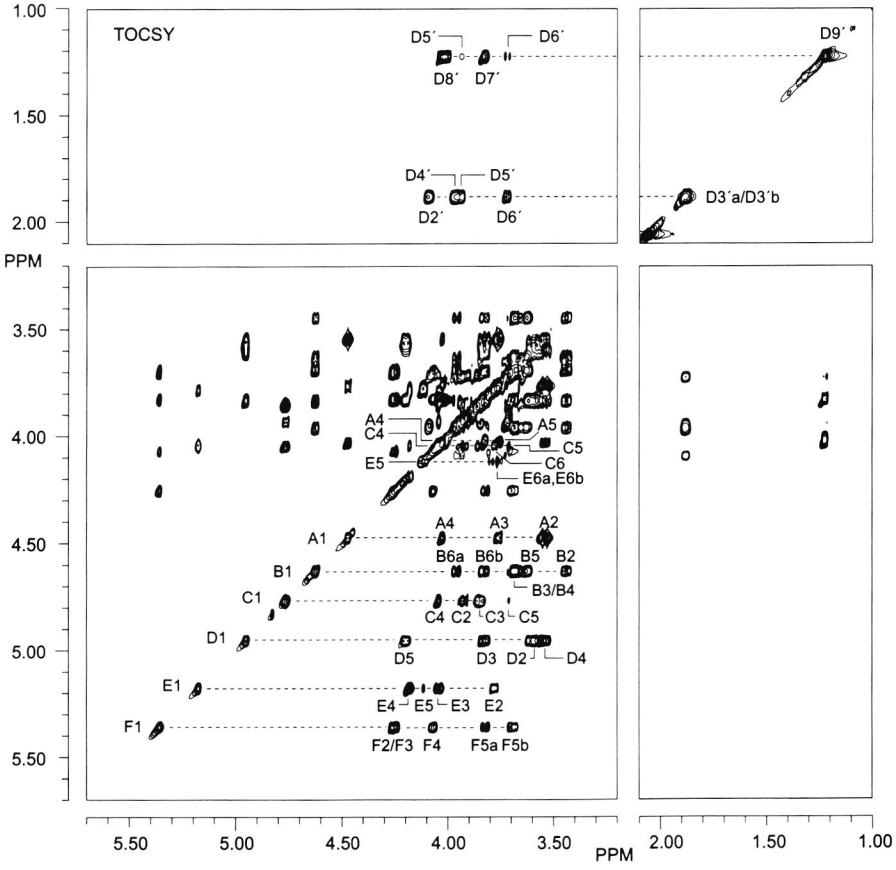

Figure 3. *500-MHz 2D TOCSY spectrum (mixing time 300 ms) of n-EPS, recorded in D_2O at 64 °C. Diagonal peaks of the anomeric protons, of H-4 of residues **A** and **C**, H-5 of residue **E**, and H-3′a,3′b,9′ of residue **D** are indicated. Labels near cross-peaks refer to the protons of the scalar-coupling network belonging to the diagonal peak.*

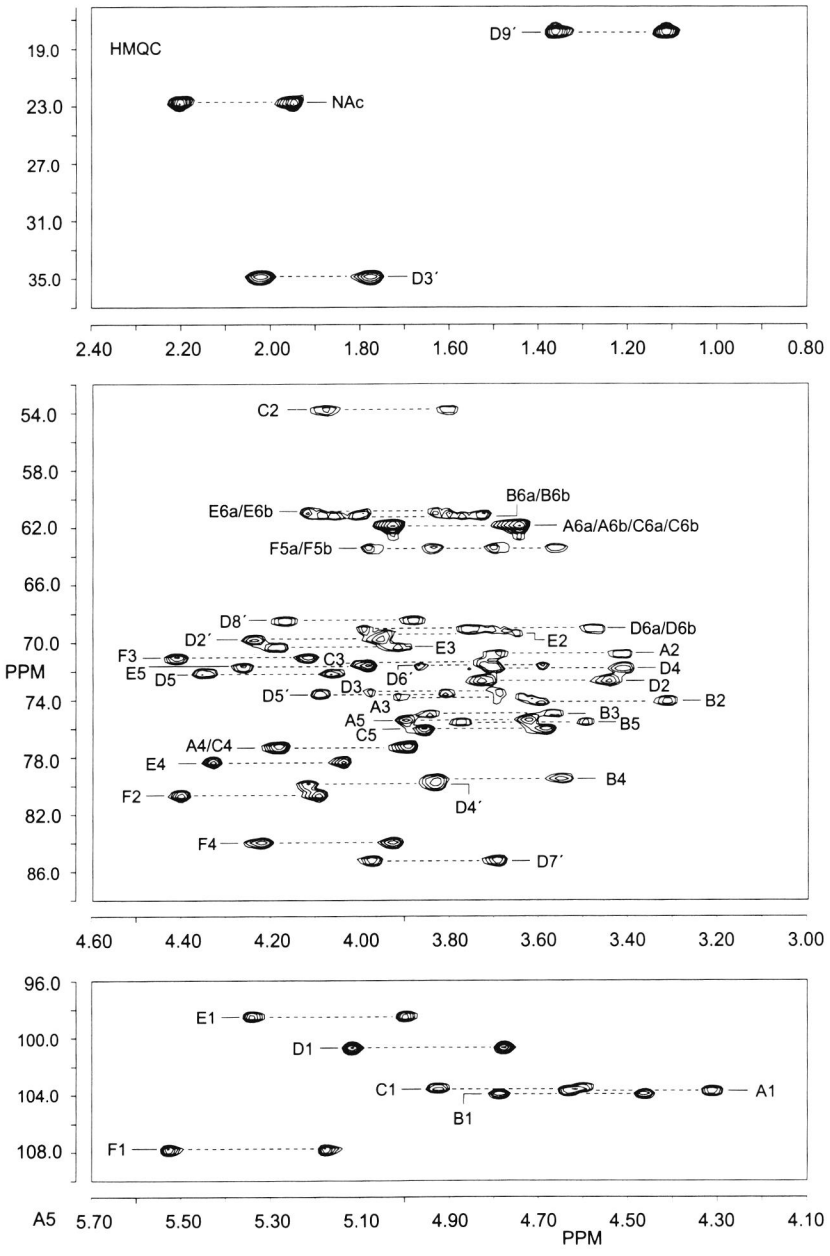

Figure 4. *500-MHz 2D ^{13}C–^{1}H undecoupled HMQC spectrum of n-EPS, recorded in D_2O at 64 °C. F1 stands for the set of cross-peaks between H-1 and C-1 of residue* **F**, *etc.*

Taking into account the ^{1}H chemical shifts, the ^{13}C-^{1}H HMQC spectrum (Figure 4) delivered the ^{13}C chemical shifts of n-EPS (Table 1). The observed $^{1}J_{C\text{-}1,H\text{-}1}$ values for residues **A** (160 Hz), **B** (161 Hz), and **C** (162 Hz) confirmed their β anomeric configurations, and the $^{1}J_{C\text{-}1,H\text{-}1}$ values of residues **D** (171 Hz) and **E** (172 Hz) their α anomeric configurations [14]. The $^{1}J_{C\text{-}1,H\text{-}1}$ value of residue **F** (176 Hz) (Rib*f*) gave no information

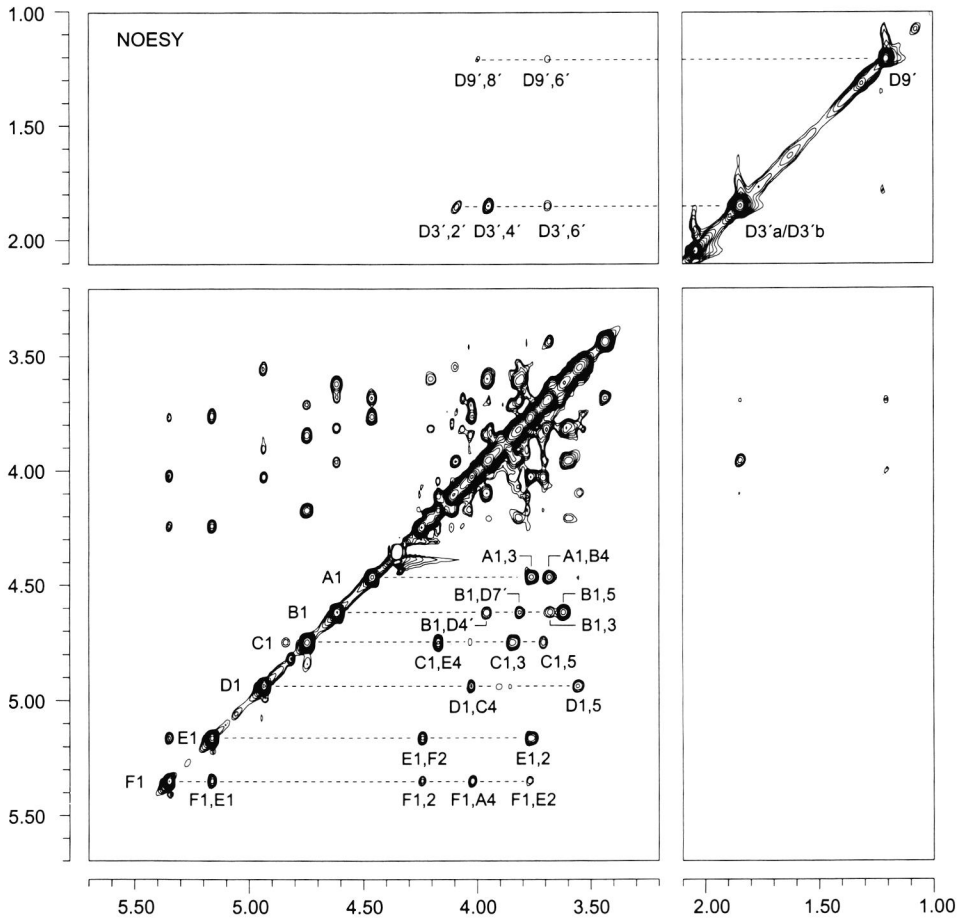

Figure 5. *500-MHz 2D NOESY spectrum (mixing time 100 ms) of n-EPS, recorded in D_2O at 64 °C. F1 corresponds to the diagonal peak belonging to residue **F** H-1; F1,2 refers to an intraresidual cross-peak between **F** H-1 and **F** H-2, and F1,E2 means an interresidual connectivity between **F** H-1 and **E** H-2, etc.*

about the anomeric configuration of this residue. Comparison of the chemical shift of **F** C-1 (δ 107.7) with the C-1 resonances of α-D-Rib*f*1Me (δ 103.1) and β-D-Rib*f*1Me (δ 108.0) [15], proved residue **F** to have β anomeric configuration.

By comparison of the ^{13}C chemical shifts of n-EPS with published ^{13}C chemical shift data of methyl aldosides [15], in combination with the methylation analysis data, the substitution patterns of the residues were deduced. The downfield chemical shift of **A** C-4 (δ 77.2) and **B** C-4 (δ 79.5) demonstrated residue **A** and **B** to represent 4-substituted β-D-Gal*p* (β-D-Gal*p*1Me, $\delta_{C\text{-}4}$ 69.7) and 4-substituted β-D-Glc*p* (β-D-Glc*p*1Me, $\delta_{C\text{-}4}$ 70.6), respectively. For residue **C**, confirmed to be β-D-Gal*p*NAc by the chemical shift of C-2 (δ 53.8), the downfield chemical shift of **C** C-4 (δ 77.2) indicated residue **C** to be 4-substituted (β-D-Gal*p*NAc1Me, $\delta_{C\text{-}4}$ 69.0). The downfield chemical shift of **E** C-4 (δ 78.3) and **F** C-2 (δ 80.7) demonstrated residue **E** to be 4-substituted α-D-Gal*p* (α-D-Gal*p*1Me, $\delta_{C\text{-}4}$ 70.2) and residue **F** to be 2-substituted β-D-Rib*f* (β-D-Rib*f*1Me, $\delta_{C\text{-}2}$ 74.3). Residue **D** contained a downfield-shifted C-6 (δ 69.0) signal as compared with α-D-Glc*p*1Me ($\delta_{C\text{-}6}$ 61.6), indicating 6-substituted α-D-Glc*p*. Finally, the position of the **D** C-7′ resonance (δ 85.1) was indicative of a glycosidic linkage at this position since this resonance was shifted downfield in comparison with isolated Sug ($\delta_{C\text{-}7'}$ 74.5) [9].

The monosaccharide sequence of n-EPS was unambiguously deduced from a 2D NOESY spectrum (Figure 5). The interresidual connectivity **E** H-1,**F** H-2 indicated the **E**-(1→2)-**F** linkage. The interresidual connectivities **F** H-1, **A** H-4 and **A** H-1, **B** H-4 demonstrated the **F**-(1→4)-**A**-(1→4)-**B** sequence. On the **B** H-1 track NOEs with **D** H-4′ and **D** H-7′ were observed. The downfield position of the resonance of **D** C-7′ (δ 85.1) proved the **B**-(1→7′)-**D** sequence. The NOE between **B** H-1 and **D** H-4′ resulted from flexibility within the nononic acid part of residue **D**. Finally, the interresidual connectivities **D** H-1,**C** H-4 and **C** H-1,**E** H-4 demonstrated the **D**-(1→4)-**C**-(1→4)-**E** sequence.

Concluding remarks

Based on monosaccharide analysis, methylation analysis, and 1D/2D NMR studies (^{1}H and ^{13}C) carried out on the native polysaccharide, and by mass spectrometric and NMR analyses of the oligosaccharide obtained from the polysaccharide by de-*N*-acetylation followed by deamination and reduction, the repeating unit of the EPS produced by *S. thermophilus* 8S in reconstituted skimmed milk was demonstrated to be:

→4)-α-D-Gal*p*-(1→2)-β-D-Rib*f*-(1→4)-β-D-Gal*p*-(1→4)-β-D-Glc*p*-(1→7′)-Sug-(1→4)-β-D-Gal*p*NAc-(1→

in which Sug is 6-*O*-(3′,9′-dideoxy-D-*threo*-D-*altro*-nononic acid-2′-yl)-α-D-glucopyranose [9]. The structural elucidation of the repeating unit of the EPS revealed the attachment of a Glc*p* residue by a glycosidic linkage to O-7′ of Sug. Taking into account the novel 2′-O-yl→6 linkage in Sug, the repeating unit can be formulated as a "hepta"saccharide. Since the structures of EPSs, including their conformation, are the main factors influencing their physical properties [16], the presence of Sug in the backbone of the EPS produced by *S. thermophilus* 8S will most likely have consequences for the physical properties of the EPS. Furthermore, the ability of the EPS to form a lactone in the repeating unit might alter the physical properties of the EPS in response to pH, as earlier suggested for oligo- and polysialic acids [17,18]. Interestingly, the repeating unit of the EPS produced by *S. thermophilus* 8S contains also a Rib*f* residue. This monosaccharide is commonly occurring in polysaccharides produced by Gram-negative bacteria [19], and has never been reported as a constituent of the repeating unit of an EPS produced by a Gram-positive lactic acid bacterium.

Due to the novel composition of the EPS produced by *S. thermophilus* 8S, the genetics and biochemistry of the EPS biosynthesis as well as the physical properties of the EPS will be intriguing subjects of further studies.

5.3 Experimental

Culture conditions of microorganism and isolation of polysaccharide. — *S. thermophilus* 8S, obtained from NIZO food research (Ede, The Netherlands), was cultured in pasteurized reconstituted skimmed milk containing 0.2% (w/w) casiton. After 16 h at 37 °C, trichloroacetic acid was added (4% w/w), and the bacterial cells and precipitated proteins were removed by centrifugation (30 min, 16,300 *g*, 4 °C). To the supernatant two volumes of EtOH were added, and precipitated material was isolated by centrifugation (30 min, 16,300 *g*, 4 °C). An aqueous solution of the precipitated material was extensively dialyzed against running tap water, and, after removal of insoluble material by centrifugation, again two volumes of EtOH were added. The precipitate formed was re-dissolved in water, and subsequently subjected to a fractionated precipitation at 30, 40, 50 and 60% (v/v) acetone. The precipitated material collected from the 30 and 40% (v/v) acetone fractions were further purified by gel filtration on a column of Sephacryl S-500 (150 x 2.2 cm, Pharmacia) irrigated with 50 mM NH_4HCO_3 using refractive index detection.

*De-*N*-acetylation and deamination.* — A solution of polysaccharide (5 mg) in anhydrous hydrazine (0.5 mL), containing hydrazine sulfate (25 mg), was stirred under argon for 20 h at 100 °C. Then, the solution was concentrated *in vacuo* and co-concentrated with toluene. The residue was dissolved in water and the solution was desalted on graphitized carbon [20]. A solution of the obtained de-*N*-acetylated polysaccharide in aq. 33% HOAc (2 mL), aq. 5% $NaNO_2$ (2 mL), and water (0.5 mL) was stirred for 2 h at room temperature, then neutralized using 4 M NH_4OH, and desalted on graphitized carbon. After lyophilization, the residue was treated with $NaBD_4$ (20 mg) in 1 M NH_4OH for 1 h at room temperature, then neutralized using 4 M HOAc, and desalted on graphitized carbon. The obtained material was fractionated by high-pH anion-exchange chromatography with pulsed amperometric detection (HPAEC-PAD) on a CarboPac PA-1 pellicular anion-exchange column (25 cm × 9 mm, Dionex). The column was eluted with a gradient of NaOAc in 0.1 M NaOH (20→250 mM NaOAc at a rate of 11 mM/min) at a flow rate of 4 mL/min. PAD-detection was carried out with a gold working electrode, and triple-pulse amperometry (pulse potentials and durations: E_1 0.05 V, 300 ms; E_2 0.65 V, 60 ms; E_3 -0.95 V, 180 ms) was used.

Carboxyl reduction. — Carboxyl-reduction of the native polysaccharide was performed as described [21]. A solution of polysaccharide (2 mg) in 2-(4-morpholino)-ethanesulfonic acid (0.2 M, 1 mL, pH 4.75), containing *N*-ethyl-*N*-(3-dimethylaminopropyl)-carbodiimide-

hydrochloride (30 mg), was stirred for 90 min at room temperature. After reduction with $NaBD_4$ (10 mg, 1 h), the obtained material was neutralized with 1.5 M HCl, desalted on graphitized carbon, and lyophilized prior to analysis. To obtain a complete carboxyl reduction the procedure was repeated twice.

Gas-liquid chromatography and mass spectrometry. — GLC analyses were performed on a CP-Sil 5CB fused silica capillary column (Chrompack CP9002, 25 m x 0.32 mm) using a temperature program from 140 °C to 300 °C at 4 °C/min followed by 10 min at 300 °C. GLC-EIMS analyses were carried out on a Fisons MD800/8060 system (electron energy, 70 eV) equipped with a DB-1 fused silica capillary column (J&W Scientific, 30 m x 0.32 mm) using a temperature program from 140 °C to 300 °C at 4 °C/min followed by 10 min at 300 °C. Positive-ion mode nanoES-CID tandem mass spectra were obtained on a Micromass Q-TOF hybrid tandem mass spectrometer equipped with a nanospray ion source (Bijvoet Center, Department of Biomolecular Mass Spectrometry) essentially according to [22]. Argon was used as a collision gas with a collision energy of 75 eV.

Monosaccharide and methylation analysis. — For monosaccharide analysis samples were subjected to methanolysis (methanolic 1 M HCl, 18 h, 85 °C), followed by re-*N*-acetylation and trimethylsilylation (1:1:5 hexamethyldisilazane-trimethylchlorosilane-pyridine), and the resulting mixtures of methyl glycosides were analyzed on GLC [23,24]. The absolute configurations of the monosaccharides were determined by GLC analysis of the trimethylsilylated (−)-2-butyl glycosides [25,26]. For methylation analysis, poly- and oligosaccharides were permethylated using CH_3I and solid NaOH in Me_2SO as described previously [27]. The methylated saccharides were subsequently hydrolyzed with 2 M trifluoroacetic acid (2 h, 120 °C) and reduced with $NaBD_4$. After neutralization and removal of boric acid by coevaporation with methanol, the mixture of partially methylated alditols was acetylated with acetic anhydride (3 h, 120 °C), and analyzed by GLC and GLC–EIMS [23,28].

NMR spectroscopy. — Prior to NMR analysis, samples were exchanged twice in 99.9 atom% D_2O (Isotec) with intermediate lyophilization and finally dissolved in 99.96 atom% D_2O (Isotec). 1D and 2D NMR spectra were recorded on a Bruker AMX-500 spectrometer (Bijvoet Center, Department of NMR Spectroscopy) at probe temperatures of 27 or 64 °C. Chemical shifts for ^1H were expressed in ppm relative to internal acetone (δ 2.225) and for ^{13}C to the α-anomeric signal of external [1-^{13}C]glucose ($\delta_{C\text{-}1}$ 92.9). 1D ^1H spectra were

recorded with a sweep width of 5000 Hz in data sets of 16384 points. The HOD signal was suppressed by applying a WEFT pulse sequence [29]. 2D TOCSY spectra were recorded using a 'clean' MLEV-17 mixing sequence with an effective spin-lock time of 15-300 ms. 2D NOESY experiments were performed with mixing times of 100 and 200 ms, and 2D ROESY experiments were recorded with a mixing time of 300 ms. The natural abundance ^{13}C-^{1}H 2D HMQC experiment was recorded without decoupling during acquisition of the ^{1}H FID. In the 2D experiments the HOD signal was suppressed by presaturation for 1 s. Homonuclear 2D spectra were recorded using a spectral width of 4032 Hz in both directions, and the heteronuclear HMQC experiment with a spectral width of 4032 Hz and 16350 Hz for ^{1}H and ^{13}C, respectively. Resolution enhancement of the spectra was performed by a Lorentzian-to-Gaussian transformation or by multiplication with a squared-bell function phase shifted by $\pi/(2.3)$, and when necessary, a fifth order polynomial baseline correction was performed. All NMR data were processed using the TRITON NMR software package (Bijvoet Center, Department of NMR Spectroscopy).

Acknowledgements

This study was supported by the PBTS Research Program with financial aid from the Ministry of Economic Affairs and by the Integral Structure Plan for the Northern Netherlands from the Dutch Development Company. The authors thank F. Kingma (NIZO food research, Ede, The Netherlands) for cultivation of *S. thermophilus* 8S and C. Versluis (Bijvoet Center, Department of Biomolecular Mass Spectrometry, Utrecht University, The Netherlands) for recording the ES-MS/MS spectra.

References

[1] L. De Vuyst, B. Degeest, *FEMS Microbiol. Rev.*, 23 (1999) 153-177.
[2] J. Cerning, *FEMS Microbiol. Rev.*, 87 (1990) 113-130.
[3] E.J. Faber, J.P. Kamerling, J.F.G. Vliegenthart, *Carbohydr. Res.*, 2000, Submitted.
[4] T. Doco, J.-M. Wieruszeski, B. Fournet, D. Carcano, P. Ramos, A. Loones, *Carbohydr. Res.*, 198 (1990) 313–321.
[5] J. Lemoine, F. Chirat, J.-M. Wieruszeski, G. Strecker, N. Favre, J.-R. Neeser, *Appl. Environ. Microbiol.*, 63 (1997) 3512-3518.
[6] W.A. Bubb, T. Urashima, R. Fujiwara, T. Shinnai, H. Ariga, *Carbohydr. Res.*, 301 (1997) 41-50.
[7] E.J. Faber, P. Zoon, J.P. Kamerling, J.F.G. Vliegenthart, *Carbohydr. Res.*, 310 (1998) 269-276.
[8] E.J. Faber, M.J. van den Haak, J.P. Kamerling, J.F.G. Vliegenthart, *Carbohydr. Res.*, 2000, Submitted.
[9] E.J. Faber, J.A. van Kuik, J.P. Kamerling, J.F.G. Vliegenthart, Manuscript in preparation.
[10] B. Domon, C.E. Costello, *Glycoconjugate J.*, 5 (1988) 397-409.
[11] N.A. Kocharova, J.E. Thomas-Oates, Y.A. Knirel, A.S. Shashkov, U. Dabrowski, N.K. Kochetkov, E.S. Stanislavsky, E.V. Kholodkova, *Eur. J. Biochem.*, 291 (1994) 653-661.
[12] G.W. Robijn, D.J.C. van den Berg, H. Haas, J.P. Kamerling, J.F.G. Vliegenthart, *Carbohydr. Res.*, 276 (1995) 117-136.
[13] H. Parolis, L.A.S. Parolis, S.M.R. Stanley, G.G.S. Dutton, *Carbohydr. Res.*, 200 (1990) 449-456.
[14] K. Bock, C. Pedersen, *J. Chem. Soc., Perkin Trans. 2*, (1974) 293-297.
[15] K. Bock, C. Pedersen, *Adv. Carbohydr. Chem. Biochem.*, 41 (1983) 27-66.
[16] R. Tuinier, PhD Thesis Wageningen University, The Netherlands, 1999.
[17] M.R. Lifely, A.S. Gilbert, C. Moreno, *Carbohydr. Res.*, 94 (1981) 193-203.
[18] M.R. Lifely, A.S. Gilbert, C. Moreno, *Carbohydr. Res.*, 134 (1984) 229-243.
[19] Y.A. Knirel, N.K. Kochetkov, *Biochemistry*, 59 (1994) 1325-1383.
[20] N.H. Packer, M.A. Lawson, D.R. Jardine, J.W. Redmond, *Glycoconjugate J.*, 15 (1998) 737-747.

[21] R.L. Taylor, H.E. Conrad, *Biochemistry*, 11 (1972) 1383-1388.

[22] A.B. Samuelsen, E.H. Cohen, B.S. Paulsen, L.P. Brüll, J.E. Thomas-Oates, *Carbohydr. Res.*, 315 (1999) 312-318.

[23] M.F. Chaplin, *Anal. Biochem.*, 123 (1982) 336-341.

[24] J.P. Kamerling, J.F.G. Vliegenthart, in A.M. Lawson (Ed.), *Clinical Biochemistry - Principles, Methods, Applications. Vol. 1, Mass Spectrometry*, Walter de Gruyter, Berlin, 1989, pp. 176-263.

[25] G.J. Gerwig, J.P. Kamerling, J.F.G. Vliegenthart, *Carbohydr. Res.*, 62 (1978) 349-357.

[26] G.J. Gerwig, J.P. Kamerling, J.F.G. Vliegenthart, *Carbohydr. Res.*, 77 (1979) 1-7.

[27] I. Ciucanu, F. Kerek, *Carbohydr. Res.*, 131 (1984) 209-217.

[28] P.-E. Jansson, L. Kenne, H. Liedgren, B. Lindberg, J. Lönngren, *Chem. Commun. Univ. Stockholm*, 8 (1976) 1-74.

[29] K. Hård, G. van Zadelhoff, P. Moonen, J.P. Kamerling, J.F.G. Vliegenthart, *Eur. J. Biochem.*, 209 (1992) 895-915.

Chapter 6

Modeling of the structure in aqueous solution of the exopolysaccharide produced by *Lactobacillus helveticus* 766

Elisabeth J. Faber, J. Albert van Kuik, Johannis P. Kamerling, and Johannes F.G. Vliegenthart

Bijvoet Center, Department of Bio-Organic Chemistry, Utrecht University, PO Box 80.075, NL-3508 TB Utrecht, The Netherlands.

Abstract

A method is described for constructing a conformational model in water of a heteropolysaccharide built up from repeating units, and is applied to the exopolysaccharide produced by *Lactobacillus helveticus* 766. The molecular modeling method is based on energy minima, obtained from molecular mechanics calculations of each of the constituting disaccharide fragments of the repeating unit *in vacuo*, as starting points. Subsequently, adaptive umbrella sampling of the potential-of-mean-force is applied to extract rotamer populations of glycosidic dihedral angles of oligosaccharide fragments in solution. From these analyses, the most probable conformations are constructed for the hexasaccharide-repeating unit of the polysaccharide. After exploring the conformational space of each of the individual structures by molecular dynamics simulations, the different repeating unit conformations are used as building blocks for the generation of oligo- and polysaccharide models, by using a polysaccharide building program. The created models of the exopolysaccharide produced by *L. helveticus* 766 exhibit a flexible twisted secondary structure and tend to adopt a random coil conformation as tertiary structure.

Elisabeth J. Faber, J. Albert van Kuik, Johannis P. Kamerling, and Johannes F.G. Vliegenthart, *Manuscript in preparation.*

6.1. Introduction

Polysaccharides are essential elements of life, having a large number of different functions in plants, animals and microorganisms [1]. Although the physiological function of microbial exopolysaccharides (EPSs) produced by lactic acid bacteria is hardly understood, the interest of the food industry in their texturizing properties in fermented dairy products [2] is increasing. In order to get insight into the relationship between the structures of EPSs produced by lactic acid bacteria and their physical properties, in addition to the primary structures ([3], and references cited therein), the secondary and tertiary structures of the EPSs have to be elucidated. For helix forming carbohydrate polymers, X-ray diffraction patterns from polycrystalline and oriented fibers and films can be interpreted in terms of reliable three-dimensional models [4]. NMR spectroscopy and computational methods can be used to obtain conformational data of these polymers in solution. A typical example of the modeling of bacterial polysaccharides *in vacuo*, is the prediction of hollow helical structures for the EPS produced by *Lactobacillus sake* 0-1 [5]. In the last study, low energy conformations of the pentasaccharide repeating unit were extrapolated to regular polysaccharide structures using a polysaccharide builder program. In a more complete investigation, a combination of molecular modeling and NMR spectroscopy was used to derive the conformation of the polysaccharide produced by *Streptococcus mitis* J22 [6]. The applied NMR techniques involved uniform ^{13}C-enrichment of the polysaccharide, which allowed for accurate measurements of heteronuclear $^{3}J_{CH}$ values. These data were used to generate starting conformations for molecular dynamics simulations *in vacuo*.

Here, we report on the development of a method to calculate the secondary and tertiary structures of polysaccharides consisting of repeating units, by taking into account solvent effects by explicitly including water molecules. The method includes molecular mechanics (MM) calculations, adaptive umbrella sampling (AUS) of the potential-of-mean-force (PMF), and molecular dynamics (MD) simulations. The repetitious nature of the polysaccharides enables to begin with the exploration of the conformational space of small fragment molecules that are gradually elongated. Finally, the obtained results are extrapolated to molecules of the size of 50 and 500 backbone residues. The method is applied to EPS **1**, produced by the lactic acid bacterium *Lactobacillus helveticus* 766, which is a homofermentative thermophilic lactic acid bacterium used in the manufacturing of various cheeses [7].

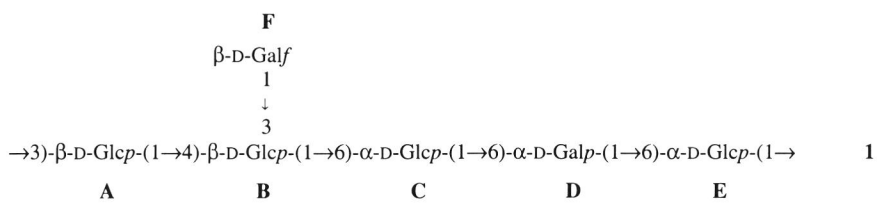

1

6.2. Results and discussion

As a first approach in calculating repeating-unit-containing polysaccharide conformations, it is assumed that monosaccharide residues separated by at least one repeating unit in the polysaccharide chain are not in close spatial contact and therefore, do not influence each others behavior. This strategy allows for the conformational investigation of a repeating unit on both sides elongated by monosaccharides of neighboring repeating units. The results can then be extrapolated to the conformation of the polysaccharide. After the determination of the abundance of the various conformations of the repeating unit, the flexibilities of these conformations are explored by MD simulations, and from these results, polysaccharide structures are constructed. At this stage, occupied space violations of monosaccharides belonging to different repeating units are taken into account.

Due to the relative rigidity of the monosaccharide rings, the conformational differences in the polysaccharide backbone originate mainly from the glycosidic dihedral angles, and therefore these angles are investigated first. Minimal energy calculations of the six constituting disaccharide fragments of the polysaccharide repeating unit are performed *in vacuo* using the CHEAT force field [8,9]. For each of the disaccharides β-D-Glc*p*-(1→4)-β-D-Glc*p*-OMe (**A→B**), α-D-Glc*p*-(1→3)-β-D-Glc*p*-OMe (**E→A**), and β-D-Gal*f*-(1→3)-β-D-Glc*p*-OMe (**F→B**) the glycosidic dihedral angles ϕ (O_{5M}-C_{1M}-O_{XN}-C_{XN}), and ψ (C_{1M}-O_{XN}-C_{XN}-$C_{(X-1)N}$) must be considered [10], and potential energy maps are generated to determine the lowest energy conformations for these glycosidic angles. For the (1→6)-linked disaccharides β-D-Glc*p*-(1→6)-α-D-Glc*p*-OMe (**B→C**), α-D-Glc*p*-(1→6)-α-D-Gal*p*-OMe (**C→D**), and α-D-Gal*p*-(1→6)-α-D-Glc*p*-OMe (**D→E**) the additional glycosidic dihedral angle ω (O_{6N}-C_{6N}-C_{5N}-C_{4N}) is involved [10]. Here, three separate minimal energy calculations are performed for the ϕ and ψ glycosidic angles, reflecting the *gauche-gauche* (*gg*), *gauche-trans* (*gt*), and *trans-gauche* (*tg*) orientations of the ω angle*. The potential energy maps for each of the investigated disaccharides are presented in Figure 1.

---

* $^4C_1$ chair conformation of a hexopyranose and Newman-projections of the three staggered conformations about the C_5-C_6 bond. In this figure *g* and *t* are abbreviations of *gauche* (±60°) and *trans* (180°), respectively, indicating qualitatively the value of a dihedral angle. The angle of the O_6-C_6-C_5-O_5 moiety is indicated by the first character and the angle of the O_6-C_6-C_5-C_4 moiety by the second.

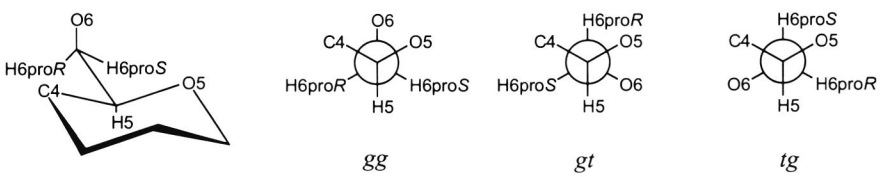

gg *gt* *tg*

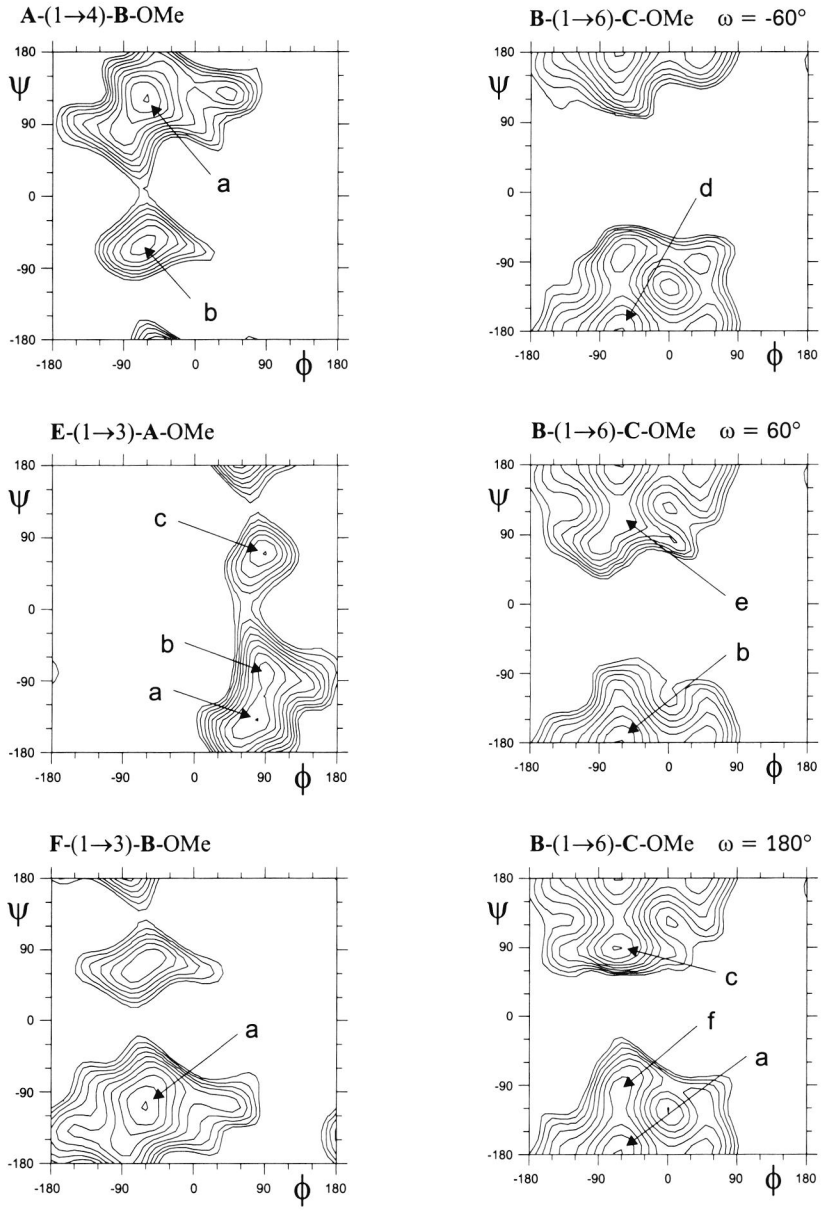

Figure 1. *Energy contour plots for each of the constituting disaccharides of the* L. helveticus *766 EPS. Contours are plotted at regular intervals of 1 kcal/mol up to 10 kcal/mol with respect to the global energy minimum. Global minima are indicated with a and local minima that are at the most 3 kcal/mol higher than the global minima are indicated with b to f.*

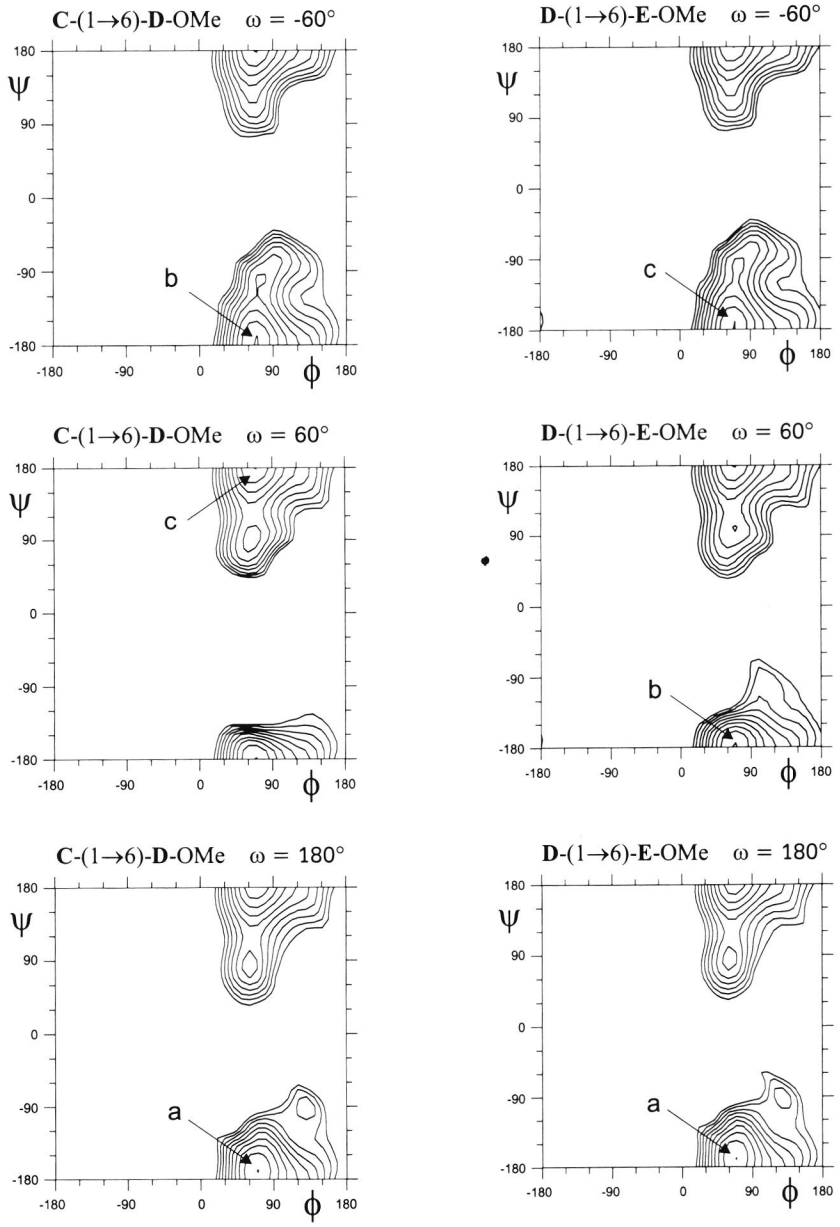

Figure 1. *Continued.*

In each map, the global energy minimum, as well as the different local energy minima are indicated. The glycosidic dihedral angles and energy minima with energies that are at the most 3 kcal/mol higher than the global minima are listed in Table 1. Inspection of the energy minima of the different potential energy surfaces of the glycosidic linkages shows that for the disaccharides **A→B** and **E→A** the main flexibilities can be attributed to the dihedral angles ψ, for the disaccharides **B→C** and **C→D** to both ψ and ω, and for the disaccharide **D→E** to ω. Furthermore, **F→B** is the least flexible disaccharide in having only one energy minimum.

Table 1. *Minimal energy conformations of the six constituting disaccharide fragments of* L. helveticus *766 EPS.*

Disaccharide fragments		Minima	Dihedral angles			ΔE^a
			ϕ	ψ	ω	
A-(1→4)-**B**	β-D-Glc*p*-(1→4)-β-D-Glc*p*-OMe	a	-60	119	-	0.0
		b	-55	-53	-	2.7
B-(1→6)-**C**	β-D-Glc*p*-(1→6)-α-D-Glc*p*-OMe	a	-64	178	-178	0.0
		b	-64	178	61	0.0
		c	-62	91	-178	0.7
		d	-65	179	-68	1.3
		e	-77	84	44	1.3
		f	-61	-90	171	2.1
C-(1→6)-**D**	α-D-Glc*p*-(1→6)-α-D-Gal*p*-OMe	a	68	-170	-172	0.0
		b	67	-176	-58	1.3
		c	66	180	70	1.7
D-(1→6)-**E**	α-D-Gal*p*-(1→6)-α-D-Glc*p*-OMe	a	67	-168	-178	0.0
		b	67	-177	61	0.3
		c	67	-176	-68	2.1
E-(1→3)-**A**	α-D-Glc*p*-(1→3)-β-D-Glc*p*-OMe	a	78	-139	-	0.0
		b	90	-80	-	0.6
		c	87	73	-	2.9
F-(1→3)-**B**	β-D-Gal*f*-(1→3)-β-D-Glc*p*-OMe	a	-63	-107	-	0.0

[a] Relative energy (kcal/mol)

Adaptive umbrella sampling of the potential-of-mean-force

In order to study the rotamer distribution of the ψ and ω glycosidic angles in water, potential-of-mean-force (PMF) calculations [11] are performed with the GROMOS force field using the method of adaptive umbrella sampling (AUS). The umbrella potential is applied to only one dihedral angle. In order to obtain a correct rotamer distribution of this dihedral angle, the unrestricted dihedral angles need to be sampled sufficiently during the AUS simulations. This is feasible, when the global energy minimum for this dihedral is much lower than the other minima, rendering the latter contributions negligible. Similarly, when low energy barriers between global and local minima make frequent transitions possible during an AUS simulation, resulting in the conformational exploration of all minima. Starting structures for the AUS simulations are created with the glycosidic dihedral angles corresponding to the lowest energy conformations. To include possible interactions of monosaccharides that are close in space, most calculations are performed on oligosaccharide fragments larger than disaccharides. However, the total number of monosaccharide residues is limited to four, to keep the simulation period within 10 ns. All Fourier coefficients have converged after this period, which indicates that the total sampling time has been sufficiently long. The optimal sizes of the selected fragments are deduced by iterative processes as follows. In a first approach, disaccharide fragments are used for the AUS simulations. The whole protocol is repeated with a larger fragment if in the modeling procedure interactions to neighboring residues became apparent. Finally, the ψ angle of **E→A** is evaluated using the methyl glycoside analog of the disaccharide fragment. The ψ angles of **A→B** and **F→B** are evaluated separately using the trisaccharide **A→[F→]B**-OMe, and the ψ and ω angles of **B→C**, **C→D** and **D→E** using the trisaccharides **B→C→D**-OMe and **C→D→E**-OMe, and the tetrasaccharide **D→E→A→B**-OMe, respectively. In Table 2 probability distributions calculated from the free energy differences are presented. For the ϕ dihedral angles, no transitions are observed in any of the AUS simulations. This is consistent with the potential energy maps (Figure 1) which show single minimum-energy regions for the ϕ angles. Therefore, it is assumed that during 10 ns AUS simulations the conformational space of ϕ is adequately explored. For element **A→B**, the results are consistent with the conformational analysis data of β-cellobioside [12]. This disaccharide occupies primarily one minimum-energy region (ϕ / ψ = -90°/120°), whereas only one other stable conformational region exists (ϕ / ψ = -90°/-50°). This second minimum-energy region does not differ from the primary minimum-energy region with respect to the ϕ dihedral angle, confirming the main flexibility to be located in the ψ angle of element **A→B**.

Table 2. *Probability distribution* [a] *of the ψ and ω dihedral angles of the six constituting disaccharide fragments of* L. helveticus *766 EPS.*

Dihedral angle	**A**-(1→4)-**B**	**B**-(1→6)-**C**	**C**-(1→6)-**D**	**D**-(1→6)-**E**	**E**-(1→3)-**A**	**F**-(1→3)-**B**
ψ						
	120 (>98)	180 (82)	180 (89)	-170 (>98)	-130(>98)	-100 (>98)
		80 (16)	80 (10)			
		-75 (2)	-90 (1)			
ω						
(*gt*)	-	-170 (69)	-170 (87)	-170 (70)	-	-
(*gg*)	-	60 (29)	70 (5)	60 (28)	-	-
(*tg*)	-	-80 (2)	-70 (8)	-80 (2)	-	-

[a] Probability distributions are given in parentheses in %.

From the combined results of these AUS runs it emerges that the **E**→**A**→[**F**→]**B** structural element essentially adopts one conformation with **E**→**A** ϕ/ψ = 100°/-130°, **A**→**B** ϕ/ψ = -90°/120°, and **F**→**B** ϕ/ψ = -80°,-100°. The distribution profiles of the ω angles of the (1→6)-linked disaccharide fragments (Figure 2A) show that the →6)-α-D-Glc*p* fragments of

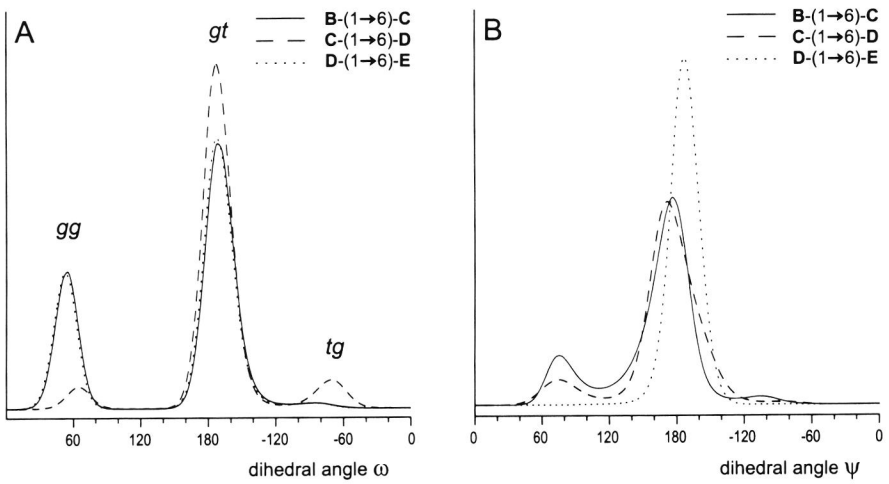

Figure 2. *Probability distribution profiles of dihedral angles (A) ω and (B) ψ of the (1→6)-linked fragments of the* L. helveticus *766 EPS, obtained by potential-of-mean-force calculations in water.*

B→C and **D→E** adopt both the *gg* and *gt* conformation. These conformations occur in ratios similar to the rotamer distribution about the C_5-C_6 bond in gentiobiose (β-D-Glc*p*-(1→6)-D-Glc*p*): *gg* (34 %), *gt* (66 %) [13]. In the distribution profile of the →6)-α-D-Gal*p* fragment of **C→D**, ω is located mainly in the *gt* orientation. This is in agreement with the probability distribution of the hydroxy-methyl group of free β-D-Gal*p*: *gt* (70 %), *tg* (25 %) [14]. The resemblance of the calculated and published dihedral angle ratios of the smaller fragments reveals that monosaccharide residues that are not directly involved in the sampled glycosidic linkage have only a small effect on the rotamer distribution. Further analysis of the AUS trajectories reveals rapid transitions as well as distinct dihedral angle populations for the free ψ angles during the AUS of the ω angles. This shows that ψ is adequately sampled and that correlations exist between the ψ and ω dihedral angles. As an example of these observations, a scatter plot of the sampled ω angle versus the corresponding free ψ angle of the **B→C** fragment is presented in Figure 3.

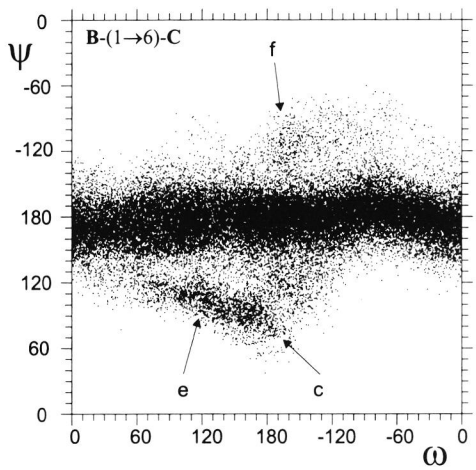

Figure 3.
*Scatter plot of the ψ and ω dihedral angles of the AUS simulation of the ω dihedral angle in the **B→C** fragment.*

The local minima c, e and f, obtained from the minimal energy calculations, are all represented. The distribution profiles of the ψ angles of the (1→6)-linked disaccharide fragments (Figure 2B) show that ψ is predominantly 180° and the **B→C** and **C→D** fragments reveal an additional population of ψ around 60°. A relatively low energy barrier between both populations suggests flexibility in the ψ angle. In contrast, the distribution profiles of the ω angles indicate high energy barriers between *gg*, *gt*, and *tg* (Figure 2A). During the AUS of the ψ angles, the trajectories of the free ω angles show between one and three transitions only, confirming that the high energy barriers between the ω populations make

adequate sampling of these free angles difficult. Therefore, it is assumed that the AUS simulations of ψ from the (1→6)-linkages are less reliable than those of ω.

The conformational preferences, resulting from the PMF calculations, are used to create starting structures for the MD simulations [14-17]. For the (1→6)-linkages, only the distribution information of ω angles is used. This is permitted, since the flexibility of the ψ angles is expected to allow adequate sampling in the free MD simulations. In order to include all glycosidic linkages present in the EPS, and to consider possible influences of monosaccharides from adjacent repeating units, the repeating unit of the EPS is elongated with two residues at the reducing side and with one at the non-reducing side (**2**). It should be noted that elongated repeating unit **2** is chosen in such a way that the most flexible part is in the center.

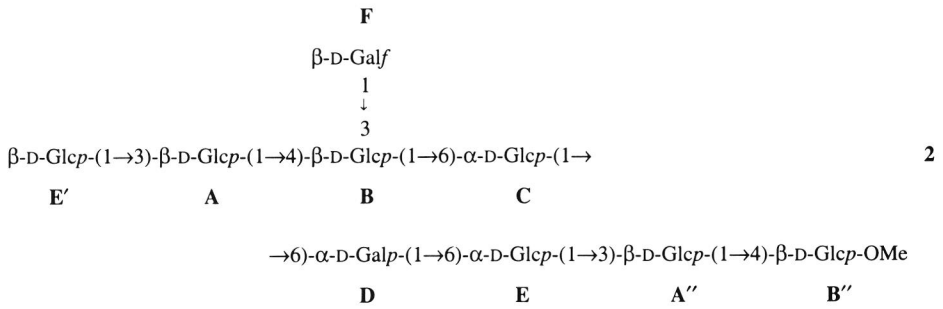

Based on the rotamer distributions obtained from the AUS runs, the eight most probable conformations (I to VIII) are constructed from the ϕ and ψ angles in their global energy minima (Table 1) and the ω angles according to Table 3.

Table 3. *Orientation of the ω dihedral angles and probability of the local minimum-energy conformations I to VIII for structure 2.*

Fragment	I	II	III	IV	V	VI	VII	VIII
	Orientation							
B-(1→6)-**C**	-170	60	-170	60	-170	60	-170	60
C-(1→6)-**D**	-170	-170	-170	-170	-70	-70	-70	-70
D-(1→6)-**E**	-170	-170	60	60	-170	-170	60	60
	Probability (%)							
	46	19	18	8	4	2	2	1

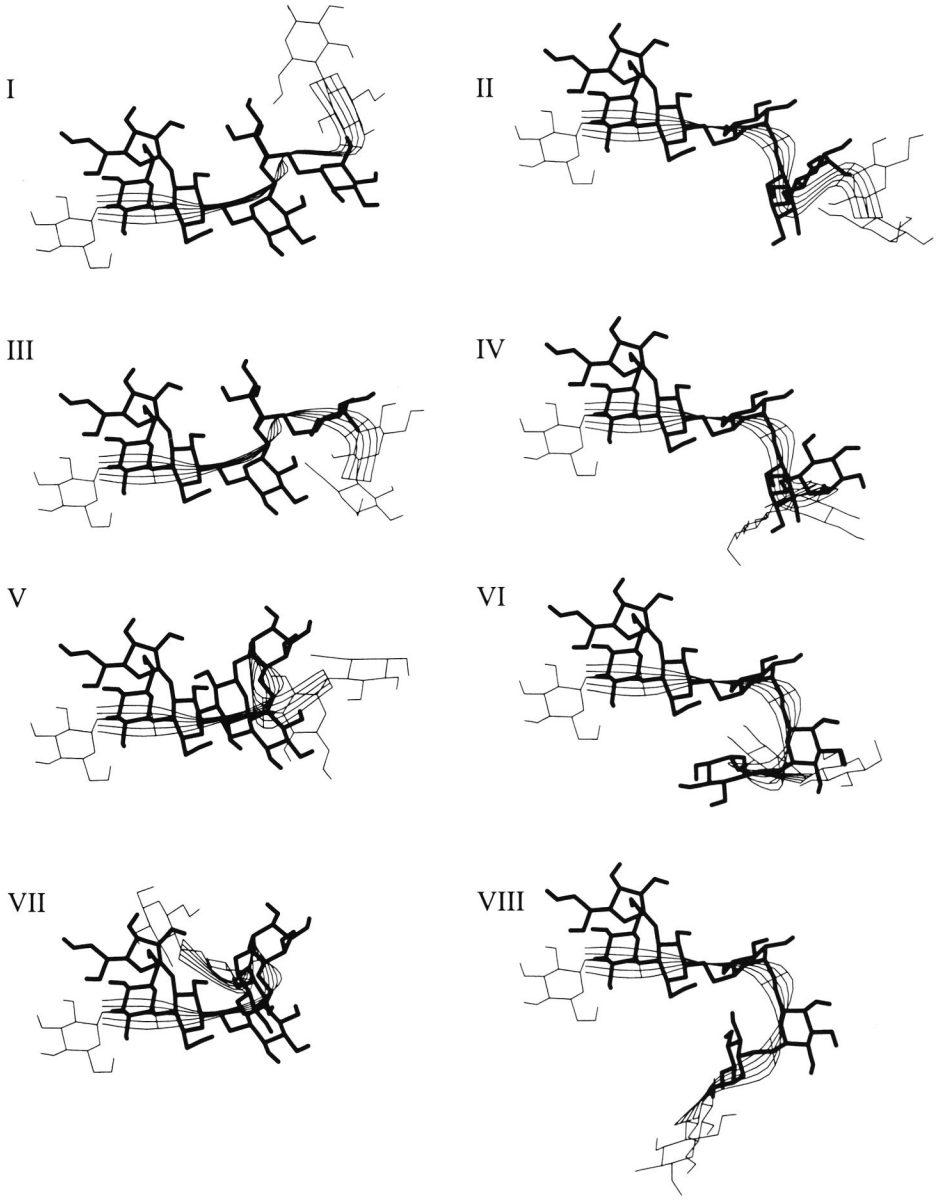

Figure 4. *Local minimum-energy conformations of the eight most probable conformational families (I to VIII) found by PMF calculations of* **2**. *Ribbons are drawn through the glycosidic bonds, perpendicular on the* C_{1M}-O_{XN}-C_{XN} *plane, to visualize the backbone of the molecule.*

In Figure 4 the differences are illustrated between the eight constructed conformations. The structures include a ribbon, which is drawn through the glycosidic bonds, perpendicular on the C_{1M}-O_{XN}-C_{XN} plane, to visualize the backbone of the molecule. All conformers show some bends or twists; for example, V and VII have a back-folded conformation in which several residues come into close contact.

Molecular dynamics simulations

In order to sample the conformational space of I to VIII, MD simulations in water [14-17] of 1 ns are performed and the trajectory-averaged dihedral angles are listed in Table 4. Inspection of the MD trajectories reveals flexibility within the conformations as illustrated by the superposition of several frames from the MD trajectory of II (Figure 5).

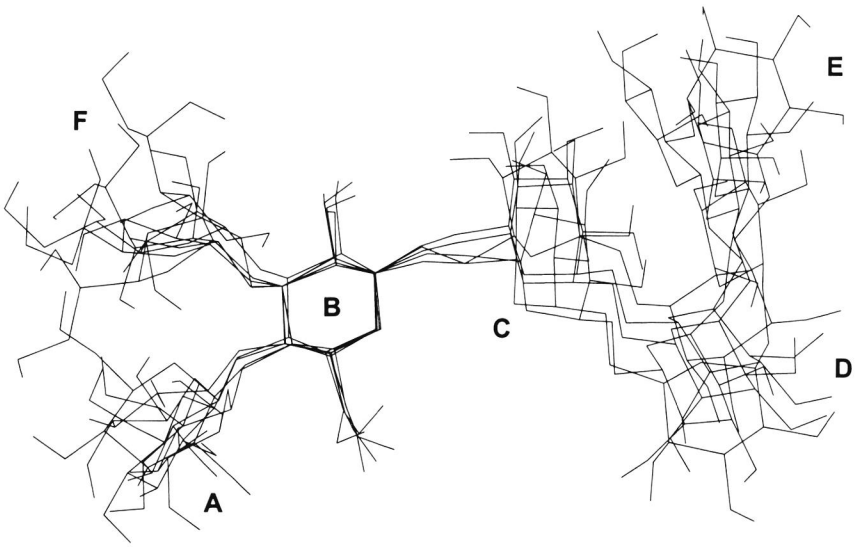

Figure 5. *Starting conformation of II, along with four conformations within the same conformational space.*

Furthermore, hydrogen bonds between non-neighboring residues are frequently observed. The most predominant hydrogen bond, observed in all MD runs, exists between the hydroxyl groups **F** OH-3 and **A** OH-6. The presence of this hydrogen bond in all simulated repeating

Table 4. *Trajectory-averaged dihedral angles of the MD simulations for the repeating unit conformations I to VIII.*

	I	II	III	IV	V	VI	VII	VIII
	E′-(1→3)-**A**							
ϕ	97	92	91	91	96	97	98	94
ψ	-125	-134	-130	-133	-130	-128	-127	-126
	A-(1→4)-**B**							
ϕ	-71	-77	-64	-71	-91	-73	-75	-68
ψ	121	120	126	121	115	121	121	123
	B-(1→6)-**C**							
ϕ	-87	-79	-83	-90	-85	-83	-82	-84
ψ	-176	173	-101 [a]	172	-165	170	-170/-105 [b]	179
ω	-167	62	-156	57	-163	59	-158	59
	C-(1→6)-**D**							
ϕ	91	94	88	92	100	97	99	99
ψ	178/-140 [b]	159	-174	174	-171	177	-175	-178
ω	-162	-162	-173	-167	-74	-83/-163 [b]	-76	-72/-164 [b]
	D-(1→6)-**E**							
ϕ	88	88	98	99	103	97	91	94
ψ	-161	-159	173	-171	-174	-162	-179	175
ω	-171	-171	60	60	-160	-162	55	58
	E-(1→3)-**A″**							
ϕ	99	98	95	89	95	101	88	90
ψ	-121	-125	-126	-136	-126	-122	-140	-133
	A″-(1→4)-**B″**							
ϕ	-81	-89	-94	-89	-90	-79	-90	-98
ψ	111	106	104	106	104	109	106	101
	F-(1→3)-**B**							
ϕ	-84	-76	-91	-76	-80	-76	-77	-82
ψ	-105	-100	-107	-104	-97	-101	-98	-104

[a] Deviating average value due to transition, see text.
[b] Average value of distinct regions in MD simulation.

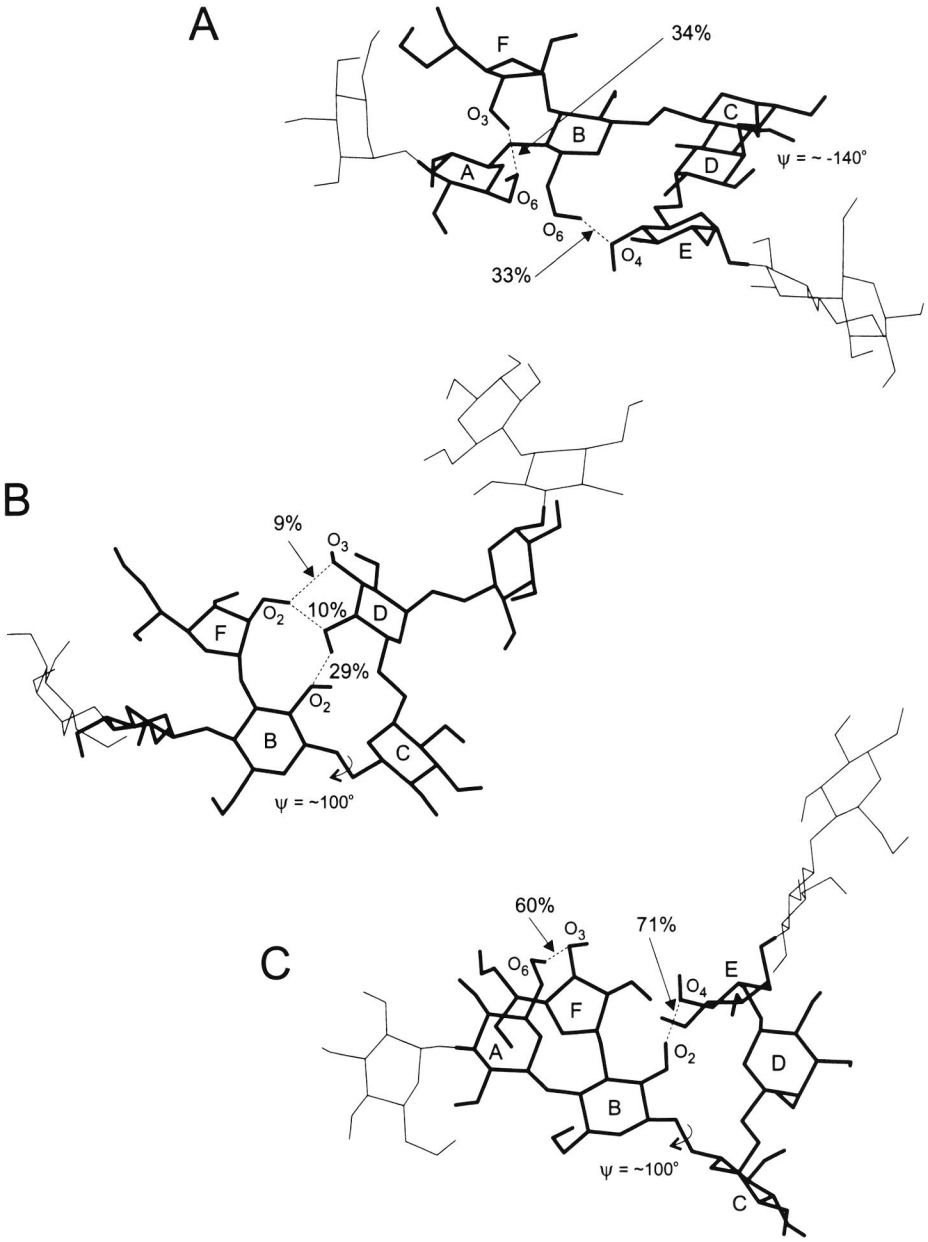

Figure 6. *Snap shot of the MD-trajectory of conformation (A) I, (B) III, and (C) VII, illustrating hydrogen bond formation between non-neighboring residues.*

unit conformations confirms the relative rigidity of the **A**→[**F**→]**B** fragment. The MD trajectories show no transitions of the glycosidic dihedral angles for the (1→3)- and (1→4)-linked residues, and only a few for the (1→6)-linked residues. The ψ angle of the **C**→**D** linkage in the MD trajectory of I reveals a transition from 178° to -140°. Inspection of I after the transition suggests that the intramolecular hydrogen bond between **B** OH-6 and **E** OH-4 (Figure 6A) is of importance in stabilizing conformation I with ψ = -140°. The ψ angle of the **B**→**C** linkage in conformation III reveals an instantaneous transition of this dihedral from its starting value of 178° (Table 1) to the low probability average value of -101°. Observed intramolecular hydrogen bonds between hydroxyl groups of residues **B** and **D**, and **F** and **D** (Figure 6B) are likely to stabilize this conformation. For the **B**→**C** linkage a similar transition is observed in the MD trajectory of VII (ψ = -170° to ψ = -105°). Here the intramolecular hydrogen bond between **B** OH-2 and **E** OH-4 is probably the stabilizing factor of the conformation in which ψ = -105° (Figure 6C). In the MD simulations of VI and VIII transitions of the ω angle in the **C**→**D** linkage from approximately -75° to -164° after about 0.2 ns, convert VI and VIII into the more stable II and IV, respectively.

Polysaccharide building

From the conformational ensembles generated by the MD simulations of I to VIII, polymer structures can be constructed by connecting randomly selected conformations from these ensembles. If polymers are constructed from conformations of different ensembles their selection is in random order, but in accordance with the relative occurrence of the ensembles. Oligosaccharide structures of typically 10 repeating units are generated possessing single repeating unit conformers I to IV (Figure 7A). Oligosaccharides solely composed of repeating unit conformers V to VIII are not evaluated, since the occurrence of multiple repeating units with these conformations are, due to their low molar ratios (Table 3), not likely. The generated models differ with respect to their secondary structure. The oligosaccharides built from I and III have extended structures with nonuniform bents. The oligosaccharide model built from II shows a helix-like structure, in which multiple repeating units form one helical turn. The structure of IV is less regular than II, but still possesses a helix-like turn. From conformers I to VIII a polysaccharide model containing 100 repeating units is generated using the molar ratios obtained from the AUS simulations (Table 3). This degree of polymerization is less than 10% of the average size of EPSs produced by lactic acid bacteria [18]. The obtained polysaccharide model (Figure 7B) gives a plausible description of the conformations of the polysaccharide chain in solution. It exhibits a flexible twisted secondary structure and tends to adopt a random coil conformation as a tertiary structure.

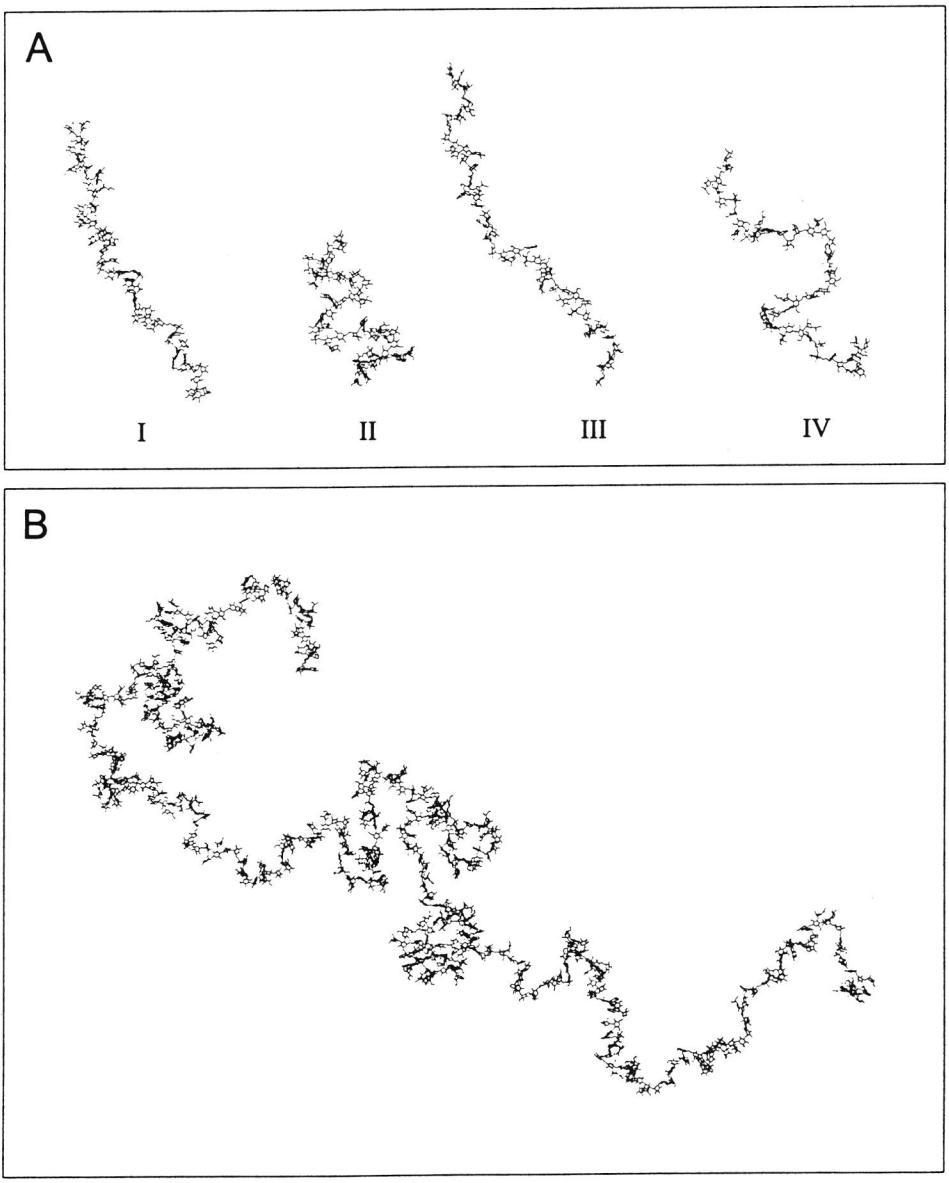

Figure 7. *(A) Oligosaccharide structures generated from I to IV and (B) polysaccharide structure generated from I to VIII in a molar ratio according to Table 3. The oligosaccharide chains consist of 50 and the polysaccharide chain of 500 backbone residues (10 and 100 repeating units).*

Concluding remarks

For the EPS produced by *L. helveticus* 766 it was found that the global and local energy minima obtained by MM calculations for the constituting disaccharide fragments are good starting points to explore the conformations of this polysaccharide. Adaptive umbrella sampling of the potential-of-mean-force was applied successfully to obtain rotamer distributions of flexible glycosidic dihedral angles in solution. The MD simulations of the most probable conformations of the elongated repeating unit **2** indicate only minor differences in the trajectory-averaged dihedral angles in comparison with the same dihedral angles obtained from the AUS simulations. The few transitions, which do occur, are probably caused by the interaction of some non-neighboring residues. For the prediction of the conformation of polysaccharides it is important to study oligosaccharide fragments of a certain size in order to include the most prominent long-range interactions. This may lead to an iterative process since these long-range interactions may only become apparent during the building of a polysaccharide from previously obtained repeating unit conformations. It must be kept in mind that the interactions of non-bonded residues can influence the ratio of different local conformations in the polysaccharide, because this ratio was based on AUS simulations of smaller oligosaccharide fragments. This holds especially for the EPS produced by *L. helveticus* 766, since the presence of three consecutive (1→6)-linkages within the repeating unit make the EPS very flexible, and therefore a large number of different long-range interactions are possible. Including these effects in the AUS simulations by extending the oligosaccharide fragments for these simulations is not feasible, since all conformational differences in the free dihedral angles have to be taken into account during the AUS simulations. The construction of oligo- and polysaccharide models demonstrates the secondary and tertiary structure of the *L. helveticus* 766 EPS. Characterization of these polysaccharide models in terms of persistence length will be subject of further research.

6.3 Experimental

Molecular Mechanics calculations. — Minimal energy calculations *in vacuo* were performed with CHEAT [8,9], a CHARMm based force field for carbohydrates. In this force field hydroxyl groups are represented by extended atoms to prevent intramolecular hydrogen bond formation *in vacuo*. Minimal energy contour plots were calculated on a 5° by 5° grid and were plotted at intervals of 1 kcal/mol with respect to the calculated global energy minimum.

Adaptive umbrella sampling of the potential-of-mean-force. — Potential-of-mean-force (PMF) calculations [11] were performed with the GROMOS force field using the method of adaptive umbrella sampling. All simulations were divided into jobs of 10 ps. Dihedral angle values were partitioned into 72 classes, each having a width of 5°. The derivative of the PMF was evaluated as a 12-term Fourier series. Each system was simulated for 10 ns, and the final PMF for each system was used to obtain the rotamer population distributions of the sampled dihedral angle.

Molecular dynamics. — MD simulations in water were performed using the GROMOS program [15] with the improved force field for carbohydrates [14]. Each repeating unit was placed in a computational truncated octahedral periodic box containing between 1075 and 1781 SPC/E [16] water molecules. All bond lengths were kept fixed using the SHAKE procedure [17]. Simulations were performed at constant temperature (300K) and pressure (1 atm.) with a relaxation time of 0.1 and 0.5 ps, respectively. For the simulations a cut-off radius of 0.8 nm, a time step of 2 fs and a total simulation time of 1 ns was used. A hydrogen bond is considered to be present for donor and acceptor hydrogen atoms with an O-H··O distance of less than 2.5 Å and a bond angle larger than 120°.

Polysaccharide building. — From the conformational ensembles I to VIII, obtained by MD simulations, polysaccharide models were generated using an in-house made building program. In brief, the program selects at random elongated repeating units. The selected repeating units are connected from residue **E** of the first repeating unit to residue **A** of the second, using the dihedral angles ϕ of **E**→**A**″ and ψ of **E**′→**A**. The overlapping monosaccharide residues **E**′, **A**″ and **B**″ are removed. After assembling each repeating unit, the polymer is checked for occupied space violations, and if necessary repeating units are rearranged or the polysaccharide is rebuilt.

Acknowledgements

This study was supported by the PBTS Research Program with financial aid from the Ministry of Economic Affairs and by the Integral Structure Plan for the Northern Netherlands from the Dutch Development Company.

References

[1] E.A. MacGregor, C.T. Greenwood, *Polymers in Nature*, Chapter 6, John Wiley & Sons, Chichester, 1980, pp. 240-328.

[2] J. Cerning, *FEMS Microbiol. Rev.*, 87 (1990) 113-130.

[3] E.J. Faber, J.P. Kamerling, J.F.G. Vliegenthart, *Carbohydr. Res.*, 2000, Submitted.

[4] V.S.R. Rao, P.K. Qasba, P.V. Balaji, R. Chandrasekaran, in V.S.R. Rao, P.K. Qasba, P.V. Balaji, R. Chandrasekaran, *Conformation of Carbohydrates*, Harwood Academic Publishers, Amsterdam, 1998, pp. 223-254.

[5] G.W. Robijn, A. Imberty, D.J.C. van den Berg, A.M. Ledeboer, J.P. Kamerling, J.F.G. Vliegenthart, S. Pérez, *Carbohydr. Res.*, 288 (1996) 57-74.

[6] Q. Xu, C.A. Bush, *Biochemistry*, 35 (1996) 14521-14529.

[7] G.W. Robijn, J.R. Thomas, H. Haas, D.J.C. van den Berg, J.P. Kamerling, J.F.G. Vliegenthart, *Carbohydr. Res.*, 276 (1995) 137-154.

[8] P.D.J. Grootenhuis, C.A.G. Haasnoot, *Mol Simul.*, 10 (1993) 75-95.

[9] M.L.C.E. Kouwijzer, P.J.D. Grootenhuis, *J. Phys. Chem.*, 99 (1995) 13426-13436.

[10] IUPAC-IUB Joint Commission on Biochemical Nomenclature (JCBN), *Eur. J. Biochem.*, 131 (1983) 5-7.

[11] R.W.W. Hooft, B.P. van Eijck, J. Kroon, *J. Chem. Phys.*, 97 (1992) 6690-6694.

[12] L.M.J. Kroon-Batenburg, J. Kroon, B.R. Leeflang, J.F.G. Vliegenthart, *Carbohydr. Res.*, 245 (1993) 21-42.

[13] L. Poppe, *J. Am. Chem. Soc.*, 115 (1993) 8421-8426.

[14] S.A.H. Spieser, J.A. van Kuik, L.M.J. Kroon-Batenburg, J. Kroon, *Carbohydr. Res.*, 322 (1999) 264-273.

[15] W.F. van Gunsteren, *GROMOS, Groningen Molecular Simulation Package*, University of Groningen, The Netherlands (1987).

[16] H.J.C. Berendsen, J.P.M. Postma, W.F. van Gunsteren, J. Hermans, in B. Pullman (Ed.), *Intermolecular Forces*, Reidel, Dordrecht, 1981, pp. 331-342.

[17] J.-P. Ryckaert, G. Ciccotti, H.J.C. Berendsen, *J. Comput. Phys.*, 23 (1977) 327-341.

[18] J. Sikkema, T. Oba, *Snow Brand R&D Reports*, 107 (1998) 1-31.

Summary

Microbial exopolysaccharides (EPSs) are employed as additives to a wide variety of food products, where they serve as thickening, stabilizing, emulsifying or gelling agents. EPSs produced by lactic acid bacteria, which carry the GRAS (generally recognized as safe) status, are used *in situ* to improve body and texture of fermented dairy products. The elucidation of the structures of these EPSs is of interest to establish the relationship between the structures and their rheological behavior. Knowledge of this relationship may lead to the development of chemically, enzymatically, and genetically modified polysaccharides, which meet particular requirements for industrial applications. The work described in this thesis deals with the isolation, purification and primary structure analysis of the EPSs produced by four *Streptococcus thermophilus* strains and a *Lactobacillus delbrueckii* subsp. *bulgaricus* strain. Furthermore, a conformational analysis of the EPS produced by a *Lactobacillus helveticus* strain is outlined.

In Chapter 1 the determination of the primary structure of the EPSs produced by *S. thermophilus* Rs and Sts in skimmed milk is described. For both polysaccharides, monosaccharide analysis demonstrated the occurrence of D-galactose and L-rhamnose in a molar ratio of 5:2. Linkage analysis and 1D/2D NMR (^{1}H and ^{13}C) studies revealed that both polysaccharides were composed of identical branched heptasaccharide repeating units with the following structure:

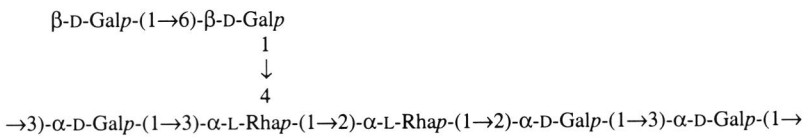

Remarkably, the two strains differ in their effects on the viscosity of stirred milk cultures. The milk culture of *S. thermophilus* Rs is non-ropy and affords 135 mg/L polysaccharide with an average molecular mass of 2.6×10^3 kDa. In contrast, the milk culture of *S. thermophilus* Sts is ropy and produces 127 mg/L polysaccharide with an average molecular mass of 3.7×10^3 kDa. Permeability measurements of non-stirred milk cultures of the strains suggest that both strains have a similar effect on the protein-polysaccharide network.

Therefore, the only clear difference between both strains, which may cause the difference in ropiness of the milk cultures, is the difference in molecular mass of the polysaccharide.

In Chapter 2 the EPS produced by *S. thermophilus* S3 in skimmed milk is characterized as described, and was found to be composed of D-galactose and L-rhamnose in a molar ratio of 2:1. The polysaccharide contained 0.4 equivalents of *O*-acetyl groups per repeating unit. Linkage analysis and 1D/2D NMR (^{1}H and ^{13}C) studies on native and de-*O*-acetylated EPS together with nanoES-CID tandem mass spectrometry studies on oligosaccharides generated by a periodate oxidation protocol, showed the polysaccharide to have the following hexasaccharide repeating structure:

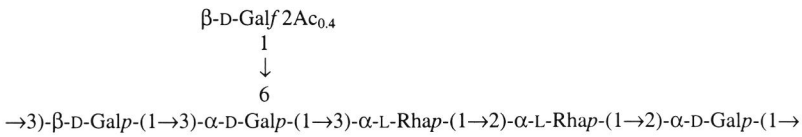

In Chapter 3 the elucidation of the primary structure of the EPS produced by *Lb. delbrueckii* subsp. *bulgaricus* 291, when grown in skimmed milk, is outlined. The lactic acid bacteria produced 80 mg/L exopolysaccharide with an average molecular mass of 1.4×10^3 kDa and a monosaccharide composition of D-glucose and D-galactose in a molar ratio of 3:2. Methylation analysis, mass spectrometry, and 1D/2D NMR (^{1}H and ^{13}C) studies performed on the native polysaccharide, and on oligosaccharides obtained from a mild acid hydrolyzate of the native polysaccharide, showed the polysaccharide to consist of branched pentasaccharide repeating units with the following structure:

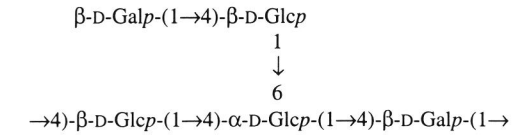

Surprisingly, the repeating unit of the EPS produced by *Lb. delbrueckii* subsp. *bulgaricus* 291 was found to be identical to the de-*O*-acetylated repeating unit of the EPS produced by

Lactococcus lactis subsp. *cremoris* B891. To our knowledge there are no reports on the appearance of identical heteropolysaccharide repeating units produced by different genera of lactic acid bacteria. Therefore, the production of an identical EPS by *Lb. delbrueckii* subsp. *bulgaricus* 291 and *L. lactis* subsp. *cremoris* B891 is remarkable.

In Chapter 4 the isolation and identification is reported of a novel sugar constituent from the heteropolysaccharide excreted by *Streptococcus thermophilus* 8S when grown in skimmed milk. The structure was determined by means of chemical analysis, mass spectrometry, NMR spectroscopy, along with molecular dynamics simulations, and shown to be 6-*O*-(3′,9′-dideoxy-D-*threo*-D-*altro*-nononic acid-2′-yl)-D-glucopyranose.

In Chapter 5 the complete elucidation is described of the primary structure of the *S. thermophilus* 8S EPS. The EPS was shown to be a heteropolysaccharide containing D-galactose, D-glucose, D-ribose, *N*-acetyl-D-galactosamine, and 6-*O*-(3′,9′-dideoxy-D-*threo*-D-*altro*-nononic acid-2′-yl)-D-glucose in a molar ratio of 2:1:1:1:1. Methylation analysis and 1D/2D (^{1}H and ^{13}C) NMR studies performed on the native polysaccharide, and mass spectrometric and NMR analysis of the oligosaccharide obtained from the polysaccharide by de-*N*-acetylation followed by deamination and reduction, demonstrated the "hepta"saccharide repeating unit to be:

→4)-α-D-Gal*p*-(1→2)-β-D-Rib*f*-(1→4)-β-D-Gal*p*-(1→4)-β-D-Glc*p*-(1→7′)-Sug-(1→4)-β-D-Gal*p*NAc-(1→

in which Sug is 6-*O*-(3′,9′-dideoxy-D-*threo*-D-*altro*-nononic acid-2′-yl)-α-D-glucopyranose.

Finally, in Chapter 6 a method is described for constructing a conformational model in water of a heteropolysaccharide built up from repeating units, and is applied to the exopolysaccharide produced by *Lactobacillus helveticus* 766. This EPS is composed of hexasaccharide repeating units with the following primary structure

β-D-Gal*f*
1
↓
3
→3)-β-D-Glc*p*-(1→4)-β-D-Glc*p*-(1→6)-α-D-Glc*p*-(1→6)-α-D-Gal*p*-(1→6)-α-D-Glc*p*-(1→

The molecular modeling method was based on energy minima, obtained from molecular mechanics calculations of each of the constituting disaccharide fragments of the repeating unit *in vacuo*, as starting point. Subsequently, adaptive umbrella sampling of the potential-of-mean-force was applied to extract rotamer populations of glycosidic dihedral angles of oligosaccharide fragments in solution. From these analyses, the most probable conformations were constructed for the hexasaccharide-repeating units of the polysaccharide. After exploring the conformational space of each of the individual repeating units by molecular dynamics simulations, the different repeating unit conformations were used as building blocks for the generation of oligo- and polysaccharide models, by using a polysaccharide building program. The created models of the exopolysaccharide produced by *L. helveticus* 766 exhibit a flexible twisted secondary structure and tend to adopt a random coil conformation as tertiary structure.

Samenvatting

Bacteriële exopolysachariden (EPSen) worden gebruikt als additieven in een groot aantal voedingsmiddelen, waar zij dienen als verdikkingsmiddel, stabilisator, emulgator of geleermiddel. EPSen geproduceerd door melkzuurbacteriën, welke de zogenaamde GRAS (generally recognized as safe) status bezitten, worden *in situ* gebruikt om de samenhang en structuur van gefermenteerde zuivelproducten te verbeteren. De structuuropheldering van EPSen is van belang om de relatie tussen de structuur en de rheologische eigenschappen te bepalen. Inzicht in deze relatie kan leiden tot de ontwikkeling van chemisch-, enzymatisch- en genetisch gemodificeerde polysachariden met eigenschappen die deze polysachariden interessant maken voor industriële toepassingen. Het werk beschreven in dit proefschrift omvat de isolatie, zuivering en primaire structuuropheldering van de EPSen geproduceerd door vier *Streptococcus thermophilus* stammen en één *Lactobacillus delbrueckii* subsp. *bulgaricus* stam. Daarnaast wordt een conformatieanalyse van het EPS geproduceerd door een *Lactobacillus helveticus* stam gepresenteerd.

In Hoofdstuk 1 wordt de opheldering van de primaire structuur van de EPSen geproduceerd door *S. thermophilus* Rs and Sts in magere melk beschreven. Uit monosacharideanalyse aan beide EPSen werd duidelijk dat de polysachariden zijn opgebouwd uit D-galactose en L-rhamnose in een molaire verhouding van 5:2. Met behulp van methyleringsanalyse en 1D/2D NMR (^{1}H en ^{13}C) experimenten kon worden vastgesteld dat beide EPSen uit identieke vertakte repeterende eenheden bestaan zoals hierna is weergegeven:

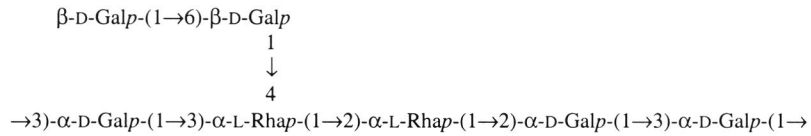

Opmerkelijk genoeg verschillen de twee stammen in hun effect op de viscositeit van geroerde melkculturen. De melkcultuur van *S. thermophilus* Rs is niet slijmerig en bevat 135 mg/L polysacharide met een gemiddelde molmassa van 2.6×10^3 kDa. Daarentegen, is de melkcultuur van *S. thermophilus* Sts slijmerig en bevat 127 mg/L polysacharide met een gemiddelde molmassa van 3.7×10^3 kDa. Permeabiliteits metingen aan niet geroerde

melkculturen van de twee stammen suggereren dat beide stammen een overeenkomstig effect hebben op het eiwit-polysacharide netwerk. Daarmee is het enige duidelijke verschil tussen beide stammen welke het verschil in slijmerigheid van de melkculturen kan veroorzaken, het verschil in molmassa van de polysachariden.

In Hoofdstuk 2 wordt de structuur van het EPS geproduceerd door *S. thermophilus* S3 in magere melk opgehelderd. Uit een monosacharideanalyse is gebleken dat dit EPS is opgebouwd uit D-galactose en L-rhamnose in een molverhouding van 2:1. Het polysacharide bevat 0.4 mol *O*-acetyl per 1.0 mol repeterende eenheid. Methyleringsanalyse en 1D/2D NMR (^{1}H en ^{13}C) experimenten aan het natieve EPS en aan een EPS-derivaat verkregen door de-*O*-acetylering, samen met nanoES-CID tandem massaspectrometrie studies aan oligosacharide geproduceerd met behulp van een perjodaat-oxidatie protocol, lieten zien dat het polysacharide is opgebouwd uit hexasacharide repeterende eenheden met de volgende structuur:

β-D-Gal*f* 2Ac$_{0.4}$
1
↓
6
→3)-β-D-Gal*p*-(1→3)-α-D-Gal*p*-(1→3)-α-L-Rha*p*-(1→2)-α-L-Rha*p*-(1→2)-α-D-Gal*p*-(1→

In Hoofdstuk 3 wordt beschreven hoe de primaire structuur van het EPS van *Lb. delbrueckii* subsp. *bulgaricus* 291 gegroeid in magere melk is opgehelderd. De melkzuurbacterie produceert 80 mg/L exopolysacharide met een gemiddelde molmassa van 1.4×10^{3} kDa en een monosacharide samenstelling van D-glucose en D-galactose in een molverhouding van 3:2. Met behulp van methyleringsanalyse, massaspectrometrie, en 1D/2D NMR (^{1}H en ^{13}C) experimenten aan zowel het natieve EPS als aan oligosacharide die zijn verkregen via mildzure hydrolyse van het natieve EPS, kon worden vastgesteld dat het EPS uit vertakte pentasacharide repeterende eenheden bestaat, zoals hierna is weergegeven:

β-D-Gal*p*-(1→4)-β-D-Glc*p*
1
↓
6
→4)-β-D-Glc*p*-(1→4)-α-D-Glc*p*-(1→4)-β-D-Gal*p*-(1→

De repeterende eenheid van het EPS geproduceerd door *Lb. delbrueckii* subsp. *bulgaricus* 291 blijkt identiek te zijn aan de repeterende eenheid van het EPS-derivaat, verkregen door de-*O*-acetylering van het natieve EPS geproduceerd door *Lactococcus lactis* subsp. *cremoris* B891. Voor zover ons bekend, is het voorkomen van identieke heteropolysacharide repeterende eenheden geproduceerd door verschillende genera melkzuurbacteriën niet eerder gerapporteerd. De productie van de identieke EPS door *Lb. delbrueckii* subsp. *bulgaricus* 291 en *L. lactis* subsp. *cremoris* B891 is daarom dan ook opmerkelijk.

In Hoofdstuk 4 wordt de isolatie en identificatie van een nieuw koolhydraat bestanddeel van het heteropolysacharide uitgescheiden door *S. thermophilus* 8S beschreven. Met behulp van chemische analyses, massaspectrometrie, NMR spectroscopie en moleculaire-dynamische-simulaties is de structuur vastgesteld als 6-*O*-(3′,9′-dideoxy-D-*threo*-D-*altro*-nonaanzuur-2′-yl)-D-glucopyranose.

In Hoofdstuk 5 wordt de structuuropheldering van de primaire structuur van het complete *S. thermophilus* 8S EPS beschreven. Het EPS is een heteropolysacharide bestaande uit D-galactose, D-glucose, D-ribose, *N*-acetyl-D-galactosamine, en 6-*O*-(3′,9′-dideoxy-D-*threo*-D-*altro*-nonaanzuur-2′-yl)-D-glucose in een molverhouding van 2:1:1:1:1. Met behulp van methyleringsanalyse en 1D/2D (^{1}H en ^{13}C) NMR experimenten aan het natieve EPS in combinatie met massaspectrometrie en NMR analyses van het oligosacharide verkregen door de-*N*-acetylering, deaminering en reductie van het natieve EPS kon de structuur van de "hepta"sacharide repeterende eenheid worden vastgesteld:

→4)-α-D-Gal*p*-(1→2)-β-D-Rib*f*-(1→4)-β-D-Gal*p*-(1→4)-β-D-Glc*p*-(1→7′)-Sug-(1→4)-β-D-Gal*p*NAc-(1→

waarin Sug staat voor 6-*O*-(3′,9′-dideoxy-D-*threo*-D-*altro*-nonaanzuur-2′-yl)-α-D-glucopyranose.

In Hoofstuk 6 wordt tenslotte een methode beschreven voor het construeren van conformatiemodellen in water van een heteropolysacharide opgebouwd uit repeterende eenheden. De ontwikkelde methode is toegepast op het exopolysacharide geproduceerd door *Lb. helveticus* 766. Dit EPS bestaat uit hexasacharide repeterende eenheden met de volgende primaire structuur:

β-D-Gal*f*
1
↓
3
→3)-β-D-Glc*p*-(1→4)-β-D-Glc*p*-(1→6)-α-D-Glc*p*-(1→6)-α-D-Gal*p*-(1→6)-α-D-Glc*p*-(1→

De *molecular modeling* methode is gebaseerd op energie minima welke zijn verkregen via moleculaire-mechanica-berekeningen *in vacuo* aan elk van de samenstellende disacharide-fragmenten van de repeterende eenheid. Vervolgens is met behulp van *adaptive umbrella sampling* van de *potential-of-mean-force*, de energie potentiaal rond glycosidische tweevlaks hoeken, de rotameer populatie van de glycosidische tweevlaks hoeken van oligosacharide-fragmenten in oplossing bepaald. Met behulp van deze gegevens zijn de meest waarschijnlijke conformaties van de hexasacharide repeterende eenheid opgebouwd. Na het bestuderen van de conformationele ruimte van ieder van de repeterende eenheden met behulp van moleculaire-dynamische-simulaties, zijn de verschillende repeterende eenheid conformaties gebruikt als bouwstenen om oligo- en polysacharidemodellen te genereren. De geconstrueerde modellen van het polysacharide geproduceerd door *L. helveticus* 766 bezitten een flexibele gedraaide secundaire structuur en neigen een *random-coil* conformatie als tertiaire structuur aan te nemen.

Curriculum vitae

Elisabeth Johanna Faber werd geboren op 13 juni 1970 te Minnertsga. Na het behalen van het LBO diploma Levensmiddelentechnologie aan het Onderwijscentrum voor Landbouw, Tuinbouw en Levensmiddelentechnologie te Leeuwarden en het behalen van het MLO diploma Technische Microbiologie aan de Middelbare Laboratorium school te Leeuwarden, is zij in september 1989 gestart met de studie Chemie aan de Internationale Agrarische Hogeschool Larenstein, sectie Laboratoriumtechniek te Wageningen. Tijdens deze periode werd stage gelopen bij de vakgroep Plantenfysiologie en Microbiologie van de Universiteit van Tromsø, Noorwegen en werd een afstudeeropdracht uitgevoerd bij de afdeling Technologie van NIZO Food Research, Ede. Aansluitend is zij gedurende een half jaar bij hetzelfde bedrijf werkzaam geweest als onderzoeksmedewerker. In januari 1994 werd begonnen aan de verkorte doctoraal studie Moleculaire Wetenschappen aan de Landbouwuniversiteit te Wageningen. Het hoofdvak ter afsluiting van deze studie werd uitgevoerd aan de vakgroep Moleculaire Fysica en aan de vakgroep Bosbouw.

Van 1 april 1996 tot en met 1 april 2000 was zij als Assistent in Opleiding werkzaam bij de sectie Bio-Organische Chemie van het Bijvoet Centrum voor Biomoleculair Onderzoek van de Faculteit Scheikunde van de Universiteit Utrecht (Prof. Dr. J.F.G. Vliegenthart en Prof. Dr. J.P. Kamerling) al waar zij het in dit proefschrift beschreven onderzoek uitvoerde. Tijdens het promotieonderzoek nam zij deel aan de "4th European Training Course on Carbohydrates" in Alzate Brianza, Italië (1996), aan de "Advanced NMR spectroscopy Course" in Nijmegen en Utrecht (1997), en aan de "Mass Spectrometry Course" in Utrecht (1998). Onderdelen van het in dit proefschrift beschreven onderzoek zijn onder meer gepresenteerd tijdens de jaarlijkse bijeenkomst van de Duitse, Franse en Nederlandse verenigingen voor Glycobiologie te Giessen, Duitsland (1996) en Nuland (1998) en op het "XIX International Carbohydrate Symposium" in San Diego, USA (1998).

Since 1 november 2000 is zij werkzaam als Projectleider NMR i.o. bij de afdeling Voedingsmiddelen & Voedingssupplementen Analyse van de Nederlandse Organisatie voor toegepast-natuurwetenschappelijk onderzoek (TNO) te Zeist.

List of publications

Measurement procedure for concentration of active rennet in cheese.
P. Zoon, C. Ansems, E.J. Faber, *Neth. Milk Dairy J.*, 48 (1994) 141-150.

The exopolysaccharides produced by *Streptococcus thermophilus* Rs and Sts have the same repeating unit but differ in viscosity of their milk cultures.
E.J. Faber, P. Zoon, J.P. Kamerling, J.F.G. Vliegenthart, *Carbohydr. Res.*, 310 (1997) 269-276.

Introduction of the exopolysaccharide gene cluster from *Streptococcus thermophilus* Sfi6 into *Lactococcus lactis* MG1363: production and characterization of an altered polysaccharide.
F. Stingele, S.J.F. Vincent, E.J. Faber, J.W. Newell, J.P. Kamerling, J.-R. Neeser, *Mol. Microbiol.*, 32 (1999) 1287-1295.

Biochemical and structural characterization of the glucan and fructan exopolysaccharides synthesized by the *Lactobacillus reuteri* wild-type strain and by mutant strains.
G.H. van Geel-Schutten, E.J. Faber, E. Smit, K. Bonting, M.R. Smith, B. ten Brink, J.P. Kamerling, J.F.G. Vliegenthart, L. Dijkhuizen, *Appl. Environ. Microbiol.* 65 (1999) 3008-3014.

Structure elucidation of glycoprotein glycans and of polysaccharides by NMR spectroscopy.
B.R. Leeflang, E.J. Faber, P. Erbel, J.F.G. Vliegenthart, *J. Biotechnol.* 77 (2000) 115-122.

Structure of the exopolysaccharide produced by *Streptococcus macedonicus* Sc136
S.J.F. Vincent, E.J. Faber, J.-R. Neeser, F. Stingele, J.P. Kamerling, *Glycobiology*, (2000) in press.

Structure of the exopolysaccharide produced by *Streptococcus thermophilus* S3.
E.J. Faber, M van den Haak, J.P. Kamerling, J.F.G. Vliegenthart, *Carbohydr. Res.*, (2000) submitted.

Structure of the extracellular polysaccharide produced by *Lactobacillus delbrueckii* subsp. *bulgaricus* 291.
E.J. Faber, J.P. Kamerling, J.F.G. Vliegenthart, *Carbohydr. Res.*, (2000) submitted.

Molecular characterization of a novel glucansucrase from *Lactobacillus reuteri* synthesizing a unique and highly branched glucan with $\alpha(1,4)$ and $\beta(1,4)$ glycosidic bonds.
G.H. van Geel-Schutten, S. Kralj, H. Rahaoui, R.J. Leer, S.A.F.T. Hijum, E.J. Faber, L. Dijkhuizen, *Appl. Environ. Microbiol.*, (2000) submitted.

The exopolysaccharide produced by *Streptococcus thermophilus* 8S contains a novel open chain nononic acid.
E.J. Faber, J.A. van Kuik, J.P. Kamerling, J.F.G. Vliegenthart, *Manuscript in preparation.*

Characterization of the exopolysaccharide produced by *Streptococcus thermophilus* 8S containing an open chain nononic acid.
E.J. Faber, D.J. van Haaster, J.P. Kamerling, J.F.G. Vliegenthart, *Manuscript in preparation.*

Modeling of the structure in aqueous solution of the exopolysaccharide produced by *Lactobacillus helveticus* 766.
E.J. Faber, J.A. van Kuik, J.P. Kamerling, J.F.G. Vliegenthart, *Manuscript in preparation.*

Dankwoord

Aan het einde van vier jaar onderzoek wil ik hier mijn dank betuigen aan eenieder die aan de totstandkoming van dit poefschrift heeft bijgedragen.

Allereerst wil ik mijn promotores bedanken voor de mogelijkheid die zij mij hebben geboden om het in dit proefschrift beschreven onderzoek uit te voeren. Hans Kamerling, ik bewonder jouw enthousiasme voor het PBTS-project en wil je bedanken voor de heldere discussies, de bemoedigende opmerkingen en voor al de punten en komma's die dit proefschrift nodig had. Ook Hans Vliegenthart wil ik hartelijk danken voor zijn steun, vertrouwen, en voor de geboden vrijheid waarin ik de afgelopen vier jaar heb kunnen werken.

Verschillende medewerkers van NIZO Food Research ben ik dankbaar voor hun hulp bij het onderzoek. Met name Nel Zoon voor haar fysische inbreng en Fedde Kingma voor alweer een liter yogurt. Daarnaast wil ik alle collega's waarmee ik heb samengewerkt in het kader van het PBTS-project exopolysachariden bedanken voor hun betrokkenheid en de opbouwende kritiek tijdens onze bijeenkomsten.

Mischa van den Haak en Daan van Haaster hebben in het kader van hun bij- en hoofdvak meegewerkt aan de isolatie en structuuropheldering van enkele EPSen, waarvoor ik hen zeer erkentelijk ben. Cees Versluis bedank ik voor het opnemen van de Q-TOF spectra.

En dan zijn er natuurlijk mijn collega's en oud-collega's waarvan ik niet alleen het 'vak' heb geleerd, maar door wie ik het zowel tijdens als buiten de werkuren altijd naar mijn zin heb gehad. Yuri en Carel, met veel plezier denk ik terug aan de wetenschappelijke maar vooral ook aan de niet-zo-wetenschappelijke discussies die wij hadden. Ik ben blij dat jullie mij ook in de laatste fase van mijn promotie bij willen staan. Albert en Bas, bedankt voor al die keren dat ik bij jullie mocht "aankloppen". Albert, zonder jou zou figuur 6 in Hoofdstuk 4 er nu heel anders uitzien en Bas, ik zal die gesprekken op dat andere gebied niet vergeten. Simon, thanks for all the answers to my 'Do you know ....?' questions, and Sebastien, although our work is not included in this thesis, I would like to thank you for our collaboration and friendship, and I sincerely hope that in the future we can hold up to the principle: "science over competition".

De secretaresses van de BOC (en dat zijn er in de afgelopen vier jaar een heel aantal geweest), ik bedank jullie vanaf het kopje koffie dat ik tijdens mijn sollicitatiegeprek van jullie kreeg, tot de enveloppen waarin ik mijn proefschrift heb verstuurd. Jan, Ingrid en Aloys, jullie wil ik bedanken voor het maken van posters, dia's en de voorkant van dit proefschift. Dankzij jullie kon ik altijd goed voor de dag komen op symposia en congressen, en die poster prijs is dus eigenlijk voor jullie.

Natuurlijk mogen ook de rest van mijn collega's "binnen" en "buiten" de BOC niet in dit dankwoord ontbreken. Het valt moeilijk precies aan te geven waarvoor ik jullie dank verschuldigd ben omdat een ieder op zijn eigen manier bijgedragen heeft tot de prettige samenwerking maar vooral ook aan de gezellige sfeer op het lab en aan de koffietafel. Bedankt.

Tenslotte gaan mijn gedachten uit naar mijn familie en vrienden en in heb bijzonder naar mijn ouders. Lieve papa en mama, jullie hebben me altijd gesteund en gestimuleerd om het beste uit mezelf te halen. Ik ben jullie dankbaar voor de vrijheid die jullie mij hebben gegeven ook al konden jullie daardoor niet altijd bevatten waar ik mee bezig was.

Lieve Hans, de meeste dank ben ik aan jou verschuldigd. Je onvoorwaardelijke liefde, je steun en je geduld hebben mij de energie gegeven om dit te bereiken; ik had het niet alleen gekund.

Abbreviations

1D, 2D	one-, two-dimensional
Ac	acetyl
AUS	adaptive umbrella sampling
CID	collision induced dissociation
COSY	correlation spectroscopy
cr-EPS	carboxyl reduced exopolysaccharide
dAc-EPS	deacetylated exopolysaccharide
DQF	double quantum filtered
EI	electron ionization
EPS	exopolysaccharide
ES	electrospray
f	furanose
FID	free induction decay
Gal	galactose
GLC	gas liquid chromatography
Glc	glucose
GRAS	generally recognized as save
Hex	hexose
HMBC	heteronuclear multiple bond correlation
HMQC	heteronuclear multiple quantum coherence
HPAEC	high-performance anion-exchange chromatography
HP-GPC	high-performance – gel permeation chromatography
HSQC	heteronuclear single quantum coherence
hyd-EPS	hydrolyzed exopolysaccharide
L.	*Lactococcus*
Lb.	*Lactobacillus*
MALDI-TOF	matrix-assisted laser desorption / ionisation – time of flight
Man	mannose
MD	molecular dynamics
Me	methyl
MM	molecular mechanics
MS	mass spectrometry

NAc	*N*-acetyl
n-EPS	native exopolysaccharide
NMR	nuclear magnetic resonance
NOE	nuclear Overhauser enhancement
NOESY	nuclear Overhauser enhancement spectroscopy
p	pyranose
PAD	pulsed amperometric detection
Pent	pentose
PMF	potential of mean force
Q-TOF	quadrupole - time of flight
Rha	rhamnose
RI	refractive index
Rib	ribose
ROESY	rotating frame Overhauser enhancement spectroscopy
S.	*Streptococcus*
TOCSY	total correlation spectroscopy
WEFT	water-eliminated Fourier transform

Printed by Universal Press, Veenendaal

Publication of this thesis was financially supported by TNO Nutrition and Food Research Institute Zeist, Netherlands

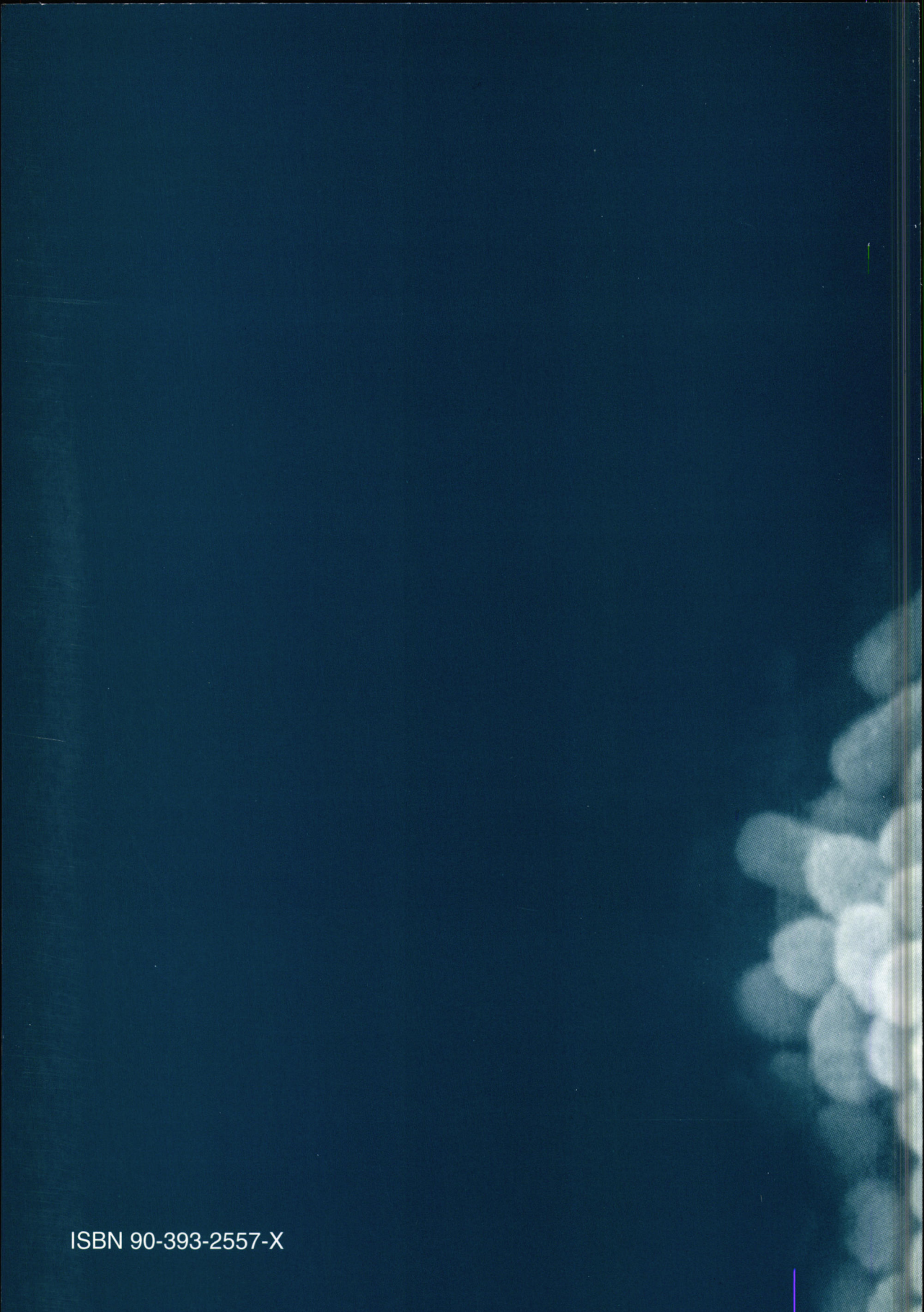

ISBN 90-393-2557-X